THE UNIVERSITY OF CALGARY

Spontaneous and Electrically Induced Activity of Medial Septum/Diagonal Band Neurons

BY

Richard Douglas Ford

A THESIS

SUBMITTED TO THE FACULTY OF GRADUATE STUDIES

IN PARTIAL FULFILLMENT OF THE REQUIREMENTS FOR THE

DEGREE OF MASTER OF SCIENCE

DEPARTMENT OF PSYCHOLOGY

CALGARY, ALBERTA

FEBRUARY, 1988

ISBN 0-315-42454-0

THE UNIVERSITY OF CALGARY

FACULTY OF GRADUATE STUDIES

The undersigned certify that they have read, and recommend to the Faculty of Graduate Studies for acceptance, a thesis entitled, "Spontaneous and Electrically Induced Activity of Medial Septum/Diagonal Band Neurons" submitted by Richard D. Ford in partial fulfillment of the requirements for the degree of Master of Science.

Dr. Brian H. Bland (Supervisor)
Department of Psychology

Dr. Jos J. Eggermont
Department of Psychology

Dr. Eugene S. Edgington
Department of Psychology

Dr. Brian A. MacVicar
Department of Medical Physiology

Date February 26, 1988

ABSTRACT

Extracellularly recorded spike trains from 65 medial septum/diagonal band neurons in urethane anaesthetized rats were compared to hippocampal slow wave activity using three axes. Cells which discharged in rhythmic bursts, phase locked to hippocampal theta were termed phasic while those that discharged irregularly, unrelated to the phase of theta were termed tonic. The second axis involved whether or not the cell discharge rate varied linearly with changes in theta frequency. Cells were termed theta-on if: a) their discharge rate was positively correlated to the frequency of hippocampal theta (linear), or b) they discharged at a rate which was significantly greater during slow wave theta than during large amplitude irregular activity (nonlinear). Cells were termed theta-off if: a) their discharge rates were negatively correlated to the frequency of theta (linear), or b) they discharged at significantly lower rates during theta compared to large amplitude irregular activity (nonlinear). Out of 37 theta-on cells, 10 were phasic linear, 12 were phasic nonlinear, 7 were tonic linear and 8 were tonic nonlinear. Sixteen cells were determined to be theta-off cells, of which 9 were phasic linear, 4 were phasic nonlinear, and 3 were tonic linear. These results show that medial

septum/diagonal band neurons in a urethane anaesthetized preparation are not only related to slow wave theta by their discharge pattern, but also by their discharge rate.

Stimulation of the dorsomedial-posterior nuclei of the hypothalamus resulted in a linear relationship between discharge rate and stimulation intensity in phasic linear (n = 3) and tonic linear (n = 1) theta-on cells. Discharge rates were also linearly related to stimulation intensity (n = 6) and theta frequency (n = 5) in phasic nonlinear theta-off cells. The effects of stimulation on tonic nonlinear theta-on cell discharge rates were more variable than the effects observed in phasic nonlinear theta-on cells. Tonic nonlinear theta-on cell discharge rates increased (n = 1), or decreased (n = 2) linearly with increased stimulation intensity. In addition, one tonic nonlinear theta-on cell increased its discharge rate with stimulation, but not in a linear fashion, and another was not affected by stimulation. The effects of stimulation on the spontaneous relationship between cell discharge rates and hippocampal theta were discussed.

ACKNOWLEDGEMENTS

The expertise, patience and friendship of Dr. Brian Bland was greatly appreciated since this project could not have been completed without it.

A special thank you to my wonderful parents for their Love and support in this extended endeavour.

Thank you to Leanne, Martyn and Bill, as well as my Brothers in Zeta Psi for their friendship, encouragement, etc., which has been of infinite value in reaching my goal.

CONTENTS

	PAGE
ABSTRACT	iii
ACKNOWLEDGEMENTS	v
TABLE OF CONTENTS	vi
LIST OF TABLES	vii
LIST OF FIGURES	viii
INTRODUCTION	1
ANATOMY	4
Septal Anatomy	4
Hippocampal Anatomy	8
Septal-Hippocampal Connections	16
Dorsomedial-Posterior Nuclei: Anatomic Connections with the Septum and Hippocampal Formation	22
PHYSIOLOGY AND PHARMACOLOGY	25
Hippocampal Theta	25
Septal-Hippocampal Connections	30
Unit Activity and Hippocampal Theta	37
OBJECTIVES	53
METHODS	57
Subjects	57
Apparatus	57
Surgical Procedure	58
Experimental Procedure	62
Data Analysis	63
Statistical Analysis	66
RESULTS	70
Spontaneous Activity	70
Stimulation Induced Activity	107
DISCUSSION	124
Spontaneous Activity	124
Cell Discharge Patterns	124
Linear vs. Nonlinear Discharge Rates	126
Theta-on vs. Theta-off	127
Topography of MS/vDBB Neuron Types	130
Stimulation Induced Activity	131
Conclusions	135
Spontaneous Activity	135
Stimulation Induced Activity	145
REFERENCES	148

LIST OF TABLES

Table	Title	Page
Table 1	List of abbreviations	3
Table 2	Theta-on and theta-off cells in the MS/vDBB	80
Table 3	Theta-on cell data summary	83
Table 4	Theta-off cell data summary	93
Table 5	Summary for linear regression of theta frequency on stimulation intensity	108
Table 6	Summary for linear regression of unit discharge rate on stimulation intensity ...	114

INTRODUCTION

The medial septal nucleus (MS) and the vertical limb nucleus of the diagonal band of Broca (vDBB) are considered to be of central importance in the generation of hippocampal electroencephalographic (EEG) activity. The MS and vDBB are centrally located between the ascending pathways of the brainstem and the hippocampal formation (HF). The observed relationship between hippocampal slow wave activity, behavior, and sensory processing has resulted in the extensive study of cell behavior and the hippocampal EEG. Specifically, the study of rhythmic bursting neurons and the relationship of these cells to the hippocampal theta rhythm has received a great deal of attention.

The rhythmic bursting neurons of the MS and vDBB are generally thought of as the pacemakers of the hippocampal slow wave theta rhythm. Anatomic, pharmacologic, physiologic, and behavioral research have resulted in an extensive body of literature which describes the relationship of MS/vDBB cell discharge patterns to the theta rhythm. Activation of various brainstem and hypothalamic nuclei is thought to influence both MS/vDBB cells, and hippocampal theta.

Unlike previous research, which has neglected cell discharge rates, this study will analyze the relationship between spontaneous discharge rates of MS/vDBB neurons and simultaneously recorded hippocampal slow wave activity. Since the theta rhythm is not the only slow wave activity recorded in the hippocampus, changes in the spontaneous cell activity which accompany shifts in the hippocampal EEG state will be studied, in addition to the relationship between cell discharge rate and slow wave theta frequency. Finally, slow wave theta frequency is known to be modified by increased activation from the brainstem and hypothalamus, therefore, it is also of interest to determine the nature of this effect on the cell discharge rates of MS/vDBB neurons.

The following chapters will provide an overview of the literature which is relevant to the relationship between septal unit activity and the hippocampal EEG. Areas which will be covered include septal-hippocampal anatomy, physiology, and pharmacology. It is important to note that a great deal of the literature is based on information obtained from *Ratus norvegicus*, however, some information has been obtained from other species. Information obtained from species other than *Ratus norvegicus* will be identified.

Table 1

List of abbreviations

Dentate Gyrus	DG
Diagonal Band of Broca	DBB
Dorsomedial Hypothalamus	DMH
Dorsomedial-Posterior nuclei of the Hypothalamus	DM-PH
Hippocampal Formation	HF
Horizontal limb nucleus of the Diagonal Band of Broca	hDBB
Lateral Hypothalamic Area	LHA
Lateral Septal Nucleus	LS
Medial Forebrain Bundle	MFB
Medial Septal Nucleus	MS
Medial Septum/Digonal Band Complex	MS/vDBB
Posterior Hypothalamic Nucleus	PH
Vertical Limb Nucleus of the Diagonal Band of Broca	vDBB
Acetylcholine	ACh
Acetylcholinesterase	AChE
Choline acetyltransferase	ChAT
γ-Amino butyric acid	GABA
Glutamic acid decarboxylase	GAD
Horseradish peroxidase	HRP
Phaseolus vulgaris leuco-agglutinin	PHA-L
Autocorrelation histogram	ACH
Interspike interval histogram	ISIH
Interstimulus interval	ISI
Theta cycle spike histogram	TCSH
Theta duration histogram	TDH
Electroecephalograph	EEG
Large amplitude irregular activity	LIA

ANATOMY

Septal Anatomy

The study of septal function has generally centered around its role as a component of the limbic system. This is due primarily to its topographic and connectional relationships to other limbic structures (Swanson and Cowan, 1976). The septum is located medially between the horns of the lateral ventricles, ventral to the corpus callosum, anterior and dorsal to the decussation of the anterior commissure, rostral to the ventral hippocampal commissure and fimbria, and caudal to the nucleus accumbens and frontal cortex (Costa, Panula, Thompson and Cheney, 1983). This important limbic structure consists of several nuclei and is a centre of convergence for fiber tracts of the diencephalic and telencephalic structures which comprise the limbic system.

The septum has been divided by Swanson and Cowan (1976, 1979) into medial, lateral, posterior, and ventral divisions. These distinctions were based on topographic, cytoarchitectonic, and connectional data obtained from rats. Differences between early anatomic studies were primarily related to terminology and were not substantive (Swanson and Cowan, 1976). Recent research has also supported, and utilized the septal organization described

in 1976 and 1979 by Swanson and Cowan (Costa, et al., 1983; Nyakas, Luiten, Spencer and Traber, 1987).

The medial division is divided into the MS dorsally, and the nucleus of the diagonal band of Broca (DBB) ventrally. The medial division contains the largest and most darkly stained neurons within the septum, as observed in preparations stained using Golgi, Nissl, Bodian, Weil, or luxol fast blue methods (Swanson and Cowan, 1976, 1979). Between the large neurons are smaller cells with long spine-free dendrites. These cells are more numerous ventrally. Although they identified large and small neurons, they also stated that these cells had a wide range of sizes.

The DBB is further subdivided into a vertical limb (vDBB) which lies ventral to the MS, along the midline, and the horizontal limb (hDBB) which extends laterally from the ventral portion of the vertical limb (Raisman, 1966; Swanson and Cowan, 1976; 1979). The boundary between vertical and horizontal divisions of the DBB is found, rostral-caudally, at the decussation of the anterior commissure (Swanson and Cowan, 1976, 1979; Nyakas, et al., 1987). The vDBB and the MS form the medial septum/diagonal band complex (MS/vDBB), which together form the septal-hippocampal projection (to be discussed in subsequent chapters).

Using a modified Golgi technique, Tombol and Petsche (1969) identified neurons of the MS and the vDBB in rabbits. They found large, medium, and small cells of various shapes with distinct interconnections. The small neurons were ovoid in shape and sent axon collaterals to the medium and large size cells. The medium neurons were either multiangular, or fusiform in shape, with local axon collaterals forming axodendritic synapses on medium and large size cells. The large neurons were also multiangular, or fusiform, however, the axon collaterals of these cells could not be traced in their preparations. Axons of the medium and large size cells appeared to leave the septum in a dorsal direction, while the axons of the smaller cells appeared to remain within the MS/vDBB. Cells of the vDBB have been shown to project to cells of the MS (Swanson and Cowan, 1979). It has also been demonstrated that the smaller cells of the medial division are more numerous in the ventral areas (Swanson and Cowan, 1976, 1979).

The lateral septal nucleus (LS) forms the lateral division which has been divided into the dorsal, intermediate and ventral components (Swanson and Cowan, 1976). The LS contains medium sized neurons with the distinction between the three components based on differences in cell size and density, and the depth of

staining. Neurons of the LS were shown to have radiating dendrites with many spiney processes (Swanson and Cowan, 1976). Lateral septal neurons project to the MS/vDBB forming one of two identified intrinsic connections of the septal nuclei (Swanson and Cowan, 1979).

The posterior division of the septum is composed of the triangular septal nucleus and the septofimbrial nucleus (Swanson and Cowan, 1976). These authors described the cells of the triangular septal nucleus as small, almost granule-like. They are densely packed within the rostral-ventral part of the ventral hippocampal commissure. The cells of the septofimbrial nucleus are similar in size and appearance to those found in the LS and are embedded within the precommissural fornix (Swanson and Cowan, 1976).

The ventral division of the septum is composed of a heterogeneous group of cell types which is referred to as the bed nucleus of the stria terminalis. Swanson and Cowan (1976) stated that it is called the bed nucleus of the stria terminalis because it receives afferent fibers from the amygdala via the stria terminalis. It is composed of small to medium sized neurons with a strip of larger cells at its lateral border (Swanson and Cowan, 1979). It is bordered ventrally by the medial preoptic and anterior hypothalamic areas and rostrally by the nucleus accumbens.

Hippocampal Anatomy

The HF is a bilateral, telencephalic, limbic structure which, in rodents, is horn shaped and forms the floor of the lateral ventricles. Anteriorly and dorsally it approaches the midline, inferior to the corpus callosum and caudal to the septum (Gaarskjaer, 1986). From the anterior-dorsal position it curves postero-laterally toward the occipital cortex and ventrally forming a semicircle around the thalamus (longitudinal axis). From the most posterior portion of the HF, which is referred to as the occipital pole, it curves antero-medially toward the temporal cortex (Gaarskjaer, 1986). The portion of the HF that lies dorsal to the thalamus is termed the dorsal HF while the portion that extends into the temporal lobe is referred to as the ventral HF. The HF is a structure which has been described by many authors including Ramón y Cajal (1911) and Lorente de Nó (1934). Hippocampal formation refers to the hippocampus proper (cornu ammonis, or Ammon's horn), the dentate area, and the subicular complex (Meibach and Siegel, 1977a). The hippocampus proper and the dentate area have a simple laminar structure which is shaped like two interlocking gyri, separated by the hippocampal fissure.

The cytoarchitecture of the HF as drawn by Brodal (1947), is provided in figure 1. Pyramidal cells are the

Figure 1. Cytoarchitecture of the hippocampal formation, as drawn by Brodal (1947). The dentate gyrus interlocks with hippocampus proper. The subicular complex is continuous with the hippocampus proper and the entorhinal area.

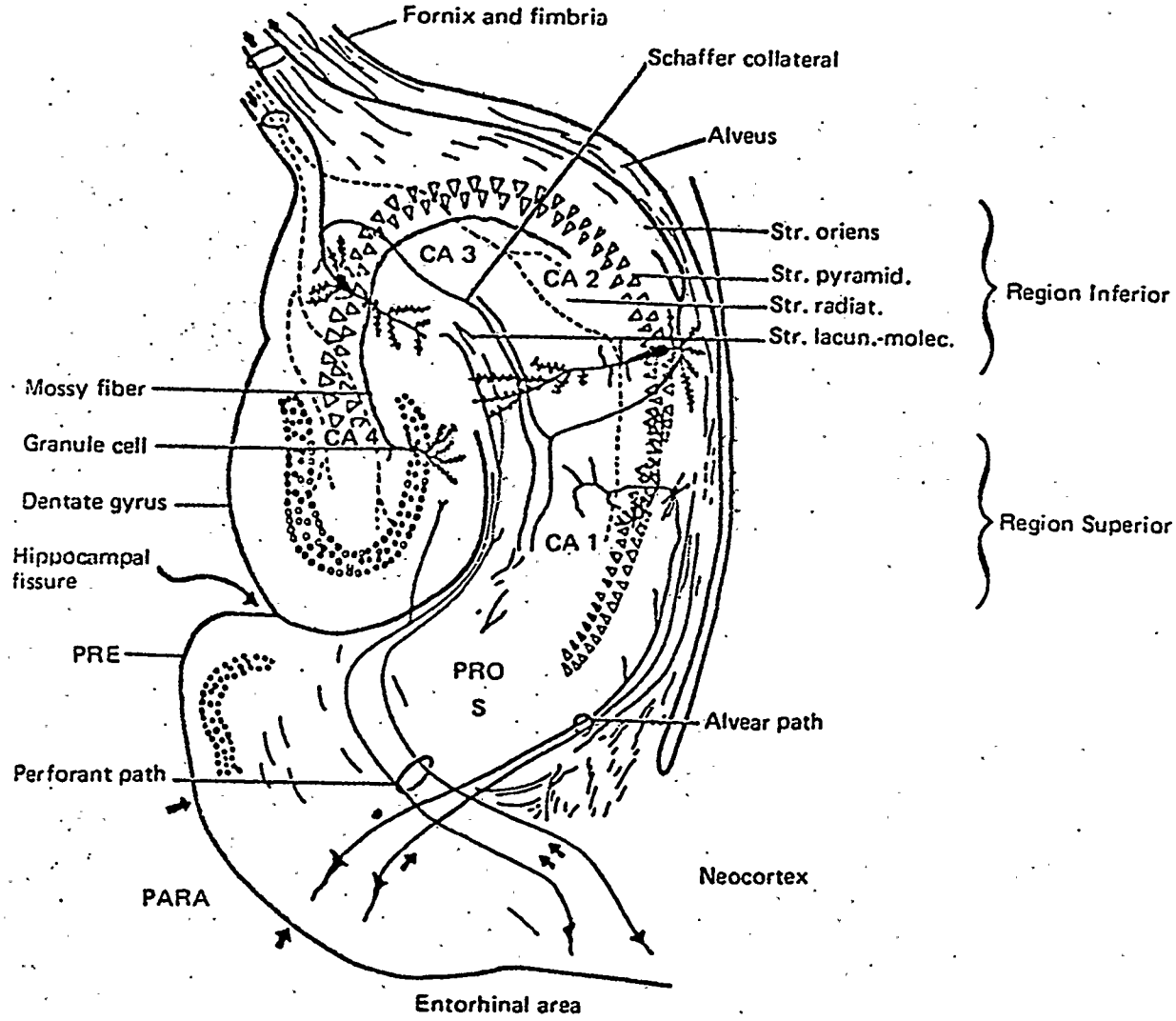
Fornix and fimbria
Schaffer collateral
Alveus
Str. oriens
Str. pyramid.
Str. radiat.
Str. lacun.-molec.
Region Inferior
Region Superior
CA 3
CA 2
CA 4
CA 1
Mossy fiber
Granule cell
Dentate gyrus
Hippocampal fissure
PRE
PRO S
Alvear path
Perforant path
PARA
Neocortex
Entorhinal area

main cell type of the hippocampus proper, forming the only cell layer of the structure (stratum pyramidale). The short basal dendritic trees of the pyramidal cells make up the stratum oriens. The outermost layer, or alveus, contains the pyramidal cell axons which extend through stratum oriens. Stratum radiatum is composed of the proximal portions of the apical dendrites, which are packed closely together in radial rows directed toward the hippocampal fissure. The distal portions of the apical dendrites compose stratum lacunosem-moleculare. The hippocampal fissure separates the hippocampus proper from the dentate area, specifically the upper blade of the dentate gyrus (DG).

The primary cell type of the DG is the granule cell, which forms the second layer of the DG, stratum granulosum. The lamellae of the DG that borders the hippocampal fissure, stratum moleculare, contains the dendritic trees of the granule cells. The dendrites of the granule cells only project to the periphery of the DG. The dentate hilus is situated between the granule layers of the upper and lower blades of the DG, and is continuous with the pyramidal cells of the hippocampus proper (Blackstad, 1956). According to the results of Amaral's (1978) Golgi stained preparations, there are eight different types of neurons in the hilus. Granule cells, basket cells, mossy

cells, and multipolar cells were four of the more common cell types found in the dentate hilus.

The subicular complex, which is continuous with the hippocampus proper, can be considered part of a transitional zone between the single cell layered archicortex, and the multi-layered entorhinal cortex (mesocortex). This structure is subdivided into the subiculum, prosubiculum, presubiculum, and parasubiculum.

The hippocampus proper has also been subdivided on the basis of anatomical and functional considerations. Ramón y Cajal (1911) originally divided the hippocampus into the areas regio inferior and regio superior based on the anatomical difference between the pyramidal cells (Raisman, Cowan and Powell, 1965). Later, Lorente de Nó (1934) further defined the regions of the hippocampus proper into four fields: CA1, CA2, CA3, and CA4 (CA for cornu ammonis). Fields CA1 and CA3 correspond to Ramón y Cajal's (1911) regio superior and regio inferior, respectively.

Regio inferior (CA3) is characterized by the presence of mossy fibers which originate in the DG. Field CA4, which is continuous with the dentate hilus, is composed of cells which are scattered and not the typical shape for pyramidal cells. Although Lorente de Nó (1934) characterized these cells as part of the hippocampus

proper, Blackstad (1956) considered them to be part of the dentate hilus.

In addition to pyramidal cells, many interneurons are found in the hippocampus proper and the DG (Ramón y Cajal, 1911; and Lorente de Nó, 1934). The most common interneurons are basket cells. These are found primarily in the stratum pyramidale, adjacent to stratum oriens (Raisman, et al., 1965). They get their name from the fact that their axons loop back through stratum radiatum to form a basket plexus on pyramidal cell bodies.

The pyramidal cells of CA3 also receive an extensive synaptic input from the ipsilateral granule cells of the DG (Gaarskjaer, 1986). Through the use of Timm's and Golgi staining, anterograde transport of [^{3}H] amino acids, and retrograde transport of horseradish peroxidase (HRP), mossy fibers from granule cells have been shown to form synapses ipsilaterally on the pyramidal cells of CA3 (stratum pyramidale) and their apical dendrites. The mossy fibers form the stratum lucidum, observed only in CA3 (Raisman, et al., 1965; Gaarskjaer, 1986). Mossy fibers also project ipsilaterally to various cells of the dentate hilus. Gaarskjaer (1986) stated that there is considerable controversy over whether or not mossy fibers project to CA1. Lorente de Nó (1934) described CA2 to as a transition zone between regio superior (CA1) and regio inferior (CA3)

partly because of the lack of mossy fibers (Gaarskjaer, 1986. Moreover, the mossy fiber pathway becomes less prominent in the ventral hippocampus (Gaarskjaer, 1986).

Mossy fibers are not the only source of intrinsic connections within the HF. Cells of field CA4 and the hilus have been shown, using degeneration techniques (Blackstad, 1956; Raisman, et al., 1965), and axonal transport of HRP and [^{3}H] amino acids (Berger, Semple-Rowland, and Basset, 1980), to project bilaterally to the stratum moleculare of the DG. This is the only projection of the dentate area which leaves the HF (only to reenter the contralateral HF). Cells of the DG do not project ouside the HF (Raisman, et al., 1965; Swanson and Cowan, 1977).

Degeneration studies have shown that Schaffer collaterals (pyramidal cell axon collaterals) from fields CA3 and CA4 terminate ipsilaterally in strata radiatum and oriens of the DG and all CA fields. Commissural fibers from field CA3 and CA4 project through the fimbria and the ventral hippocampal commissure, and terminate contralaterally in the DG and all CA fields. Schaffer collaterals from field CA1 project ipsilaterally to strata radiatum and oriens of field CA1 and the commissural fibers project to the contralateral field CA1 (Hjorth-Simonsen,

1973; Raisman, et al., 1965). These studies have been supported using autoradiography (Swanson and Cowan, 1977).

Anterograde degeneration (Fink-Heimer silver impregnation) demonstrated that regio superior (CA1) projects ipsilaterally through the alveus to the subiculum and presubiculum, thus confirming the previous Golgi studies of the late 1800's and early 1900's (Hjorth-Simonsen, 1973). Swanson and Cowan (1977), using autoradiography, identified significant ipsilateral projections from fields CA1 - CA3 to the subiculum. They also observed a projection from CA3 to the presubiculum and the parasubiculum. Pyramidal cells in field CA1 of the dorsal hippocampus project ipsilaterally to the presubiculum and the parasubiculum, in addition to the subiculum. This doesn't seem to be the case for pyramidal cells in field CA1 of the ventral hippocampus (Swanson and Cowan, 1977).

The HF receives two major sources of afferent fibers. One main source of hippocampal afferent fibers is the MS/vDBB complex. The other source of afferent input, the perforant path, consists of two basic fiber tracts originating in the medial and lateral entorhinal cortex, and innervating the dentate molecular layer and the stratum lacunosum-moleculare of field CA3 (Hjorth-Simonsen, 1972; Hjorth-Simonsen and Jeune, 1972; Steward and Scoville,

1976). The perforant path and a temporo-alvear tract from the entorhinal cortex to the hippocampus proper, via the alveus (Raisman, et al., 1965;), have also been confirmed using autoradiography (Swanson and Cowan, 1977).

Septal-Hippocampal Connections

Degeneration studies provided the initial evidence that a major source of afferent fibers to the HF originates in the MS and the vDBB (Raisman, 1966; Mosko, Lynch and Cotman, 1973). The septal-hippocampal pathway has been extensively studied, both anatomically and physiologically. Recent information regarding this pathway has been obtained through anterograde transport of [^{3}H] amino acids (Swanson and Cowan, 1979; Milner, Loy and Amaral, 1983), retrograde transport of HRP (Monmaur and Thomson, 1983; McKinney, Coyle and Hedreen, 1983; Milner, et al., 1983; Amaral and Kurz, 1985), anterograde transport of HRP using light microscopy (Crutcher, Madison and Davis, 1981) and electron microscopy (Chandler and Crutcher, 1983), electrophysiology (Rawlins, Feldon and Gray, 1979; McNaughton and Miller, 1984), and anterograde transport of *Phaseolus vulgaris* leuco-agglutinin (PHA-L) (Nyakas, et al., 1987).

Injections of [^{3}H] amino acids into the MS and the vDBB resulted in labelled fibers in the dorsal fornix, all CA fields, and the DG (Meibach and Siegel, 1977b; Swanson

and Cowan, 1979). More laterally placed injections resulted in the presence of labelled fibers in the lateral part of the dorsal fornix and the adjacent, medial portion of the fimbria, which terminated in the posterior hippocampus and subicular complex (Meibach and Siegel, 1977b). Septal-hippocampal projections did not originate in any other septal nuclei (Meibach and Siegel, 1977b; Swanson and Cowan, 1979).

Injections of HRP into the hippocampus proper and into the DG resulted in HRP positive cells in the MS/vDBB (Meibach and Siegel, 1977b; McKinney, et al., 1983; Milner, et al., 1983; Monmaur and Thomson, 1983; Amaral and Kurz, 1985) . Results from anatomical tracing using anterograde transport of HRP have indicated that the septal-hippocampal pathway projects to regio inferior (CA2 and CA3) and the dentate area; specifically to the hilus, supragranular and infragranular zones of the ventral DG; and the hilus and infragranular zone of the dorsal DG (Crutcher, et al., 1981). In addition, retrograde tracing with HRP has shown that the more lateral septal-hippocampal neurons project to the posterior and ventral HF (Amaral and Kurz, 1985), thus confirming the results of Meibach and Siegel (1977b). Whether the MS/vDBB projects ipsilaterally (Monmaur and Thomson,1983, and Meibach and Siegel, 1977b) or bilaterally

(Milner, et al.,1983; Amaral and Kurz, 1985) is still unclear.

The combination of electron microscopy with HRP has proven useful for the identification of septal-hippocampal projection terminals. Results from the anterograde tracing with HRP have confirmed the projection from the MS/vDBB to the hilus and the supragranular zone of the DG (Chandler and Crutcher, 1983). Their results did not demonstrate septal-hippocampal projections outside of the dentate area, a fact which conflicts with most research. Fibers containing HRP reaction product projected through the dorsal fornix, fimbria, and alveus and entered the dentate area through fields CA3 and CA4. Within the hilus, terminals were observed in, or near the granule cell layer, primarily forming axodendritic synapses, although axosomatic synapses were also present. Electron micrographs also indicated that the postsynaptic cells were characteristic of both granule and basket cells. Analysis of evoked field potentials in the dentate area, produced by stimulation of the MS and LS, also supports the conclusion that there is a direct pathway from the MS to the hilus and the DG (McNaughton and Miller, 1984).

The most recent study of the septal-hippocampal pathway (Nyakas, et al., 1987) used an anterograde tracing method which employed PHA-L. The vDBB was the only

septal-hippocampal input to the pyramidal and granule cell layers of the dorsal hippocampal formation, while the pyramidal and granule cell layers of the ventral HF received inputs from both the MS and vDBB.

Fibers containing PHA-L could be separated into two distinct types. Thick, coarse fibers (type I) infiltrated the entire stratum oriens, dentate hilus, all regions of regio inferior (CA2 and CA3), and the stratum lacunosum-moleculare of field CA1. Thin, delicate fibers (type II) were most densely concentrated in the subpyramidal zone of stratum pyramidale and stratum lacunosum-moleculare of field CA1; and stratum moleculare and the supragranular zone of stratum granulosum. Iontophoretic injections of PHA-L into various locations of the MS/vDBB provided unequivocal evidence that a MS/vDBB projection to field CA1 does exist. As was indicated with HRP and autoradiography, PHA-L injections which were placed laterally in the MS/vDBB projected to more posterior and ventral portions of the HF.

A reciprocal projection from HF to the septum has also been demonstrated using neuroanatomic and electrophysiologic techniques. Early degeneration studies (Raisman, 1966; Raisman, Cowan and Powell, 1966) indicated that the anterior portion of field CA1 projects ipsilaterally through the fimbria and postcommissural

fornix, through the septofimbrial and triangular nuclei, to the MS and vDBB. This projection has not been confirmed in studies which employed [^{3}H] amino acids, HRP, or PHA-L techniques (Swanson and Cowan, 1977, 1979; Meibach and Siegel, 1977a; Gerfen and Sawchenko; 1984). The posterior CA1, although it followed the same pathway, terminated more laterally in the ventromedial quadrant of the LS. Fields CA3 and CA4 projected through the fimbria to and possibly through the lateral parts of the septofimbrial nucleus, to the nucleus of the hDBB, and lateral parts of the LS.

Swanson and Cowan (1977, 1979) used [^{3}H] amino acid autoradiography to identify hippocampal-septal pathways. Their results indicated the presence of a projection from fields CA1 - CA3, through the lateral parts of the posterior septal nuclei, to the LS. More specifically, there was a high degree of topographic organization, with projections from fields CA2 and CA3 of the dorsal hippocampus projecting bilaterally through the medial fimbria to more dorsal parts of the LS. Fields CA2 and CA3 of the ventral hippocampus projected through the lateral edge of the fimbria to more ventral locations within the LS. The same organization was found for field CA1, with the exception that it only projected to the ipsilateral LS.

Using combined anterograde axonal transport of [^{3}H] amino acids, and retrograde axonal transport of HRP Meibach

and Siegel (1977a) also found that the topographic organization of hippocampal projections to the LS was determined by the point of origin along the longitudinal axis of the HF. The results of Meibach and Siegel (1977a) also support the conclusion that CA1 projects ipsilaterally and CA2/CA3 project bilaterally to the LS. They demonstrated that the hippocampal-septal pathway projects through the dorsal fornix, in addition to the fimbria. The existence of a hippocampal-septal projection was recently confirmed using PHA-L (Gerfen and Sawchenko, 1984).

The analysis of single unit and field potential responses in all areas of the LS, evoked by stimulation of various aspects of the fimbria/fornix, confirmed the topographic organization within the fimbria/fornix (Joels and Urban, 1985). A similar study, which recorded population spikes in the HF elicited by stimulation of medial-lateral positions within the fimbria, also supported the topographic organization of the dorsal-ventral hippocampal output within the fimbria (Andersen, Bland and Dudar, 1973).

Pyramidal cells have been identified; using retrograde transport of HRP alone (Alonso and Kohler, 1982; Chronister and DeFrance, 1979), or in combination with a fluorescent dye (Swanson, Sawchenko and Cowan, 1980); and with Fast Blue in combination with Lucifer Yellow (Schwerdtfeger and

Buhl, 1986); as a source of hippocampal efferents to the LS. Nonpyramidal cells such as polymorphic cells in stratum oriens and stratum radiatum of fields CA1 and CA3, and horizontal-fusiform cells in stratum oriens, primarily in field CA3, have been shown to contribute to the hippocampal-septal pathway (Chronister and DeFrance, 1979). Nonpyramidal cells of the hilus, in addition to those from CA1 and CA3, project to the LS (Schwerdtfeger and Buhl, 1986). The results of Alonso and Kohler (1982) indicated that only pyramidal cells project to the LS; however they also reported the presence of pyramidal and nonpyramidal projections to the MS. The reported projection to the MS is questionable due to their large injections, which they stated could be observed in adjacent nuclei. Staining of nonpyramidal cells with MS injections may have been the result of a medial-lateral topographic organization of nonpyramidal-pyramidal projections to the LS.

Dorsomedial-Posterior Nuclei: Anatomic Connections with the Septum and the Hippocampal Formation

The septal nuclei and the HF have direct interconnections with many diencephalic nuclei. For the purpose of this thesis, the most important of these nuclei are the dorsomedial (DMH) and posterior (PH) nuclei of the hypothalamus. Also, the connections of the lateral

hypothalamic area (LHA) with these nuclei, with the septal nuclei, and with the HF will be reported.

The results from studies employing retrograde transport of HRP (Luiten and Room, 1980; Kita and Oomura, 1982a) and PHA-L (Ter Horst and Luiten, 1986) have shown that the PH projects through the median forebrain bundle (MFB) to the DMH. The dorsomedial-posterior nuclei of the hypothalamus (DM-PH) project, also through the MFB, to the LHA (Luiten and Room, 1980; Kita and Oomura, 1982b; Ter Horst and Luiten, 1986). The LHA reciprocally connects to the DM-PH (Saper, Swanson and Cowan, 1979; Luiten and Room, 1980; Kita and Oomura, 1982a).

The projections of the DMH to the septum and HF were demonstrated using PHA-L in combination with anterograde transport of [^{3}H] leucine (Ter Horst and Luiten, 1986). Their results indicated that the DMH projects to the dorsal and intermediate divisions of the LS. They also found bilateral projections to the stratum pyramidale of fields CA3 and CA4 and also to the stratum granulosum of the DG. Studies using retrograde transport of HRP have also demonstrated a projection from the DM-PH to the HF; however, the distribution of reaction product was sparce when compared to the septal-hippocampal projection (Segal and Landis, 1974; Wyss, Swanson and Cowan, 1979; Riley and Moore, 1981).

The LHA also projects to the septum and the HF. Anterograde transport of [^{3}H] leucine resulted in the identification of cells in the MS and the vDBB (Saper, Swanson and Cowan, 1979; Swanson and Cowan, 1979). Fibers projecting from the LHA to the HF were identified using HRP (Segal and Landis, 1974; Wyss, Swanson and Cowan, 1979; Riley and Moore, 1981).

Descending pathways from the septum to the DM-PH and the LHA have been identified using HRP and [^{3}H] amino acids. No such pathways originating in the HF have been identified (Swanson and Cowan, 1977; Meibach and Siegel; 1977a; Kita and Oomura, 1982a,b). The LS and the MS have been shown to project through the MFB, to the LHA (Meibach and Siegel, 1977b; Kita and Oomura, 1982b). In addition, a projection from the LS to the DMH has been identified (Swanson and Cowan, 1979; Kita and Oomura, 1982a). Sparce labelling has also been demonstrated in the DBB after iontophoretic injections of HRP into the DMH, however, the authors did not specify whether this was in the vertical, or horizontal limbs (Kita and Oomura, 1982a).

PHYSIOLOGY AND PHARMACOLOGY

Hippocampal Theta

The physiological study of hippocampal slow wave theta has been in progress now for over 30 years. Hippocampal theta is a periodic, approximately sinusoidal EEG waveform with a frequency of about 4-12 Hz. It is one of three EEG patterns recorded in the HF in freely moving rats, the others being large amplitude irregular activity (LIA) and fast waves (Leung, Lopes da Silva and Wadman, 1982). The first major study to systematically document slow wave theta, also referred to as rhythmical slow activity (RSA), was carried out in 1954 by Green and Arduini. They observed theta activity from macroelectrodes implanted in the hippocampi of rabbits, cats, and monkeys. Liberson and Cadilhac, also in 1954, observed theta in guinea pigs.

It has been postulated that there are two types of hippocampal theta activity (Kramis, Vanderwolf and Bland, 1975). Pharmacologic and behavioral manipulations have indicated that there are two types of theta in the rat, rabbit, and guinea pig (see review by Bland, 1986). Briefly, type 1 theta is produced during voluntary motor movements (eg. walking, rearing, or head movements), while type 2 theta is produced in response to sensory stimulation, during behavioral immobility. The

administration of atropine sulfate blocks type 2 theta, but not type 1 theta, and systemic injections of urethane (ethyl carbamate), ethyl ether, and pentobarbital block type 1 theta. Type 2 theta is resistant to some anaesthetics, such as ethyl ether and urethane. The frequency range of type 1 theta is generally 6.5 - 12 Hz and type 2 theta during immobility is 4 - 9 Hz. The range of slow wave theta observed during urethane anaesthesia has been demonstrated to be 2 - 8 Hz.

The generators of hippocampal theta are located in the pyramidal cell layer of field CA1 (Petsche and Stumpf, 1960) and the stratum moleculare of the DG (Winson, 1974; Bland, Andersen and Ganes, 1975). Both types of theta are observed in each generator. When recording hippocampal theta, and when comparing theta to behavior, it is important that the electrode placement provide a good quality recording with maximum theta amplitude (Vanderwolf, Bland and Whishaw, 1973; Robinson, 1980). In addition to theta which occurs naturally, or in response to pharmacologic manipulations, hippocampal theta has been produced with stimulation of various hypothalamic and brainstem nuclei: the ascending synchronizing system (see review by Vertes, 1982). The concept of ascending synchronizing, and desynchronizing systems, as postulated by Vertes (1982), maintains that there is only one type of

theta, and that pharmacologic manipulations only affect certain aspects of the system.

The concept of two types of theta is refuted in a recent study by Brazhnik and Vinogradova (1986). These authors proposed that the frequency of theta is a direct function of the burst frequency of rhythmic bursting pacemaker cells (type I) in the MS/vDBB complex. They suggested that this population of cells is only 2 - 4 % of MS/vDBB cells. In addition, they suggested that increased activation from the brainstem is responsible for shifts in the burst frequency of these cells, which were unaffected by systemic injections of cholinergic antagonists. The remaining septal cells were referred to as being secondarily (type II) and tertiarily (type III) involved in the production of theta. Brazhnik and Vinogradova (1986) proposed that recruitment of these cells by increased afferent activation from the reticular formation results in the occurrence of theta.

Regardless of whether there is one type of theta or two, the importance of the brainstem in the generation of theta cannot be denied. In brief, the ascending synchronizing system begins in some of the brainstem nuclei, ascends through several fiber tracts to the septum, and finally to the HF. Stimulation of nuclei and fiber tracts along this system result in the production of

hippocampal theta (Vertes, 1982). In rabbits, rats, and cats the nucleus pontis oralis was found to be the most effective synchronizing (theta producing) site using high frequency stimulation (Macadar, Chalupa and Lindsley, 1974; Robinson and Vanderwolf, 1978; Vertes, 1980).

Studies have shown that the ascending pathway involved in theta generation travels through both the dorsal longitudinal fasciculus (Anchel and Lindsley, 1972; Destrade, 1982) and the medial longitudinal fasciculus (Vertes, 1981), but Vertes (1982) argued that the primary pathway is the medial longitudinal fasciculus. The other pathways include the MFB (Vertes, 1981; Destrade 1982) and the central tegmental tract (Macadar, et al., 1974; Robinson and Vanderwolf, 1978; Anchel and Lindsley, 1972; Vertes, 1981). These tracts are consistent across the various species used in hippocampal research (cats, rats, mice and rabbits; Vertes, 1982).

Vertes (1982) hypothesized that the ascending synchronizing system must be polysynaptic due to the lack of direct projections from the pontine reticular formation to the MS/vDBB. However, direct projections to the MS/vDBB from the DM-PH and the LHA have been demonstrated with anatomical tracing techniques (see Anatomy chapter). Bland and Vanderwolf (1972), using freely moving rats, clearly demonstrated the significance of the DM-PH in the ascending

synchronizing system. Stimulation of the DM-PH resulted in the production of theta and when the stimulation voltage was increased in a linear fashion, theta frequency increased linearly. This work was recently verified, and extended to HF theta cells in urethane anaesthetized rats (Colom, Ford and Bland, 1987). Theta cells are those which discharge rhythmically, in phase with slow wave theta, and discharge less frequently and arrhythmically during LIA (see review by Bland, 1986). Colom, et al., (1987) demonstrated that an increase in stimulation current applied to the DM-PH resulted in an increase in theta frequency, and an increase in theta cell discharge rate.

Several factors indicate that the vDBB and the MS are the critical components in the generation of the synchronous EEG theta rhythm. Production of theta through stimulation of the MS/vDBB, unlike the reticular and diencephalic sites, is best produced by a pulsed stimulation which corresponds to the frequency of theta (Kramis and Routtenberg, 1977; Kramis and Vanderwolf, 1980). Stimulation of the MS/vDBB at 100 - 400 Hz did not result in hippocampal slow wave theta as it did in the reticular formation, or hypothalamus (Kramis and Vanderwolf, 1980). The opposite effect of pulsed stimulation is obtained with lesions. Lesions of the MS/vDBB totally eliminate theta activity in the HF

(Andersen, Bland, Myhrer and Schwartzkroin, 1979; Petsche and Stumpf, 1960; Rawlins, et al., 1979; Sainsbury and Bland, 1981). Lesions of the septal-hippocampal projection, the fimbria/fornix, also disrupt slow wave theta (Rawlins, et al., 1979; Andersen, et al., 1979).

Septal-Hippocampal Connections

The importance of the septal-hippocampal projection in the generation of hippocampal theta has been demonstrated. In addition to the anatomical importance, the septal-hippocampal pathway is the major source of acetylcholine (ACh) to the HF. In a review by Bland (1986), the cholinergic nature of the septal-hippocampal pathway is fully summarized. Research has solidly demonstrated in rats, rabbits, and cats using choline acetyltransferase (ChAT; ACh synthesizing enzyme), and acetylcholinesterase (AChE; ACh catabolic enzyme) immunohistochemistry, and many other techniques that the septal-hippocampal pathway is cholinergic. The original AChE immunohistochemistry, which was combined with axonal degeneration (Lewis and Shute, 1967; Mellgren and Srebro, 1973; Mosko, et al., 1973), has been supported by studies combining AChE immunohistochemistry with [^{3}H] amino acid autoradiography (Lynch, Rose and Gall, 1978), and with the use of HRP (Baisden, Woodruff and Hoover, 1984). These

studies have shown that the distribution of AChE corresponds to the anatomical distribution of MS/vDBB afferent fibers to the HF.

The use of polyclonal (Kimura, McGeer, Peng and McGeer, 1981) and monoclonal (Mesulam, Mufson, Wainer and Levey, 1983; McKinney, et al., 1983; Houser, Crawford, Barber, Salvaterra and Vaughn, 1983; Wainer, Levey, Rye, Mesulam and Mufson, 1985) antibodies to ChAT have confirmed the results of AChE immunohistochemistry. In addition to identifying the axon terminals, the use of AChE and ChAT immunohistochemistry alone, or in combination with HRP revealed that the somata of the cholinergic projection were located within the MS and the vDBB. No AChE or ChAT positive cell bodies were, located in the LS.

HRP-AChE and HRP-ChAT combined studies have also revealed that the septal-hippocampal projection contains a noncholinergic component. A recent study of the cholinergic and noncholinergic septal-hippocampal projection which employed a double label, HRP-AChE technique (Baisden, et al. 1984) determined that 68 % of the somata were found in the vDBB while 31 % were found in the MS. Of those cells labelled in the vDBB, 46 % also stained for AChE. Similarly, in the MS, 41 % of the HRP labelled neurons stained positively for AChE. These results were confirmed in two studies employing

immunocytochemical localization of ChAT combined with HRP (Wainer, et al., 1985; Amaral and Kurz, 1985). The results of Wainer, et al. (1985) indicated that 30 - 35 % of the HRP labelled septal-hippocampal neurons located in the MS were double labelled and 45 - 55 % of the HRP labelled cells in the vDBB, were also ChAT labelled.

The results of the combined HRP-AChE and HRP-ChAT studies have also revealed similar information regarding the topographic organization and the morphology of the cholinergic septal-hippocampal cells. Using the terminology of Amaral and Kurz (1985), there is a midline cholinergic cell group, a medial noncholinergic cell group, as well as dorsal, intermediate, and ventral cholinergic cell groups. The intermediate and ventral cholinergic groups extend laterally along the dorsal and ventral boundaries of the vDBB. Cholinergic cells in the dorsal group were small while those in the ventral and intermediate groups were larger, elliptical, and multipolar (Amaral And Kurz, 1985). The ChAT labelled cells of the intermediate group were large, round, and multipolar (Amaral and Kurz, 1985).

A more recent study which combined the use of PHA-L and an AChE pharmaco-histochemical technique, also found the same distribution of potentially cholinergic septal-hippocampal cells (Nyakas, et al., 1987). Both AChE

labelled and unlabelled cells in the MS/vDBB projected to the HF as long as the injection sites were within the MS/vDBB complex. Noncholinergic cells were often intermingled with AChE and ChAT labelled cells (Nyakas, et al., 1987; Amaral and Kurz, 1985; Mesulam, et al., 1983). Nyakas, et al. (1987) argued that, because thin type II fibers originate in areas of the MS/vDBB which are rich in AChE and ChAT staining, and because they innervate areas of the HF which heavily stain for ChAT, the type II fibers are cholinergic. They also suggested that the thick type I fibers are probably both cholinergic and noncholinergic.

Immunohistochemical localization of glutamic acid decarboxylase (GAD), the enzyme which catalyzes the synthesis of gamma-aminobutyric acid (GABA) from glutamic acid, in the MS/vDBB lead to the suggestion that the noncholinergic portion of the septal-hippocampal pathway is GABAergic (Kohler and Chan-Palay, 1983; Panula, Revulta, Cheney, Wu and Costa, 1984). GAD positive cells were also located in the LS. Combining GAD immunohistochemistry with HRP staining indicated that GAD containing cells in the MS/vDBB did indeed project to the HF, while the GAD containing cells in the LS did not (Kohler, Chan-Palay and Wu, 1984). It appeared that the GAD containing cells were morphologically heterogeneous (Kohler, et al., 1984), and located in areas which contained cholinergic cells (Panula,

et al., 1984). AChE immunohistochemistry did not label GAD positive cells (Kohler, et al., 1984).

A series of studies on MS/vDBB neurons indicated that septal-hippocampal neurons were excited by iontophoretic applications of glutamic acid and that approximately 75 % also increased their discharge rates with the application of acetylcholine (Dutar, Lamour and Jobert, 1983; Lamour, Dutar, and Jobert, 1984; Dutar, Lamour, Rascol and Jobert, 1986). Acetylcholine induced inhibition was rare. Carbachol produced a similar reaction; however, the percentage of cells with decreased spontaneous activity increased to approximately 10 %. Muscarinic agonists were more effective than nicotinic agonists in eliciting an excitatory response. Also, atropine sulfate antagonized the ACh and carbachol induced excitation. Thus, cholinergic and noncholinergic septal-hippocampal neurons were also shown to be cholinoceptive.

An early study on the reciprocal connections of the septal nuclei with the HF, using evoked potentials, suggested that the LS received an excitatory connection from the HF (McLennan and Miller, 1974a). It was proposed that the LS sent an inhibitory projection to the MS via an interneuron, which also provided an inhibitory recurrent collateral to the lateral septal cells receiving the hippocampal input. These pathways were proposed because

fimbrial stimulation orthodromically activated lateral septal cells, followed by an extended period of inhibition. Antidromic activation of medial septal cells was also followed by a period of inhibition. These results have been supported by the recent studies of Lamour, Dutar and Jobert (Lamour, et al., 1984; Dutar, et al., 1986). McLennan and Miller (1974a) also suggested the presence of a direct inhibitory projection to the MS, although the short latency and the high frequency following suggest that this pathway was antidromically activated by the fimbrial stimulation (Lamour, Dutar and Jobert, 1984; Dutar, Lamour and Jobert, 1985; Dutar, Lamour, Rascol and Jobert, 1986).

Septal afferents from the HF have been identified pharmacologically. Although the literature is not extensive, there is evidence for a GABAergic projection to the LS (Shinoda, Tohyama and Shiotani, 1987). The combination of retrograde transport of biotin-wheat germ agglutinin (B-WGA), injected into the LS, with GABA immunohistochemistry revealed a GABAergic projection through the dorsal fornix from fields CA1 (ipsilaterally) and CA2 (bilaterally). Using microiontophoresis, Segal (1974) found that GABA was a potent inhibitor of the spontaneous activity of lateral septal neuons suggesting a GABAergic input, however, the intrinsic source of GABA

might also be the postulated recurrent collaterals (discussed above).

Results from unilateral kainic acid lesions of dorsal field CA3, and fimbria/fornix transection, which interrupted hippocampal-septal projections, resulted in the reduction of high affinity uptake of [^{3}H] glutamate in the LS (Fonnum and Walaas, 1978; Storm-Mathisen and Woxen Opsahl, 1978; Zaczek, Hedreen and Coyle, 1979). Recently, injections of ibotenic acid into the MS resulted in cell loss in the dorsal LS rather than in the MS (Stewart and Vanderwolf, 1987). It is presumed that ibotenic acid destroys cells which have a glutamatergic input (Cooper, Bloom and Roth, 1986). These results have been cautiously interpreted to indicate the presence of a glutamatergic pathway from the HF to the LS.

Several studies have supported the conclusion that the projection from the LS to the MS and the vDBB is GABAergic. Cell bodies containing GAD are located within the LS (Panula, et al., 1984; Kohler, et al., 1984). Stimulation of the LS *in vitro* produced a Cl- dependent inhibitory postsynaptic potential (IPSP) which was blocked by picrotoxin, a potent GABA antagonist. Also, local application of GABA resulted in a marked Cl- dependent increase in conductance (Segal, 1986). Hyperpolarizing potentials following fimbrial stimulation have been

observed in intracellularly recorded septal-hippocampal and unidentified neurons located in the MS/vDBB (Dutar, Lamour and Jobert, 1985). It was suggested that the hyperpolarizing potentials represented IPSPs since they could be observed in the absence of a preceding spike, reversed polarity in a chloride dependent fashion, and were associated with a decrease in spontaneous discharges.

Iontophoretic applications of GABA have also been shown *in vivo* to result in depression of spontaneous activity of identified septal-hippocampal neurons (Lamour, Dutar and Jobert, 1984), and unidentified MS/vDBB neurons (Segal, 1974; Lamour, Dutar and Jobert, 1984). Iontophoretic injections of GABA and glycine showed that the inhibitory effect of GABA required significantly smaller ejection currents (McLennan and Miller, 1974b). Inhibition by GABA was antagonized by the application of bicuculline (a GABA antagonist) and not strychnine (a glycine antagonist), while the weaker inhibition induced by glycine could be inhibited by strychnine and not bicuculline.

Unit Activity and Hippocampal Theta

Rhythmically discharging units related to the hippocampal theta rhythm have been observed in many structures with the greatest proportion located in the

MS/vDBB (Garcia-Austt, 1984). Ranck (1973) described theta cells in the HF of freely moving rats as cells which doubled their discharge rate during type 1 theta behaviors (eg. walking, rearing, etc.). Since these observations, theta cells have also been recorded during type 2 theta (Sinclair, Seto and Bland, 1982). Later, Bland, Seto and Rowntree (1983) modified Ranck's (1973) definition of a theta cell such that a theta cell: a) always fires in a simple manner, b) is either silent or discharging irregularly during large amplitude irregular activity, c) consistently discharges in a rhythmic manner, locked to the negative phase of the local slow wave theta, d) changes its discharge rate relative to the frequency of the slow wave theta. The morphology of theta cells is still questionable, with research suggesting that they are pyramidal cells, interneurons, and/or granule cells (Bland 1986).

Recently the discovery of a group of hippocampal neurons in urethane anaesthetized rats, whose discharge rates were inversely related to the slow wave theta frequency has resulted in a further modification of the definition of theta cells (Colom, et al., 1987). Theta cells have been divided into theta-on and theta-off cells. Theta-on cells were defined as cells which either: a) increase their discharge rate significantly during the

theta state compared to the LIA state, b) discharge rhythmically, increasing and decreasing their discharge rate with increases and decreases in theta frequency, respectively, (Colom and Bland, 1987). Those cells which discharged arrhythmically, and increased their discharge rate significantly during the theta state compared to the LIA state were referred to as tonic theta-on cells. Theta-on cells which discharged rhythmically and whose discharge rates were linearly correlated to the frequency of theta were termed phasic theta-on cells.

Theta-off cells were defined as cells that either: a) discharge irregularly during the LIA state and do not discharge during slow wave theta, or b) discharge arrhythmically during the LIA state and do not discharge during higher frequency theta, but begin to discharge rhythmically, increasing their discharge rate as theta frequency decreases (Colom and Bland, 1987). These two subtypes of theta-off cell were termed tonic and phasic, respectively.

As was reported previously, stimulation of the DM-PH with a variety of current intensities resulted in positive linear relationships between stimulation intensity, theta frequency, and unit discharge rate for theta-on cells (Colom, et al., 1987). Theta cells which increased their discharge rates in response to an increased stimulation

current no longer did so after theta activity was blocked with 50mg/kg I.P. atropine sulfate (Colom, et at., 1987). Eserine and carbachol induced theta were abolished with direct microinfusions of atropine sulfate into either stratum oriens of the hippocampus proper or stratum moleculare of the DG, which indicated that the site of atropine blockade was within the HF (Rowntree and Bland 1986). However, evidence suggests that there are also cholinoceptive neurons in the MS/vDBB (Dutar, Lamour and Jobert, 1983; Lamour, Dutar and Jobert, 1984; Dutar, Lamour, Roscol and Jobert, 1986; Segal, 1986).

Lesions of the MS eliminated rhythmicity observed in hippocampal theta cells, suggesting that an intact MS is required for hippocampal theta cell rhythmicity (Bland and Bland, 1986). Support for the importance of septal unit activity in the generation of slow wave theta was provided when Petsche, Stumpf and colleagues found, in curarized rabbits, a group of septal cells termed type B cells, which discharged in rhythmic bursts, phase locked to hippocampal theta (Petsche, Stumpf and Gogolak, 1962; Stumpf, Petsche and Gogolak, 1962). To determine the phase relationship they used a measure of average burst latency, which was calculated from the positive peak of the theta cycle to the mode of the probability distribution of spike discharges. They found that this value remained constant within a cell

but varied from cell to cell (Petsche, Gogolak and van Zweiten, 1965).

Type B cells were only located within the medial division of the septum and when theta was not present in the HF, B units were said to discharge irregularly. Type B units discharged between 0 and 50 spikes/s depending on the EEG state. In addition to increasing the burst frequency with corresponding increases in theta frequency, type B cells "generally" increased the number of spikes/burst with increased theta frequency (Petsche, et al., 1962). They also found a group of nonrhythmic units in the septum, type A units, which discharged randomly. Type A units were located throughout the septum.

The initial investigations determined that graded administration of urethane resulted in a gradual decrease in the frequency and amplitude of theta until irregular activity replaced theta in the hippocampal EEG (Stumpf, et al., 1962). Simultaneously, type B units decreased their burst rate and the number of spikes/burst. These authors also found that scopolamine, a muscarinic antagonist, not only blocked hippocampal theta, but that it also blocked type B unit rhythmicity.

High frequency stimulation of the reticular formation resulted in an increase in theta frequency and a corresponding increase in type B unit bursts. The B units

not only increased their discharge rates, they also remained in phase with the higher frequency theta rhythm (Petsche, et al., 1962). As for type A units, some were influenced by reticular stimulation and some were not (Petsche, et al., 1962). Further work divided type A MS/vDBB neurons into passive burst and facultative burst cells (Petsche, et al., 1965). Passive burst cells had a constant average burst latency, but the dispersion of spikes varied. Facultative burst cells burst irregularly, without a phase relation to theta. This study also indicated that the response of MS/vDBB cells to reticular stimulation varied. The ratio of cells which were excited to those that were inhibited was 2:1. The number of spikes/burst increased in 50 % of the cells and decreased in 50 % (no statistical analysis was performed).

Several lines of evidence suggested to Petsche, Stumpf, and colleagues that type B units were the pacemakers of the theta rhythm. The first was that during the post ictal period following a seizure induced during slow wave theta, B units fired rhythmically in the absence of theta (Petsche, et al., 1962). Secondly, B units retained their rhythmical bursting pattern when theta activity was abolished by the administration of urethane (Stumpf, et al., 1962). A third argument was based on the

fact that small lesions of the MS/vDBB abolished theta bilaterally (Petsche, et al., 1965).

Gogolak, Stumpf, Petsche and Sterc (1968) suggested that the pattern of cell discharges of type B neurons accounted for the shape of the theta wave. Using spike averaging and sampling which was triggered by the first spike of a burst, these authors suggested that the type B units were directly responsible for the shape of the theta wave. To reach this conclusion they averaged the amplitude of the theta wave, which was normalized to 100 % and compared it to the average spike histogram.

Additional work has also demonstrated rhythmical units in the MS/vDBB in acute (Macadar, Roig, Monti and Budelli, 1970; Gaztelu and Buno, 1982; Alonso, Gaztelu, Buno and Garcia-Austt, 1987) and chronic rats (Morales, Roig, Monti, Macadar and Budelli, 1971), acute rabbits (Apostol and Creutzfeldt, 1974), and acute cats (Wilson, Motter and Lindsley, 1976). Rhythmic septal unit activity has also been described during a period in which "it was not always possible to describe a theta rhythm" (Macadar, et al., 1970). Macadar and colleagues (Macadar, et al., 1970; Morales, et al., 1971), in support of Stumpf, et al. (1962), observed rhythmic MS/vDBB units in the absence of theta, after the administration of LSD-25.

Apostol and Cruetzfeldt (1974) identified three types of units (termed A, B and C) in the septal nuclei. Only two of these were observed in the MS/vDBB. Their type C (61 %) and type B (39 %) units correspond to the type B and type A units of Petsche, et al. (1962), respectively. Rhythmic bursting septal cells were reported in the LS, although the percentage of the total number of cells in this region was small (11 %).

Gaztelu and Buno (1982) found three basic types of neurons in the MS/vDBB, of which 74 % were type 1, rhythmic, and burst in phase with theta; 19 % were type 2, arrhythmic, but still temporarily related to hippocampal theta (i.e. spikes had a high probability of occurring on a specific phase of the theta cycle); and 7 % were type 3, arrhythmic, and showed no relation to theta activity. They also specified three subtypes of type 1 neurons based on their burst and intraburst characteristics, autocorrelations, and cross correlations. Stimulation of the mesencephalic reticular formation resulted in an increase in burst length and intraburst rates of type 1 cells, and increased, or decreased firing rates of type 2 cells. Type 3 units did not respond to stimulation. Type 1 cells were the only cells not recorded in the LS (Garcia-Austt, 1984). These classifications were made in

curarized rats under the influence of physostigmine, a cholinergic agonist which blocks acetylcholinesterase.

Recently this work was repeated in urethane anaesthetized rats (Alonso, et al., 1987). In addition to comparing septal unit discharge patterns to the theta rhythm, they also cross correlated septal and hippocampal unit discharges. As could be expected, a consistent phase relationship was demonstrated between septal-hippocampal type 1 neuron pairs. With mixed pairs, that is a type 1 hippocampal neuron and a type 2 septal neuron, the cross correlation was periodic, indicating that the type 2 neuron discharged at a preferred phase of the type 1 neuron.

Rhythmic bursting, nonrhythmic bursting, and nonbursting cells were recorded in the septal nuclei of curarized cats (Wilson, et al., 1976). Generally, rhythmic bursting cells did not discharge rhythmically during LIA; however, brief periods of rhythmic bursts were observed. Rhythmic bursting cells were located throughout the MS/vDBB complex, with the occasional cell located in the LS. The discharge frequency of these cells ranged from 4 - 63 spikes/s. Nonrhythmic cells were located throughout the MS/vDBB and the LS.

Stimulation of the DM-PH and LHA resulted in altered discharge rates for both rhythmic and nonrhythmic neurons of the MS/vDBB (Wilson, et al., 1976). Stimulation of the

DM-PH (100 Hz) during LIA resulted in hippocampal theta and rhythmic bursts at a frequency of 4.8 Hz. Seventy-eight percent of rhythmic bursting cells responded with rhythmic bursts, synchronized to the same phase of the theta rhythm as they were during spontaneous theta. They also noted an increase in discharge rate and the number of spikes/burst in these cells. Half of the remaining cells were unaffected, and half were partially inhibited. Stimulation of the LHA did not produce theta activity, but it did have an effect on rhythmic bursting cells. Using an arbitrary criterion of a 30 % change in discharge rate, 59 % increased, 33 % decreased, and 18 % were not affected. Cells that were inhibited with DM-PH stimulation increased their discharge rate to LHA stimulation. Of the nonrhythmic neurons, 80 % responded to stimulation with increased or decreased discharge rates. No differences were reported between DM-PH and LHA stimulation for nonrhythmic neurons.

Percentages of rhythmic busting neurons have been reported as high as 85 %; however, most of these studies were interested in the percentage of rhythmic and arrhythmic neurons during theta. These studies did not report isolating cells during LIA. Conversely, very low proportions of rhythmic bursting cells have been reported in the LS. In contrast to these data, Vinogradova,

Brazhnik, Karanov and Zhadina (1980) reported that 29 % and 27 % of MS and LS neurons burst rhythmically, in phase with theta.

The effects of deafferentiation on the rhythmic bursting activity of MS and LS neurons was examined in acute, curarized rabbits (Vinogradova, et al., 1980). The proportion of rhythmic bursting (type I) neurons in the MS and LS after cutting of the hippocampal connections were 17 % and 42 %, respectively. After septal undercutting, which disconnected the brainstem and hypothalamic afferents, the proportions of rhythmic bursting neurons were preserved (25 %), however, a 2-fold increase in the overall discharge rate of MS neurons was observed. Although they attributed these effects to deafferentation, they neglected the fact that they also cut efferent pathways in both deafferentation groups. This would result in major complications with injured and degenerating septal neurons.

Deafferentation was also combined with systemic administration of pentobarbital and anticholinergic drugs (Brazhnik and Vinogradova, 1986). The fact that pentobarbital reduced the discharge rate of rhythmic bursting cells (primarily by decreasing the burst rate and not the intraburst discharge rate) to a rate which was equivalent to the undercutting of the septum, and the fact

that atropine sulfate and scopolamine did not affect the rhythmic bursting activity of the rhythmic bursting pacemaker cells, lead to their unitary hypothesis of theta. Cells which were secondarily (nonrhythmic bursting; Wilson, et al., 1979) and tertiarily (irregular; Wilson, et al., 1979) related to the phase of the theta rhythm were often affected by the anticholinergic manipulation (Brazhnik and Vinogradova, 1986). The authors proposed that the number of secondary and tertiary cells which were discharging rhythmically would determine whether or not theta was present in the hippocampal EEG. According to Brazhnik and Vinogradova (1986), low frequency theta is abolished by atropine because the proportion of secondary and tertiary cells which are rhythmic is reduced. High frequency theta (type 1 theta) is not abolished because movement, reticular stimulation, or strong sensory stimuli result in an increase in the level of ascending activation, and recruitment of secondary and tertiary rhythmic cells. Once the threshold for theta to occur is reached (supposedly determined by the percentage of cells which are phasically related to theta at that instant), the noncholinergic, rhythmic bursting pacemaker cells pace the theta rhythm at their current burst rate, which is in the high frequency (type I) range.

Although the unitary hypothesis of theta may indeed be accurate, there are several inconsistencies between these data, which have been used to support the hypothesis, and previously reported data. For example, Vinogradova, Brazhnik, and associates are the only researchers to report rhythmic LS cells in proportions greater than 10 %. They also report a very low percentage of rhythmic neurons in the MS/vDBB. In fact they never report more than 30 %, which they claim is the critical percentage for theta to occur (Brazhnik and Vinogradova, 1986). Conceptual problems with this approach result from the low percentage of neurons they claim are the rhythmic bursting pacemaker cells (2 - 4 %). This problem arises partly because of their failure to clearly define the differences between rhythmic bursting, secondary, and tertiary cell types. The studies they refer to define them as rhythmic bursting, nonrhythmic bursting and irregular discharging cells (Wilson, et al., 1979); or as active bursting, passive bursting, and facultative bursting cells (Petsche, et al., 1965). These cell types seem to correspond to those of Gaztelu and Buno (1982), however, it is unclear whether or not the secondary and tertiary cells can burst rhythmically.

Through the use of fimbrial stimulation in urethane anaesthetized rats, MS/vDBB neurons projecting to the HF

were differentiated from those that either projected elsewhere, or were interneurons (Dutar, Lamour and Jobert, 1983; Lamour, Dutar, and Jobert, 1984; Dutar, Lamour, Rascol and Jobert, 1986). Rhythmic bursting neurons and nonrhythmic bursting neurons were reported for both septal-hippocampal and unidentified neurons. Fifty percent of the cells recorded in the MS/vDBB were septal-hippocampal neurons (Lamour, et al., 1984). Forty five percent of the septal-hippocampal neurons discharged in rhythmic bursts. In comparison, only 30 % of the unidentified cells discharged in rhythmic bursts. The mean discharge rate was also greater for the septal-hippocampal rhythmic bursting neurons than for the unidentified rhythmic bursting cells.

The latency of antidromic activation also varied within septal-hippocampal neurons (Lamour, et al., 1984; Dutar, et al., 1986). Rhythmic bursting neurons had a latency of less than 4 ms (group 1; 41.2 %). Of these neurons, only 16 % were observed to switch from a nonrhythmic to a rhythmic bursting pattern of discharges. Two groups of nonrhythmic neurons were identified; those that had latencies less than 4 ms (group 2; 49.5 %) and those with latencies greater than 4 ms (group 3; 7 %). Finally, a small percentage of rhythmically bursting

septal-hippocampal neurons with latencies greater than 4 ms were observed (group 4; 2.2 %).

The effects of iontophoretic injections of various neurotransmitter and putative neurotransmitter substances were described previously. However, there were different effects between the septal-hippocampal and the unidentified MS/vDBB neurons (Lamour, et al., 1984; Dutar, et al., 1986). Iontophoresis of ACh and carbachol increased spontaneous activity of rhythmic bursting septal-hippocampal neurons more frequently than it did for the nonrhythmic septal-hippocampal neurons (Lamour, et al., 1984). In addition, iontophoresis of ACh and carbachol increased spontaneous activity less frequently in unidentified MS/vDBB neurons, than it did for septal-hippocampal neurons. Within the group of unidentified neurons, ACh increased the spontaneous discharge rate of rhythmic bursting neurons more frequently than it did in nonrhythmic neurons (Lamour, et al., 1984).

Finally, in no instances did antidromic activation produced by stimulation in the MFB and the fimbria activate the same neuron (Dutar, et al., 1986). Only 4 of 13 neurons antidromically activated by stimulation of the MFB were rhythmic bursting neurons. MFB activated MS/vDBB neurons were excited by glutamate in 9 of 11 cases, while

ACh and carbachol excited less than half (Dutar, et al., 1986).

Research on MS/vDBB neurons has focused on the nature of the relationship between cell discharge patterns and hippocampal theta rhythm. These studies have basically isolated MS/vDBB units during the slow wave theta state and thus have primarily resulted in information regarding the phasic nature of septal cell discharges during slow wave theta. However, very little else is known regarding the behavior of MS/vDBB cells in relation to the different hippocampal EEG states. Brief accounts of the relationship between hippocampal theta and MS/vDBB spike discharge rates have been reported, but there has been no systematic investigation of whether MS/vDBB neurons discharge at different rates related to theta frequency, or whether the cells of the MS/vDBB discharge at different rates during different hippocampal EEG states.

The literature also provides very little information regarding how cells of the MS/vDBB respond to changes in ascending brainstem, and diencephalic input. Although it is known that stimulation of the ascending synchronizing system increases the discharge rates of most MS/vDBB cells and theta frequency, it is still unclear how these cells code changes in the level of activation of this ascending input, and how this is related to hippocampal theta.

OBJECTIVES

It is the purpose of this thesis to systematically determine whether or not MS/vDBB cell discharge rates reflect the differences in the spontaneous hippocampal slow wave activity in the urethane anaesthetized rat, both within the theta state and between theta and LIA. It is also the goal of this thesis to determine the importance of the ascending hypothalamic input in this relationship. Specifically, the objectives are:

Spontaneous Activity

1) To determine the characteristic discharge patterns of MS/vDBB neurons. That is, in keeping with previous hippocampal and septal cell classifications, neurons will be grouped as: a) phasic if they discharge in a rhythmic pattern which is related to the phase of hippocampal theta, or b) tonic if they discharge irregularly, or in bursts not related to the phase of the theta rhythm.

2) To differentiate MS/vDBB neurons based on whether their discharge rates are: a) linearly related to theta frequency (linear), or b) not linearly related to hippocampal theta frequency (nonlinear).

3) To differentiate theta-on cells and theta-off cells in the MS/vDBB based on a) whether the observed linear relationship between discharge rate and theta frequency is positive (theta-on), or negative (theta-off), or b) whether their discharge rates are significantly greater during theta (theta-on), or LIA (theta-off).

Stimulation Induced Activity

4) To establish the effects of DM-PH stimulation at different intensities on the discharge rates and patterns of MS/vDBB neurons.

5) To determine if the relationships observed spontaneously are the same during activation of the ascending input from the DM-PH.

It is expected that this study will confirm the presence of phasically discharging and tonically discharging cells in the MS/vDBB. Rhythmically bursting MS/vDBB cells are believed to be the pacemakers of hippocampal theta. Also, the spontaneous relationships discussed in objectives (2) and (3) have been shown to exist for hippocampal theta cells. Therefore, it is expected that MS/vDBB cell discharge rates will in some cases be linearly related to theta frequency, and in others be related to the hippocampal EEG state in a nonlinear fashion. By the same arguements, the direction of the linear relationships would be expected to be both linear negative and linear positive.

The results of Rowntree and Bland (1986) indicated that a nonrhythmic cholinergic input to the HF resulted in the production of theta, suggesting that a nonrhythmic input from the MS/vDBB might also be related to the theta state. Moreover, increased amounts of carbachol injected into the HF produced higher frequency theta, thus suggesting the possibility of a linear relationship between

the discharge rates of tonic MS/vDBB neurons and the frequency of theta.

Stimulation of the ascending brainstem and diencephalic inputs to the MS/vDBB has been shown to result in increased discharge rates in rhythmic bursting cells and to have variable effects or no effect on nonrhythmic cells (Petsche, et al., 1962; Wilson, et al., 1976). Moreover, hippocampal theta (Bland and Vanderwolf, 1972; Colom, et al., 1987) and theta cell discharge rates (Colom, et al., 1987) were shown to be linearly related to the level of DM-PH stimulation. Therefore, it is proposed that rhythmic (phasic) MS/vDBB cell discharge rates will be positively correlated to DM-PH stimulation intensity, and that nonrhythmic (tonic) MS/vDBB cell discharge rates will: a) increase or decrease linearly with increases in stimulation intensity, b) increase or decrease in a nonlinear fashion with stimulation, or c) not be affected by stimulation.

The input from the DM-PH is only one of several inputs to the MS/vDBB. Stimulation of the DM-PH not only affects theta indirectly, through the medial septum, but also directly. Therefore, the effects of DM-PH stimulation on the spontaneous relationships between cell discharges and hippocampal EEG is difficult to predict. Because of the more variable effects of stimulation on nonrhythmic MS/vDBB cells, and assuming the spontaneous relations described in

objectives (2) and (3) exist for tonic cells, it is possible that the effects of DM-PH stimulation on the spontaneous relationships will be more variable in the case of tonic cells than it is in case of phasic cells.

METHODS

Subjects

Twenty four male Long Evans, black hooded rats weighing between 250 and 450 grams (supplied by Animal Care services at the University of Calgary) served as subjects. The rats were housed in polycarbonate shoebox cages which contained one to three animals and were provided food and water to be consumed ad lib.

Apparatus

Electrical recordings from the DG and the MS/vDBB were made using tungsten (1 - 5 Mohms) and glass (2 M, NaCl; 2.5 - 5 Mohms) microelectrodes respectively. Electrical signals from each of the two microelectrodes were split and fed into two preamplifiers. One of the two Grass P511 wide band AC preamplifiers for each electrode was used for unit recording, with the low filter set at 300 Hz and the high filter set at 3 kHz. Unit signals were displayed on a 5100 series Tektronix storage oscilloscope. The other preamplifier for each electrode was used for EEG slow wave recording, with the low filter set at 1 Hz and the high filter set at 3 kHz. The EEG slow wave signals were displayed on a Grass model 7D polygraph (low filter, 1 Hz; high filter, 35 Hz) as well as on the Tektronix storage

oscilloscope. The EEG signals from the polygraph, and the unit signals from the preamplifiers were recorded on a TEAC XR-30, 7 channel FM tape recorder.

Electrical stimulation of the DM-PH was produced using a bipolar 250 μm stainless steel stimulating electrode, insulated to the tip and soldered to a male Winchester subminiature connector. Stimulation was produced with a Grass S44 stimulator connected to a Grass SIU 4678 stimulus isolation unit and a Grass CCU1A constant current unit. The stimulator was set to deliver square wave pulses of .1 ms duration at a frequency of 100 Hz. The five second stimulation epoch was recorded on the TEAC XR-30 via a synchronizing pulse from the stimulator.

The rat's body temperature was maintained at 38° C using a Harvard Instruments servosystem. Heart rate was also monitored throughout the experiment on the Grass 7D polygraph, and on a heart rate monitor designed by the technical staff of the University of Calgary Psychology department.

Surgical Procedure

Each rat was initially anaesthetized with halothane via an induction chamber. A jugular cannula and a tracheal tube were inserted during halothane anaesthesia to administer urethane anaesthetic (ethyl carbamate; .7g/ml)

and saline via the external jugular vein, and to facilitate breathing, respectively. Before the urethane could be given, halothane administration had to be discontinued and the animal allowed to recover as much as possible. The animal was then maintained at an adequate level of surgical anaesthesia throughout the experiment.

Having placed the animal in the stereotaxic instrument, an incision was made along the midline of the skull and the tissue tied back to expose the skull surface. The plane between bregma and lambda was then levelled horizontally for accurate electrode placement. An uninsulated tungsten electrode was inserted into the cortex, anterior to bregma, to serve as an indifferent electrode. The stereotaxic instrument served as the ground.

A kynar insulated, tungsten microelectrode with the tip electrolytically etched (1 - 5 Mohms) was stereotaxically inserted into stratum moleculare of the dorsal blade of the dentate gyrus (3.5 mm posterior to bregma, 2.5 mm lateral to the midline, and approximately 2.75 mm ventral to the dural surface), using the atlas of Paxinos and Watson (1986). This electrode served as the EEG slow wave reference and was cemented with dental acrylic at the site that resulted in the largest amplitude theta activity (approximately 1 - 2 mV).

Once the reference electrode was in place, the anaesthesic level was titrated such that theta activity and LIA alternated in the reference EEG record. Anaesthetic levels that were too high tended to suppress the spontaneous occurrence of theta activity. Proper anaesthetic level was also determined by the presence of vibrissa movement, a reduced heart rate, and the occurrence of slow wave theta in response to a tail pinch.

In 16 of the 24 animals utilized, a bipolar stimulating electrode was inserted through a 2 mm hole in the skull located 3.6 mm posterior to bregma, along the midline, and slowly lowered to the DM-PH. Before moving the electrode, the dura mater and the sagittal sinus were broken in order to ensure that the electrode proceeded in a vertical direction as it was lowered. The stimulating electrode was fixed with dental acrylic at the site that produced the highest amplitude theta rhythm with the least current, usually at a depth of 7.0 - 7.5 mm ventral to the dural surface. In addition to the theta rhythm, stimulation of the appropriate nucleus was accompanied by a substantial increase in the respiratory rate and vibrissa movement coincidental to the onset of stimulation.

The final step in the surgical preparation involved the placement of a glass microelectrode into the MS/vDBB complex in order to record extracellular spike trains from

isolated cells. The glass microelectrode (2.5 - 5.0 Mohms) was filled with either 2.0 M NaCl, or 0.5 M Na Acetate with 2.0 % Pontamine sky blue 6bx (Gurr Microscopy Materials). This electrode was lowered through a 2 mm hole located on the midline, 0.5 mm anterior to bregma. As was the case with the hypothalamic stimulating electrode, the dura mater and the sagittal sinus were broken prior to placement of the electrode. Once the bleeding from the sinus ceased, the electrode was lowered to a depth of 5.0 mm. After a short delay to allow the tissue to settle, it was lowered micron by micron until an action potential, or action potentials of a single neuron were observed. During this part of the procedure it was important that the animal be alternating between theta and LIA in the EEG record. This was to ensure that there was no unit selection bias based on the presence or absence of the theta rhythm. Any cell that was isolated at a depth between 5.0 and 6.5 mm ventral to the dural surface that could be maintained for more than 15 minutes, qualified for the experimental procedures, provided the action potential was of constant amplitude and shape.

Upon completion of the experimental procedure, the electrode was cut (NaCl filled) to mark its path, or a 50 μV DC current was passed through the tip (Na Acetate and Pontamine sky blue) for 5 minutes on each polarity, to mark

the actual recording sites. The animal was then administered an overdose of urethane, perfused with saline followed by an 11 % formalin solution, and the brain removed. After storing the brain for at least 48 hours in 11 % formalin, the locations of the reference electrode, the stimulating electrode, and the unit electrode were verified histologically.

Experimental Procedure

Once a cell was isolated and stable, at least 15 minutes of spontaneous electrical activity was recorded on tape, including periods of both slow wave theta and LIA. The animal was then given enough anaesthetic so that EEG theta activity only occurred in response to a tail pinch, or electrical stimulation. Slow wave and unit activity were also recorded during several 30 s tail pinches in addition to that which occurred during spontaneous activity. In the 16 rats with a stimulating electrode, cells which had been isolated and maintained for at least 15 minutes qualified for the following experimental manipulation.

A series of five second stimulation trials was delivered with current levels ranging from 100 μA to 500 μA in 50 μA steps. There were five trials at each stimulus level for a total of 45 (randomly ordered), five second

stimulation trials. Stimulation trials were separated by a 10 - 15 second interstimulus interval (ISI). In instances where the cell did not return to its resting discharge rate within the 15 s interval, the ISI was increased until the spike amplitude, or frequency returned to normal. In some cases the cell could not be maintained throughout all 45 trials; however, these data were still useful. When the cell could no longer be recorded, or the stimulus regimen was complete, another cell was isolated and recorded. The stimulation procedure was then repeated on any isolated neuron that could be maintained.

Data Analysis

Analogue unit discharge signals were passed through a WPI model 121 window discriminator and entered into the computing system as digital events. For each cell, the window was set prior to entering the data and was not altered. The EEG signal, which was also converted from analogue to digital (at a sampling rate of 1000 Hz), was entered into the computing system simultaneously with the unit discharge signal. A Digital Equipment Corp. PDP11/73 computing system was employed to analyze the spike train and its relation to slow wave theta.

A paper chart protocol including the EEG activity from both microelectrodes, and the stimulation indicator signal

was produced by displaying the signals from the FM tape on the Grass polygraph. From this protocol, several segments of spontaneous data were selected for analysis. This included segments of both slow wave theta and LIA, to be analyzed separately. Discharge rates and rhythmicity were compared across conditions for each cell. Theta frequency and discharge rates were analytically compared for their linear and phase relationships.

Spontaneously produced theta, and tail pinch induced theta were analyzed for each cell, where possible. Since the production of LIA and slow wave theta were dependent on the level of anaesthesia, at least two samples of theta were chosen. In most cases, two or three samples of 30 - 40 s each were selected for each EEG state. At least one sample of tail pinch induced theta was also selected and analyzed.

Comparison of the spontaneously produced theta samples to at least one tail pinch induced theta sample served as a partial control for the effects of urethane on MS/vDBB cell activity. As an additional control for the possible pharmacological effects of urethane on unit discharge rates, some reference recordings began with theta activity while others began with LIA. This served to counterbalance some variations in the systemic and CNS concentrations of urethane. Finally, data from each EEG state were chosen

such that the time interval between samples of slow wave theta, or LIA was as large as possible.

Several plots for each sample were produced on a Houston Instruments x-y plotter: including a first order interspike interval histogram (ISIH), a histogram of the peak to peak duration of each theta wave (TDH), an autocorrelation histogram (ACH) of the spike train, and a theta cycle spike histogram (TCSH) These plots were produced separately for all of the data. All plots were also produced for the concatenated samples of spontaneous theta, the concatenated samples of tail pinch induced theta, and the concatenated samples of LIA to give the final results for each EEG state, for each cell. LIA data were not subjected to the TCSH, nor the TDH since the programs used to produce these plots required theta to be present in the EEG record.

To create the TDH and the TCSH the peaks of the slow wave theta were marked using the PDP11/73. A histogram of the durations of each theta cycle was then created. Each cycle of theta and the simultaneous unit activity were then normalized to 360°. Each cycle was divided into 40 bins (9°/bin). A spike histogram of the total number of spikes in each of the 40 bins (sum of all cycles) was created.

The plots reported in the previous two paragraphs were used to determine the unit discharge pattern and its

relation to the theta rhythm. The ACH was used to determine whether or not there was a rhythmic discharge pattern. The ISIH was used to indicate whether the cell was a bursting neuron with a constant interburst interval, or not. The TDH provided a histogram of the duration of each theta cycle and was used to compare with the ACH. The TCSH was used to determine whether the cell discharge pattern was related to the phase of the theta rhythm.

Due to the 100 Hz artifact produced by the stimulator, the first second of slow wave activity, and the corresponding unit activity following each stimulation trial were entered into the PDP11/73 computer for analysis. As was the case for the spontaneous and sensory induced data, the pattern of discharges was determined from the ACH and ISIH, and the relationship of the spike train to slow wave theta determined from the TDH and TCSH.

Statistical Analysis

Simple linear regression was used to relate unit discharge frequency to theta frequency for the spontaneous data. A version of SPSS designed for the PDP11/73 (SPSS11) was utilized for this purpose. The spontaneous data for each EEG state were divided into one-second segments by the computer. A computer program calculated the slow wave theta frequency and the cell discharge rate for each

segment. The resulting series of paired observations (unit discharge rates and theta frequencies) was used for the regression analysis. Unit discharge rates were regressed on theta frequencies for each cell. Although the spontaneous data were correlational in nature, it was more useful to calculate R^2 values and slopes, which were more descriptive. The significance of the R^2 value was tested using a nonparametric, randomization test for single subject research (program 8.2), designed by Edgington (1987) and modified for use on the PDP11/73.

This technique involves 10,000 random pairings of the data set and calculates a probability value based on the number of pairings out of the 10,000 that produce a test statistic as large as the obtained statistic; in this case R^2. The randomization test is useful for designs which involve dependant data and not random assignment, although it was not designed for this purpose. It makes no assumptions about the underlying distribution and controls for dependency which might produce distributions that are not normal. It is worth noting that for cases with a large sample size, the probability of a type 1 error produced by parametric procedures approaches the value produced by the nonparametric test.

In those cases without a significant linear relationship between theta frequency and the cell discharge

frequency, an independent t-test was performed on the discharge rates during slow wave theta and LIA. The level of significance was determined using a randomization test for independent t-tests (program 4.5) designed by Edgington (1987) and modified for use on the PDP11/73 computer. The process involves calculating a test statistic for the obtained data. The data are then collapsed and randomly assigned to each group. A new test statistic is calculated for the permuted data. This is performed on 10,000 permutations and the proportion of values that are equal to, or greater than the test statistic for the obtained data is equal to the probability of a type 1 error.

For the stimulation data, a Honeywell Multics system and the SPSSX software package (version 1.1+) were used to analyze the interrelationships of theta activity, unit activity, and the level of activation as manipulated by the change in stimulus intensity. The frequency of the theta rhythm was determined from a raw data plot produced on the Houston Instruments x-y plotter. The unit discharge rate was calculated for each sample by the PDP11/73 computer and confirmed on the raw data plot. Stimulation level, unit discharge frequency, and slow wave theta frequency for all stimulation trials were entered by hand into the multics system. Slow wave theta frequency and cell discharge rates were separately regressed on stimulation intensity while

theta frequency and unit discharge rates for each cell were correlated with a Pearson correlation.

The order of the stimulation regimen was determined randomly, thus controlling for the carryover effects on the discharge rate and on slow wave theta frequency of one stimulation trial on a subsequent presentation. However, dependency between theta frequency and the unit discharge rate would be likely. For this reason the randomization test reported previously (Edgington, 1980) was used to test the probability level of the linear relationships for the stimulation data.

If the regression analysis did not produce results which indicated a linear relationship between discharge rate and the intensity of stimulation, the possibility of a nonlinear effect on mean discharge rate was examined. The mean discharge rate for the series of one-second post-stimulation epochs was compared to the mean discharge rate of the spontaneous data (one second segments) using an independent t-test. Once again, the nonparametric randomization test for independent t-tests (Edgington, 1987) was utilized to determine the probability level.

RESULTS

Spontaneous Activity

Hippocampal electrical activity recorded from the DG included both slow wave theta and LIA. Histology demonstrated that in all cases the reference electrode was accurately placed in either stratum moleculare, or stratum granulosum of the upper blade of the DG. The amplitude of the reference EEG theta activity was at least 1.0 mV ($\bar{X}$ = 1.27 ∓ 0.19) in all samples.

Sixty-five neurons were isolated and recorded. Histology verified that these neurons were located in the MS and the vDBB. Within these nuclei the recorded cells ranged from the midline, laterally to the border between the MS and LS; from the dorsal tip to the more ventral portions of the MS/vDBB; and throughout the rostral-caudal axis.

Samples of slow wave theta and LIA were recorded along with the accompanying discharges for each of the 65 cells. Theta produced in response to a tail pinch was also recorded in most cases. It is important to note that slow wave and unit activity during a tail pinch did not occur spontaneously, and due to the urethane anaesthesia, what has been referred to as spontaneously generated activity was not necessarily spontaneous. However, in all instances

the tail pinch-induced theta resulted in the same pattern in the ACH and ISIH, and the TCSH produced the same phase relationship between MS/vDBB discharges and slow wave theta as the spontaneously produced slow wave theta. Because the results for both conditions were the same, and because spontaneously generated theta and tail pinch-induced theta have the same cholinergic properties in urethanized preparations (Bland, 1986), the data produced during a tail pinch were combined with the spontaneously generated data. Since spontaneously produced and tail pinch-induced data were combined in all instances, and for lack of a better term, the combined data will be collectively referred to as spontaneous activity. This includes both unit activity and the coincidental slow wave theta activity.

The only difference apparent from the analysis was in the frequency of the theta rhythm. Tail pinch-induced theta occasionally resulted in higher frequency theta. However, this was useful since theta produced during urethane anaesthesia was generally of a narrow frequency range, and the larger the range in theta frequency the easier a linear relationship was to detect.

Spontaneous slow wave theta and unit activity were compared in several ways. The first axis by which cells were differentiated involved whether or not there was a phase relationship between slow wave theta and the unit

discharges. This first axis, although not the most important one in this study, has been a major centre of focus in previous research.

The ACH, the ISIH, the TDH, and the TCSH were utilized collectively to determine whether or not there was a phase relationship. The ACH was used to determine whether or not the spike train was rhythmic. A flat ACH indicated an arrhythmic discharge pattern and an ACH with regular repeating peaks indicated a rhythmic discharge pattern. If the period of the ACH was equal to the period of the theta cycle (mode of the TDH), then the rhythmicity of the unit discharges had a frequency equal to that of the theta rhythm. Finally, the TCSH indicated whether or not the cell's spike train was related to the phase of the slow wave theta. That is, the mode of the TCSH determined the phase angle at which the MS/vDBB cell discharges were most likely to occur. If the amplitude of the TCSH was constant, it was determined that a phase relationship was not present.

The discharge patterns for 38 of 65 cells (58.4 %) were determined to be related to the phase of the theta rhythm. The ACH that was produced demonstrated a rhythmic discharge pattern and comparison of the peak to peak duration of the ACH to the peak to peak duration of slow wave theta (TDH) indicated that the frequency of the

rhythmic pattern (ACH) was equal to the frequency of the theta rhythm. The corresponding ISIH was bimodal with the first peak being much larger than the second. As has been found in previous research, the phase angle varied from cell to cell, but remained constant within the data for each neuron. These 38 neurons were termed phasic due to the presence of a phase relationship with the slow wave theta rhythm.

There was some degree of variability in the ACH and the ISIH for phasic cells between cells. The actual peak to trough amplitude in the ACH varied from cell to cell. There was also some degree of variation in the ISIHs. The second peak was not always completely discrete from the first peak. However, there was very little doubt that two modes were present.

During LIA, nine of the phasic cells (23.7 %) had a rhythmic component in their ACH and eight of these also had a bimodal ISIH. The remaining cell had an ISIH that was unimodal. Instead of a well-defined second mode there was a wide distribution with constant amplitude. In all nine cells the rhythmicity was not as constant during LIA as it was during theta. Interspike intervals within a burst and between bursts were more variable during LIA than they were during theta. This resulted in less definition in the peaks of the ACH and the modes of the ISIH. Figure 2 shows

the ISIH and ACH during theta (column A) and LIA (column B) for phasic cell 23-1. Inset is a photograph of a two second oscilloscope trace of the raw data. Figure 2 clearly demonstrates that the cell remains rhythmic, but that there was greater variability in the rhythmicity of the cell during LIA. The remaining 29 of the phasic cells (76.3 %) showed no signs of rhythmicity during LIA.

The remainder of the 65 neurons (27, 41.5 %) discharged in a manner which was unrelated to the phase of the theta rhythm. These 27 units discharged in a regular or irregular pattern that produced ACHs and TCSHs with constant amplitudes and ISIHs that were unimodal and much more variable in their distribution. In some cases the neurons burst irregularly. In other cases, the cells did not burst at all; instead they discharged steadily with single spikes. This was indicated by the ACH and ISIH for each cell. These cells were termed tonic since they discharged in a pattern which was not related to the phase of the theta rhythm.

The recorded neurons were also differentiated on the basis of the presence or absence of a linear relationship between the unit's discharge frequency and the frequency of the corresponding slow wave theta. Linear regression analysis and the randomization test revealed that the discharge rate was related to theta frequency in 29 units

Figure 2. ACH and ISIH for phasic cell 23-1 (inset) during slow wave theta (A) and LIA (B). Phasic cells were rhythmic and phase locked to the theta rhythm. This produced bimodal ISIHs and ACHs with large peaks that repeated every 275 ms (approximately). This cell (and eight others; 23.7 %) remained rhythmic during LIA, however, there was greater variability in the interspike interval within and between bursts.

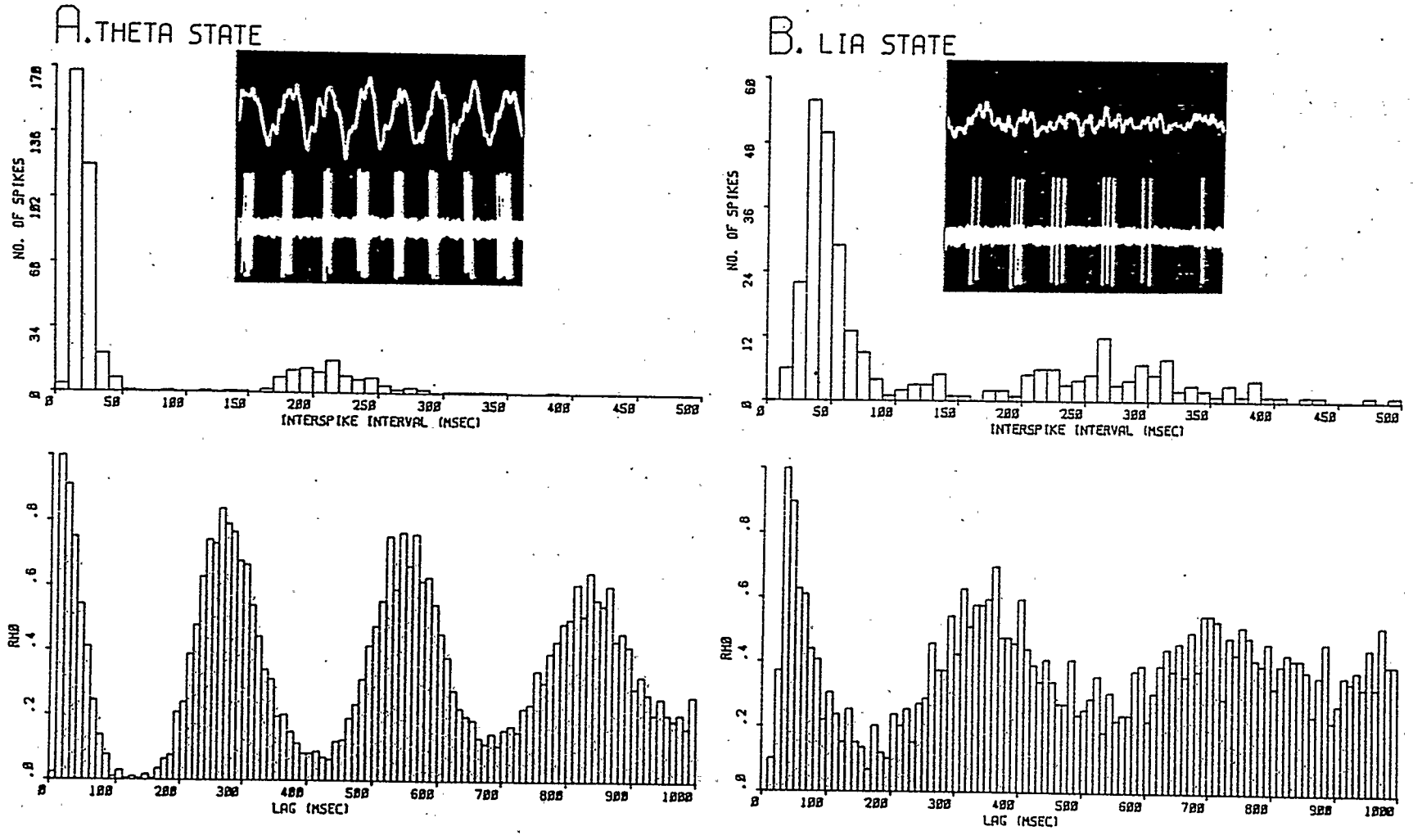
A. THETA STATE
B. LIA STATE
NO. OF SPIKES
INTERSPIKE INTERVAL (MSEC)
RHO
LAG (MSEC)

(44.6 %, $p < .01$). Nineteen of the 29 (65.5 %) linearly related neurons had discharge rates which were positively related to theta frequency while 10 (34.5 %) were negatively correlated to theta frequency. The remainder, 36 (55.4 %) did not have a linear relationship.

The linear relations, specifically the slope of the regression line, must only be interpreted within the range of theta frequencies observed during urethane anaesthesia. There are most certainly limits on the minimum and maximum discharge rates that can be produced by any neuron. These limits may exist within this theta frequency range or outside this range. Both linear and nonlinear relationships to slow wave theta may not hold with extended frequency ranges, due to maximums and minimums, and other potential factors affecting cell discharge rates in the freely moving animal.

The final axis involved the differentiation of cells based on whether they increased, or decreased their discharge rate with slow wave theta in one of two ways. A unit was determined to be a theta-on cell if: a) its discharge rate was positively correlated to theta frequency (linear), or b) its discharge frequency during slow wave theta was significantly greater than during LIA (nonlinear). Thirty seven of the 65 cells (56.9 %) qualified as theta-on cells.

Conversely, a neuron was determined to be a theta-off cell if: a) its discharge rate was negatively correlated to theta frequency (linear), or b) its rate of discharge during slow wave theta was significantly less than during LIA (nonlinear). Sixteen of sixty five neurons (24.6 %) were determined to be theta-off cells.

In addition to theta-on and theta-off cells, there were 12 cells with discharge rates which were not related to the hippocampal theta rhythm (ie. the cell discharge rate did not change significantly during a change in the EEG state from theta to LIA, or vice versa, nor was it linearly related to theta frequency). Three of these 12 cells (25.0 %) were phasic while nine (75.0 %) were tonic. These nine cells (13.8 %) were not related to theta in any discernible way and the remaining 56 neurons (86.2 %) were related to slow wave theta by their discharge rate, by a phase relationship, or both.

The central focus within this thesis involved the classification of cells into theta-on and theta-off cell types. Fifty three of 65 cells (81.5 %) were classified as either theta-on, or theta-off. That is, they were related to slow wave theta by their discharge rate. The remaining axes; phasic versus tonic, and linear versus nonlinear define the subtypes of theta-on and theta-off cells.

Table 2 provides a summary of the number of cells within each theta-on and theta-off cell subtype.

As was reported previously, 37 of 65 cells were classified as theta-on. Twenty two of these (59.4 %) were phasic while 15 (40.6 %) were tonic. On the other hand, 17 of the 37 (45.9 %) neurons had discharge rates that were linearly related to theta frequency and 20 (54.1 %) that were related to the theta state in a nonlinear manner. Combining these two axes resulted in four subtypes of theta-on cell.

Figure 3 demonstrates these four subtypes in a schematic representation. The upper row of the schematic diagram represents the hippocampal slow wave activity. The first two cell lines below this illustrate phasic cells which were linearly related to theta frequency (upper) and the slow wave state (lower): phasic linear, and phasic nonlinear theta-on cells. The bottom two representations are of tonic theta-on cells. The upper and lower cell lines illustrate the tonic linear and tonic nonlinear theta-on cells respectively. Table 3 summarizes the data for theta-on cell subtypes. Mean discharge rates during theta activity and LIA, as well as the results of the regression analysis are listed.

Ten of the 37 theta-on cells (27.0 %) were phasic linear theta-on cells. For each of these cells the

Table 2

Theta-on and theta-off cells in the MS/vDBB

	Theta-on (n)	Theta-off (n)	Subtotal (n)
Phasic			
Linear	10	9	19
Nonlinear	12	4	16
Subtotal	22	13	35
Tonic			
Linear	7	3	10
Nonlinear	8	0	8
Subtotal	15	3	18
Total	37	16	53

Figure 3. Diagrammatic representation of the schema used to classify theta-on cells that were recorded in the MS/vDBB. The upper row represents the hippocampal slow wave activity. The first two cell lines illustrate phasic (rhythmic) theta-on cells whose discharge rates were either linearly related to theta frequency (linear)or simply showed an increase related to the slow wave theta state (nonlinear). Linear and nonlinear tonic (nonrhythmic) theta-on cell types are illustrated in the last two cell lines.

THETA-ON CELLS

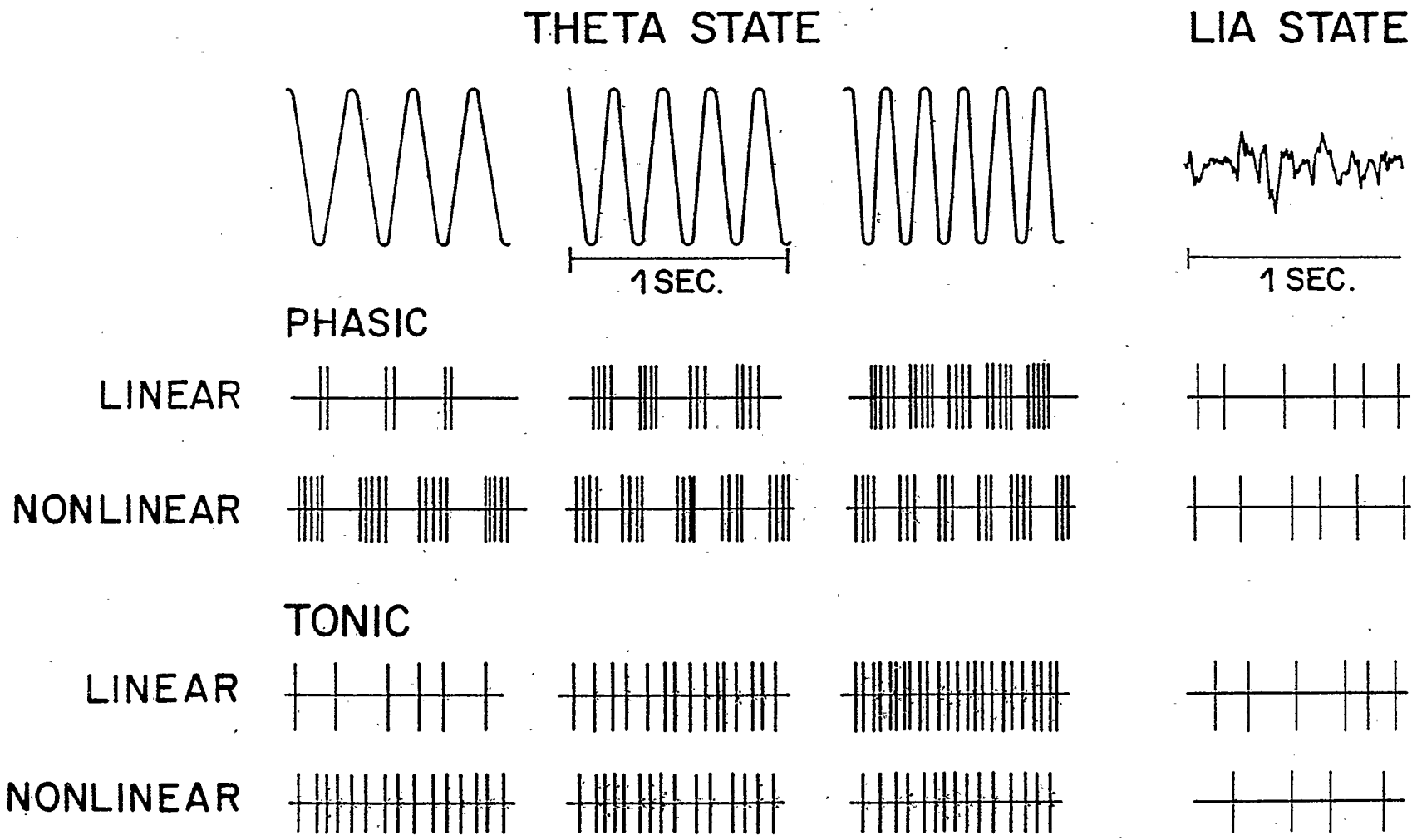

Table 3

Theta-on cell data summary

	R^2	b (spikes/s/Hz)	Discharge Rate: Theta (spikes/s)	Discharge Rate: LIA (spikes/s)
Phasic Linear (n = 10)				
Mean	0.246	7.72	19.3	11.1
S.D.	0.201	4.66	10.1	8.2
Minimum	0.070	3.76	7.9	1.8
Maximum	0.767	16.02	38.6	26.3
Phasic Nonlinear (n = 12)				
Mean	-----	-----	18.0	8.8
S.D.	-----	-----	11.0	9.2
Minimum	-----	-----	7.5	1.0
Maximum	-----	-----	48.3	36.4
Tonic Linear (n = 7)				
Mean	0.262	5.98	13.9	6.4
S.D.	0.150	3.17	6.7	4.6
Minimum	0.049	2.13	2.1	1.0
Maximun	0.462	11.23	23.6	12.2
Tonic Nonlinear (n = 8)				
Mean	-----	-----	8.7	5.3
S.D.	-----	-----	5.8	4.4
Minimum	-----	-----	1.4	0.1
Maximum	-----	-----	26.3	13.2

regression analysis produced significant results ($p < .01$) with R^2 values ranging from 0.070 to 0.767 with a mean and standard deviation of 0.246 ∓ 0.201. The slopes of the regression lines ranged from 3.76 to 16.02 spikes/s/Hz ($\bar{b}$ = 7.72 ∓ 4.66 spikes/s/Hz). These 10 cells had a mean discharge rate during theta activity which ranged from 7.9 to 38.6 spikes/s with a mean and standard deviation of 19.3 ∓ 10.1 spikes/s. In all but one case, the mean discharge rate was lower during LIA than during theta, ranging from 1.8 to 26.3 spikes/s ($\bar{X}$ = 11.1 ∓ 8.2 spikes/s). One cell was virtually silent during LIA. In nine out of 10 cases the discharge rate during LIA was less than, or equal to the minimum observed discharge rate during theta. Finally, for one phasic linear theta-on cell the mean discharge rate during LIA (22.0 spikes/s) was greater than the maximum observed discharge rate during theta (17.6 spikes/s).

A second subtype of phasic theta-on cell referred to as phasic nonlinear theta-on cells was the most common. Twelve out of 37 theta-on cells (32.4 %) were in this group. The results of the linear regression for each of these cells was not significant. The subsequent independent t-test demonstrated a significant difference ($p < .01$) between the mean discharge rates during slow wave theta and LIA for each of the 12 cells. The discharge rates during theta ranged from 7.5 to 48.3 spikes/s

($\bar{X}$ = 18.0 ∓ 11.0 spikes/s) compared to LIA, 1.0 - 36.4 spikes/s ($\bar{X}$ = 8.8 ∓ 9.2 spikes/s). Except for one cell, these cells were always active to some degree during LIA.

The last two subtypes of theta-on cells were both tonic and were only slightly less common, if at all, than the phasic subtypes. Seven out of 37 theta-on cells (18.9 %) were tonic linear theta-on cells. Once again, the linear regression analysis produced significant results ($p < .01$) for these seven cells. The R^2 values ranged from 0.049 to 0.462 with a mean and standard deviation of 0.262 ∓ 0.150. The slope of the regression line ranged from 2.13 to 11.23 spikes/s/Hz ($\bar{b}$ = 5.98 ∓ 3.17 spikes/s/Hz). The mean discharge rate during theta ranged from 2.1 to 23.6 spikes/s ($\bar{X}$ = 13.9 ∓ 6.7 spikes/s). The mean discharge rate during LIA ranged from 0.1 to 12.2 spikes/s with a mean and standard deviation of 6.4 ∓ 4.6 spikes/s. Two cells had mean discharge rates during LIA which were below two spikes/s. The mean discharge rate during LIA was lower than during theta in all but one neuron. For that cell the means for each EEG state were approximately equal. In four of the neurons the mean discharge rate during LIA was actually less than the minimum observed discharge rate during slow wave theta.

Eight of thirty seven theta-on cells (21.6 %) were tonic nonlinear theta-on cells. The mean discharge rate

during slow wave theta ranged from 1.4 to 26.3 spikes/s ($\bar{X}$ = 8.7 ∓ 5.8 spikes/s). In every case the mean discharge rate during theta was significantly larger than the mean discharge rate during LIA ($p < .01$). The mean discharge rate during LIA varied from 0.1 to 13.2 spikes/s with a mean and standard deviation of 5.3 ∓ 4.4 spikes/s. Many cells in this group had very low rates of discharge for both slow wave theta and LIA and in only one instance was a cell inactive during LIA.

Figure 4 provides examples of the four subtypes of theta-on cells. Photographs of the recordings are displayed by cell type. Each photograph contains the slow wave (upper) and unit (lower) activity from a one second oscilloscope trace. For each cell type there are three photographs, two of different theta frequencies and one of LIA. Figure 4A provides examples of linear and nonlinear phasic theta-on cells. Phasic linear theta-on cell 36-2 increased its discharge rate with an increase in theta frequency and reduced its discharge rate during LIA (left to right). Phasic nonlinear theta-on cell 25-1 had an equal discharge rate for both frequencies of theta (left and middle), but decreased its discharge rate during LIA (right).

Examples of tonic linear and nonlinear theta-on cells are shown in figure 4B. Tonic linear theta-on cell 36-3

Figure 4. The relation between slow wave activity recorded from stratum moleculare in the dentate gyrus and MS/vDBB theta-on cell discharges. A: Examples of phasic linear (upper row; cell 36-2) and phasic nonlinear (lower row; cell 25-1) theta-on cells. During higher frequency theta (middle), cell 36-2 discharged at a greater rate than during lower frequency theta (left), or during LIA (right). Cell 25-1 (phasic nonlinear theta-on) discharged at equal rates during both frequencies of theta and was virtually silent during LIA. B: Tonic linear (cell 36-3) and tonic nonlinear (cell 30-1) theta-on cells. Cell 36-3 increased its discharge rate linearly with an increase in theta frequency (left to middle) and discharged at a lower rate during LIA (right). Nonlinear cell 30-1 discharged at the same rate during lower and higher frequency theta and at a lower rate during LIA.

LIST OF FIGURES

FIGURE		PAGE
Figure 1	Cytoarchitecture of the hippocampal formation	10
Figure 2	ACH and ISIH for phasic cell 23-1 during slow wave theta and LIA	76
Figure 3	Diagrammatic representation of the schema used to classify theta-on cells	82
Figure 4	The relation between slow wave activity and MS/vDBB theta-on cell discharges	88
Figure 5	Diagrammatic representation of the schema used to classify theta-off cells	91
Figure 6	Theta-off cell discharge patterns and the simultaneous slow wave activity	96
Figure 7	The relationship between unit discharge rates and slow wave theta frequency for examples of the theta-on and theta-off cell linear subtypes	99
Figure 8	Proportions of phasic and tonic cells	103
Figure 9	Proportions of theta-on cell subtypes compared to theta-off cell subtypes	105
Figure 10	Graphic representation of the relationship relationships between unit discharge rate and stimulation intensity, and between theta frequency and stimulation intensity	113
Figure 11	An example of the effects of stimulation on a phasic nonlinear theta-on cell	117
Figure 12	Scatterplots of the data for cell 4-1 demonstrating the various spontaneous and stimulation induced relationships	121

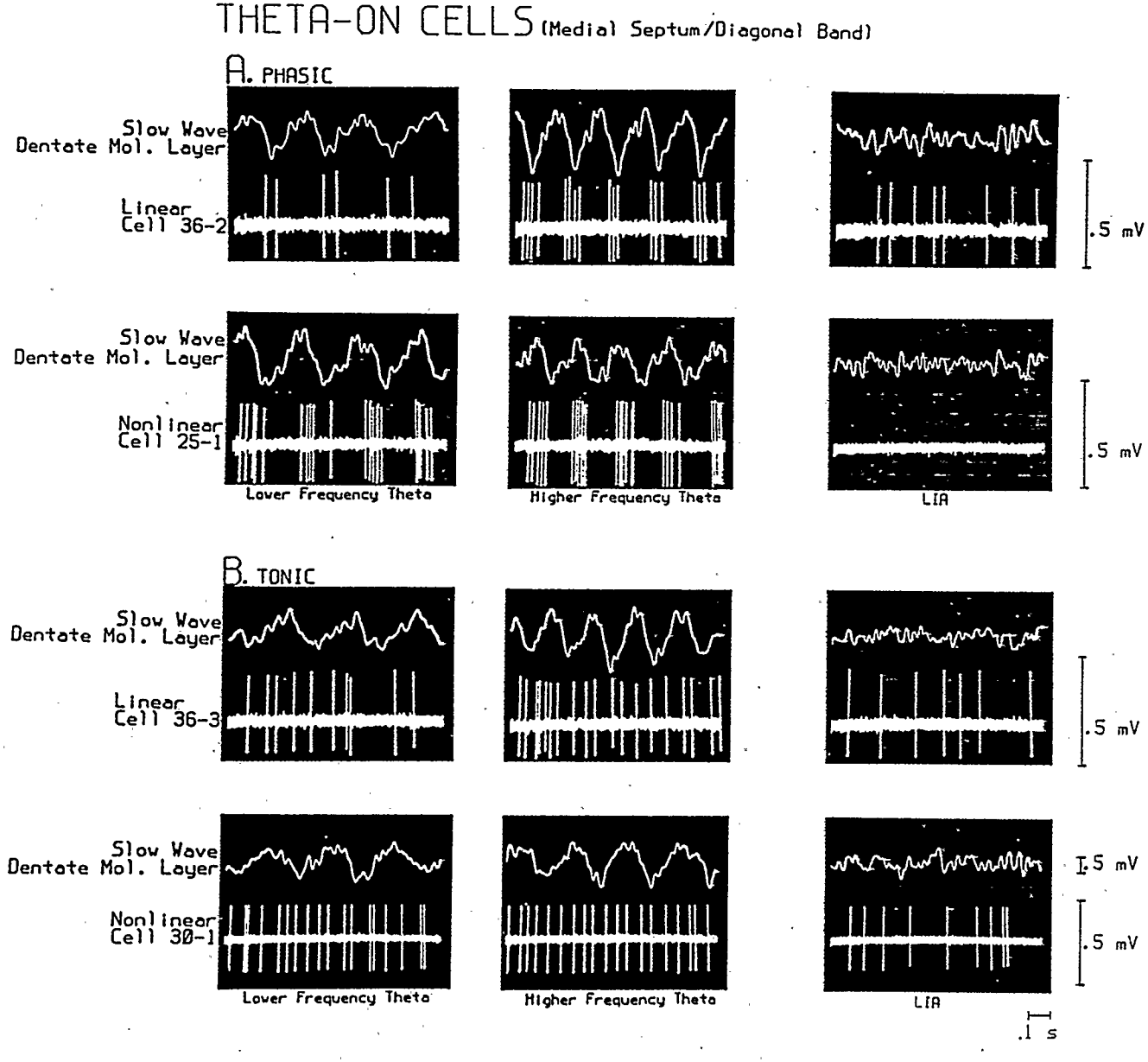
THETA-ON CELLS (Medial Septum/Diagonal Band)
A. PHASIC
Slow Wave
Dentate Mol. Layer
Linear
Cell 36-2
.5 mV
Slow Wave
Dentate Mol. Layer
Nonlinear
Cell 25-1
.5 mV
Lower Frequency Theta
Higher Frequency Theta
LIA
B. TONIC
Slow Wave
Dentate Mol. Layer
Linear
Cell 36-3
.5 mV
Slow Wave
Dentate Mol. Layer
Nonlinear
Cell 30-1
.5 mV
.5 mV
Lower Frequency Theta
Higher Frequency Theta
LIA
.1 s

had a greater discharge rate during higher frequency theta (middle) than lower frequency theta (left) and a decreased discharge rate during LIA (right). Tonic nonlinear theta-on cell 30-1 discharged at the same frequency during both frequencies of slow wave theta (left and middle) and decreased its discharge rate during LIA (right).

Whereas 56.9 % of the 65 recorded cells were theta-on cells, only 24.6 % (16) were theta-off cells. Of the 16 theta-off cells, 13 (81.2 %) were phasic and 3 (18.2 %) were tonic. Twelve of the 16 cells (75.0 %) had discharge rates which were negatively correlated to slow wave theta frequency (linear) and four of the 16 theta-off cells (25.0 %) coded the change in EEG state with an overall change in their discharge rate (nonlinear). In the case of theta-off cells, combining both of these axes resulted in three subtypes, as opposed to the four subtypes which occurred in theta-on cells. Tonic nonlinear theta-off cells were not recorded in the MS/vDBB.

Figure 5 is a schematic representation of these subtypes which are described in detail below. The upper row represents the hippocampal slow wave activity. The first two cell types illustrate phasic linear and phasic nonlinear theta-off cells. The last cell type illustrates a tonic linear theta-off cell. For a summary of the mean discharge rates during slow wave theta and LIA, and the

Figure 5. Diagrammatic representation of the schema used to classify theta-off cells recorded in the MS/vDBB. The upper row represents the hippocampal slow wave activity. The first two cell lines diagram phasic (rhythmic) theta-off cells. The first line represents the discharge pattern of a phasic linear theta-off cell and the second line represents a phasic nonlinear theta-off cell. The linear tonic (nonrhythmic) theta-on cell type is illustrated in the last cell line.

THETA-OFF CELLS

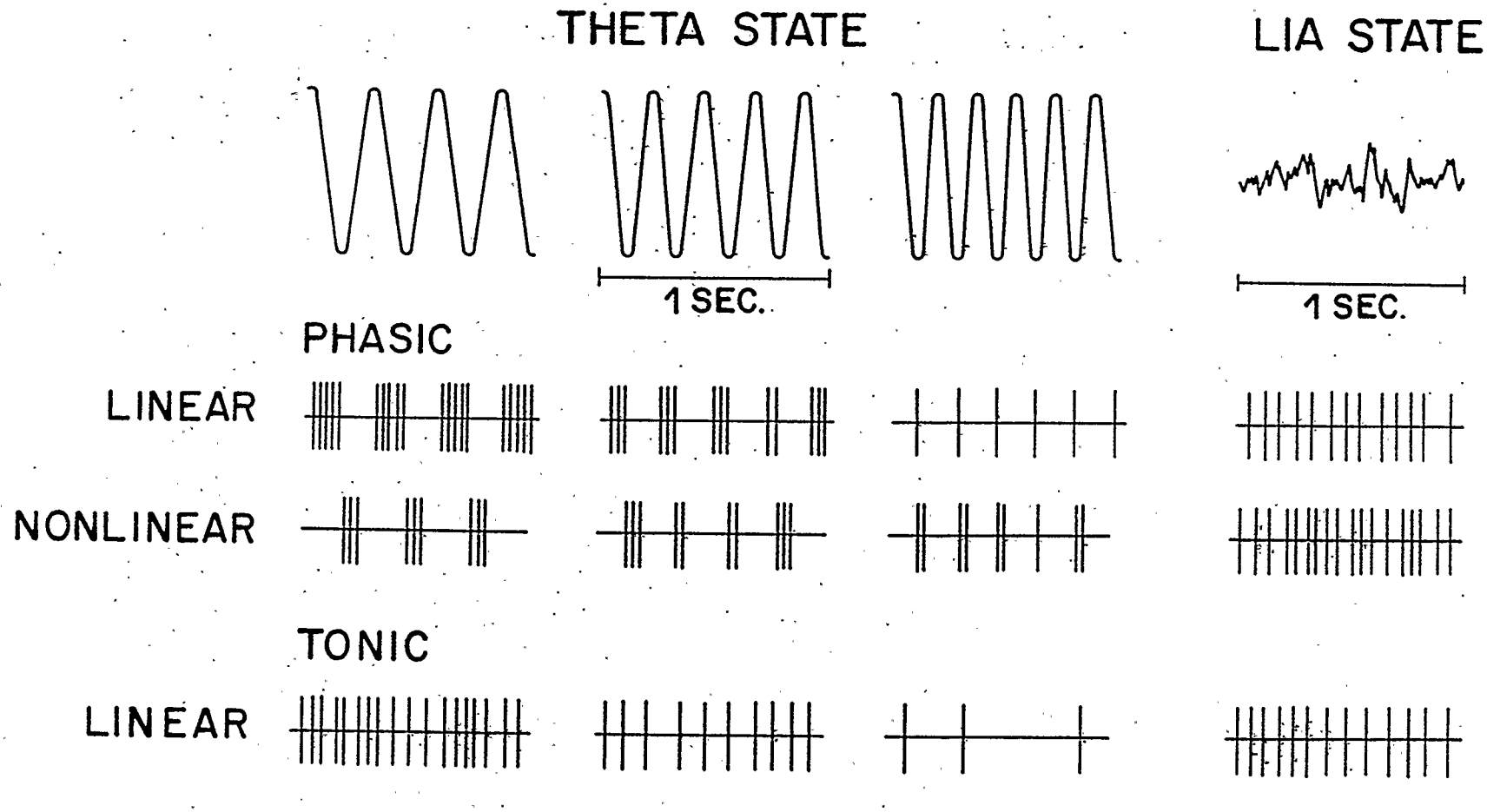

results of the regression analysis for the theta-off cell subtypes see table 4.

The most common subtype of theta-off cell was the phasic linear theta-off cell which included nine out of 16 cells (56.2 %). Values for R^2 and the slope were significant ($p < .01$) and ranged from 0.146 to 0.604, and -4.48 to -24.86 spikes/s/Hz respectively. The mean and standard deviation for R^2 were 0.236 $\mp$ 0.144 and for the slope were -12.31 $\mp$ 7.39 spikes/s/Hz. The mean discharge rate during theta was greater than the mean discharge rate during LIA in five of the nine phasic linear theta-off cells. The discharge rates were approximately equal for hippocampal theta and LIA in the other four cells. Mean discharge rates during theta ranged from 5.4 to 58.3 spikes/s ($\bar{X}$ = 27.6 $\mp$ 18.7 spikes/s) and during LIA they ranged from 4.4 to 52.9 spikes/s ($\bar{X}$ = 19.8 $\mp$ 17.9 spikes/s). At the higher frequencies of slow wave theta produced during urethane anaesthesia, five of these cells stopped discharging. The remaining four cells discharged at rates that were well below their mean discharge frequency during slow wave theta.

Four of 16 theta-off cells (25.0 %) were phasic nonlinear theta-off cells. These cells were phasic and had significantly higher mean discharge rates during slow wave theta compared to LIA ($p < .01$). The mean discharge rates

Table 4

Theta-off cell data summary

	R^2	b (spikes/s/Hz)	Discharge Rate: Theta (spikes/s)	Discharge Rate: LIA (spikes/s)
Phasic Linear (n = 9)				
Mean	0.236	-12.31	27.6	19.8
S.D.	0.144	7.39	18.7	17.9
Minimum	0.146	-4.48	5.4	4.4
Maximum	0.604	-24.86	58.3	52.9
Phasic Nonlinear (n = 4)				
Mean	-----	-----	10.2	19.8
S.D.	-----	-----	4.3	13.4
Minimum	-----	-----	6.3	7.6
Maximum	-----	-----	16.3	38.3
Tonic Linear (n = 3)				
Mean	0.249	-2.53	8.6	10.0
S.D.	0.162	0.92	6.1	3.3
Minimum	0.078	-1.60	3.6	7.0
Maximun	0.400	-3.43	15.4	13.6

during EEG theta activity ranged from 6.3 to 16.3 spikes/s ($\bar{X}$ = 10.2 ∓ 4.3 spikes/s) and during LIA ranged from 7.6 to 38.3 spikes/s ($\bar{X}$ = 19.8 ∓ 13.4 spikes/s). All four of these cells continued to be active in the presence of the hippocampal theta rhythm.

The final group of cells that were related to the theta rhythm by their discharge rate were the tonic linear theta-off cells which consisted of 3 cells (18.8 %). These cells had R^2 values which were similar to the other linear subtypes, ranging from 0.078 to 0.400, with a mean and standard deviation of 0.249 ∓ 0.162. Unlike the phasic linear theta-off cells, the tonic linear theta-off cells had slopes which were not very large. The slopes ranged from -1.60 to -3.43 spikes/s/Hz with a mean and standard deviation of -2.53 ∓ 0.92 spikes/s/Hz. Although the discharge rates of these cells decreased with increasing slow wave theta frequency, they were never silent at the higher frequencies of theta observed during urethane anaesthesia (approximately 5.5 Hz). These cells had mean discharge rates ranging from 3.6 to 15.4 spikes/s ($\bar{X}$ = 8.6 ∓ 6.1 spikes/s) during theta and from 7.0 to 13.6 spikes/s ($\bar{X}$ = 10.0 ∓ 3.3 spikes/s) during LIA.

Examples of the various theta-off cell types are provided in figure 6. Photographs were taken of the recorded data, as was done for figure 4. Part A consists

Figure 6. MS/vDBB theta-off cell discharge patterns and the simultaneous slow wave activity recorded from stratum moleculare of the dentate gyrus. A: Examples of phasic linear (cell 35-2) and phasic nonlinear (cell 21-1) theta-off cells. The discharge rate during higher frequency theta (middle) was considerably less than the discharge rate during lower frequency theta (left) for cell 35-2. During LIA (right), this cell discharged at a higher rate than the discharge rates observed at higher frequencies of theta. Phasic nonlinear theta-off cell 21-1 discharged at the same rate during both frequencies of theta and discharged at a higher rate during LIA. B: An example of a tonic linear theta-off cell (cell 24-6). Cell 24-6 discharged at a higher rate during lower frequency theta (left) and decreased its discharge rate during higher frequency theta (middle). During LIA (right), cell 24-6 discharged at a rate which was greater than its mean discharge rate during theta.

THETA-OFF CELLS (Medial Septum/Diagonal Band)

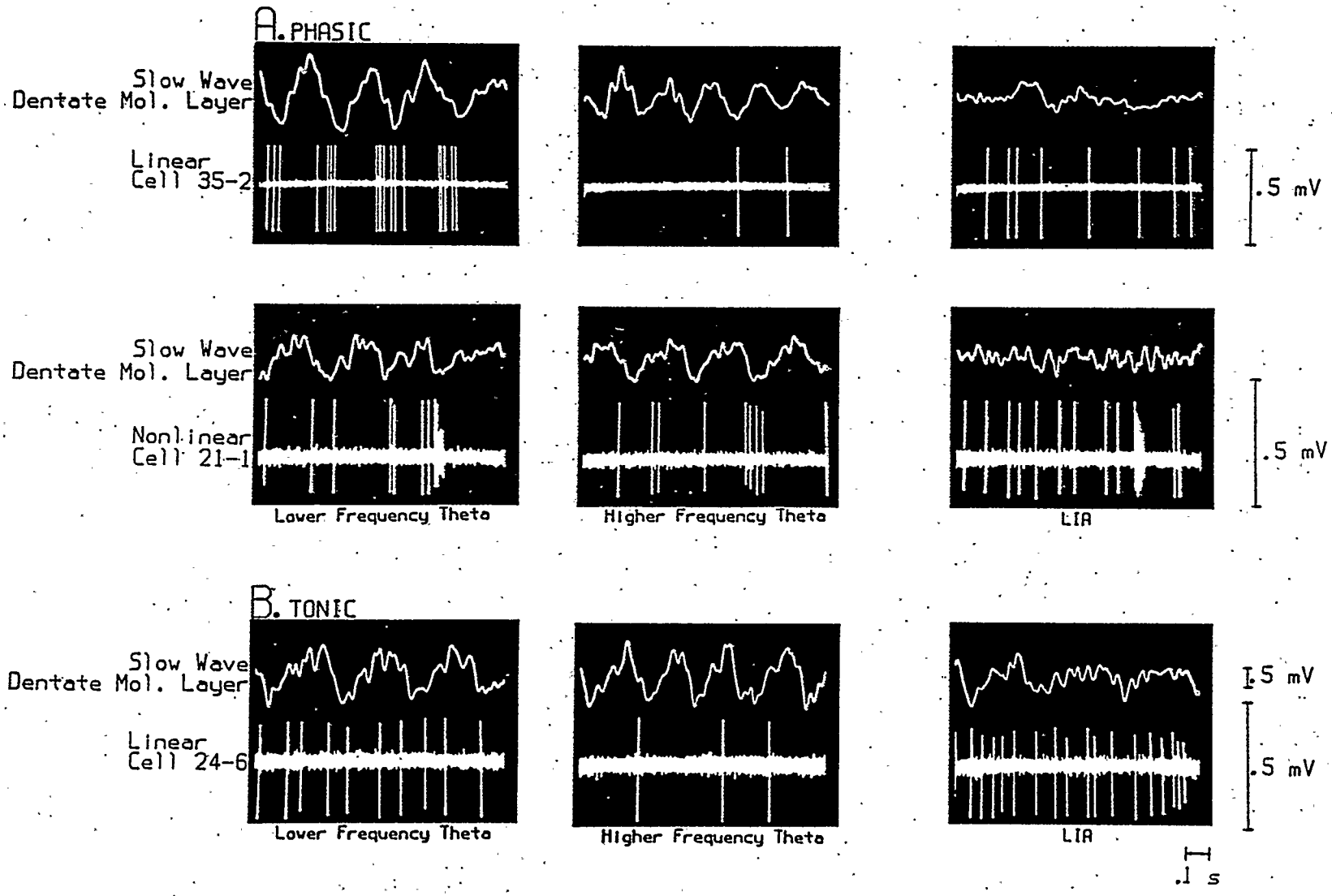

of examples of the two phasic cell types, phasic linear (cell 35-2) and phasic nonlinear (cell 21-1) theta-off cells. Part B is an example of a tonic linear theta-off cell, cell 24-6. This figure shows (part A) that an increase in theta frequency (left to right) resulted in a decrease in the discharge rate for the phasic linear theta-off cell which then increased during LIA (right). The phasic nonlinear theta-off cell discharged at a constant rate during both frequencies of slow wave theta (left and middle panels) and at a higher rate during LIA (right). Tonic linear theta-off cell 24-6, as was the case with the phasic linear theta-off cell, discharged at a rate that was less during higher frequency theta (middle) than during lower frequency theta (left) and discharged at a greater rate during LIA (right).

Figure 7 provides examples of the scatterplots and regression lines of four cells, one from each linear subtype of theta-on and theta-off cell. Figure 7A shows the scatterplot for cell 11-2. This phasic linear theta-on cell had an R^2 value of 0.767 and the slope of the regression line was 16.01 spikes/s/Hz (solid line). This particular cell had a mean discharge rate during LIA (broken line) which was less than the minimum observed discharge rate during slow wave theta activity. The scatterplot in figure 7B from tonic linear theta-on cell

Figure 7. The relationship between unit discharge rates and slow wave theta frequency for examples of the theta-on and theta-off cell linear subtypes. A: The scatterplot for phasic linear theta-on cell 11-2. The solid line is the regression line of unit discharge rate on theta frequency ($y = 16.02x - 50.24$, S.E. = 2.92) and the broken line is the mean discharge rate during LIA ($\bar{X} = 5.0 \mp 2.3$ spikes/s). B: The scatterplot for tonic linear theta-on cell 2-2. The regression line ($y = 11.23x - 23.10$, S.E. = 3.29) indicates the predicted change in discharge rate that would accompany a specific change in theta frequency, in this case 11.23 spikes/s/Hz. The discharge rate during LIA (broken line) was 12.2 ∓ 2.0 spikes/s. C: Phasic linear theta-off cell 35-3. The regression line ($y = -24.86x + 129.99$, S.E. = 6.77) demonstrates that this cell stops discharging at about 5.25 Hz. The mean discharge rate during LIA (broken line) was 13.6 ∓ 3.8 spikes/s. D: The scatterplot for tonic linear theta-off cell 36-1. The regression line ($y = -3.43x + 28.15$, S.E. = 2.26) shows that the slope of this cell had a smaller magnitude than those in A, B, and C. This cell did not stop discharging at any observed theta frequency. The mean discharge rate during LIA (broken line) was 9.9 ∓ 2.9 spikes/s. Interpretation of the regression lines must not be extended beyond the range of theta frequencies observed during urethane anaesthesia due to additional factors which may affect discharge rates in such situations.

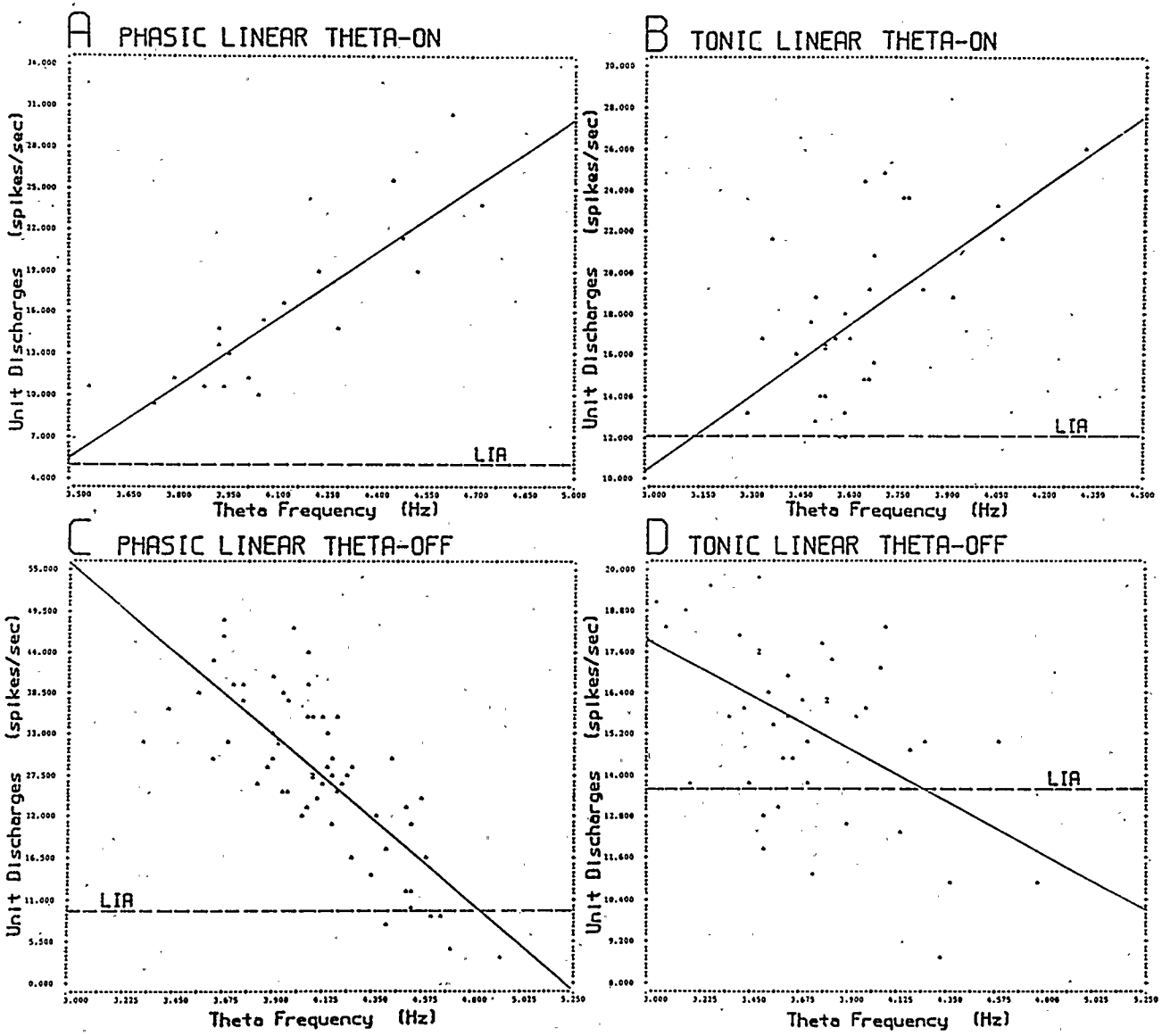
A PHASIC LINEAR THETA-ON
Unit Discharges (spikes/sec)
Theta Frequency (Hz)
LIA
B TONIC LINEAR THETA-ON
Unit Discharges (spikes/sec)
Theta Frequency (Hz)
LIA
C PHASIC LINEAR THETA-OFF
Unit Discharges (spikes/sec)
Theta Frequency (Hz)
LIA
D TONIC LINEAR THETA-OFF
Unit Discharges (spikes/sec)
Theta Frequency (Hz)
LIA

2-2 shows a similar situation compared to the plot of figure 7A. The slope (b = 11.23 spikes/s/Hz) was less than the phasic linear theta-on cell. Cell 2-2 had an R^2 value of 0.367 and a mean discharge rate during LIA (broken line) which was less than the mean rate during theta.

Figure 7C is the scatterplot of a phasic linear theta-off cell, cell 36-1. It had the steepest slope (b = -24.86 spikes/s/Hz) and the highest R^2 value (R^2 = 0.604) of the phasic linear theta-off cells. This cell also was one of five cells which became quiescent at higher theta frequencies. During LIA the mean discharge rate was greater than during the higher theta frequencies, but was still well below the mean discharge rate during theta (broken line). The scatterplot in figure 7D, is from a tonic linear theta-off cell, cell 35-3. The small slope (b = -3.43 spikes/s/Hz) was typical of this group of cells and was smaller than the slopes for phasic linear theta-off cells. Its R^2 value of 0.268 was very close to the mean for this group. As was also typical of this subtype, the mean discharge rate during LIA (broken line) was well within the range of discharge rates observed during hippocampal theta activity. Unlike the phasic linear theta-off cells, none of the tonic linear theta-off cells shut off during higher frequency slow wave theta.

Summarizing the data further, figure 8 compares the proportions of phasic (n = 38) and tonic (n = 27) cells which were linear and nonlinear theta-on, and linear and nonlinear theta-off, as well as the proportions of phasic and tonic cells which were unrelated by discharge rate to hippocampal slow wave theta. For linear and nonlinear theta-on cells the proportions of phasic and tonic cells were approximately equal. The major differences occurred between the tonic and phasic theta-off cells and in the proportions that were unrelated. Only three of 27 tonic cells (11.1 %), compared to nine of 38 phasic cells (23.7 %) were linear theta-off cells. Nonlinear theta-off cells were less common than the other subtypes for phasic cells and nonexistent within the tonic cells. The least common type of phasic cell were those that were unrelated by discharge rate to slow wave theta (n = 3, 7.9 %). For the tonic cells, those that were unrelated to theta (n = 9, 33.3 %) were more common than any subtype, theta-on or theta-off.

Figure 9 provides a different perspective for comparison. It compares proportions of theta-on and theta-off cells that were phasic, linear and nonlinear; and tonic, linear and nonlinear. The fact that there were more than twice as many theta-on cells than theta-off cells is of basic importance, but there were also two major

Figure 8. Proportions of phasic and tonic cells which were: theta-on, linear and nonlinear, theta-off, linear and nonlinear, and unrelated by discharge rate to slow wave theta. Major differences in the proportion of phasic and tonic cells occur in the linear theta-off (phasic, 23.7 %; tonic, 11.1 %) nonlinear theta-off (phasic, 10.5 %; tonic 0.0 %) and those that were unrelated (phasic, 7.9 %; tonic, 33.3 %).

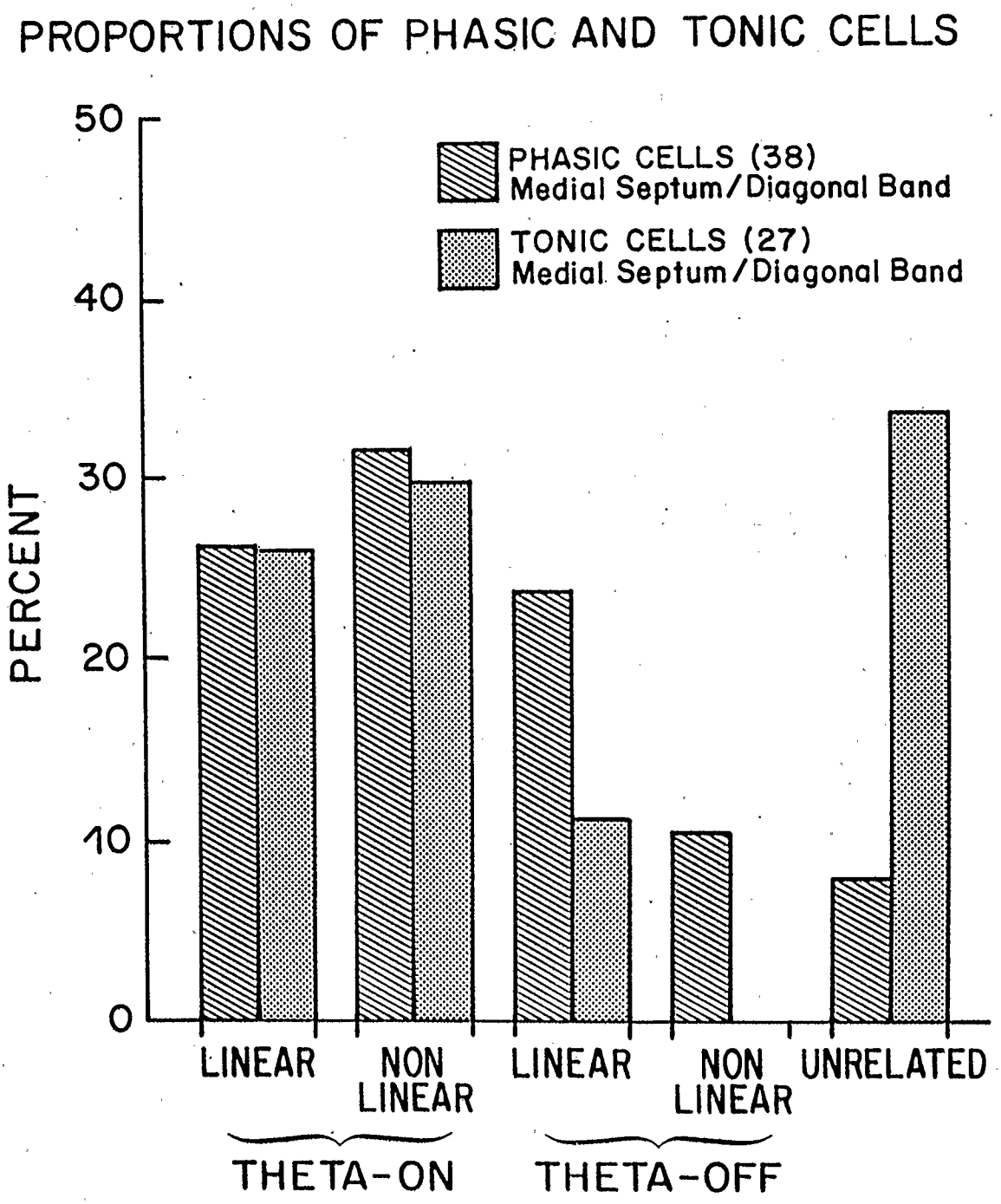
PROPORTIONS OF PHASIC AND TONIC CELLS
PHASIC CELLS (38)
Medial Septum/Diagonal Band
TONIC CELLS (27)
Medial Septum/Diagonal Band
PERCENT
50
40
30
20
10
0
LINEAR
NON LINEAR
LINEAR
NON LINEAR
UNRELATED
THETA-ON
THETA-OFF

Figure 9. Proportions of theta-on cell subtypes compared to theta-off cell subtypes. Proportions of cells that were phasic linear (theta-on, 27.0 %; theta-off, 56.2 %) differed to a large degree. Tonic nonlinear cells that decreased their rate of discharge during the theta state were not observed.

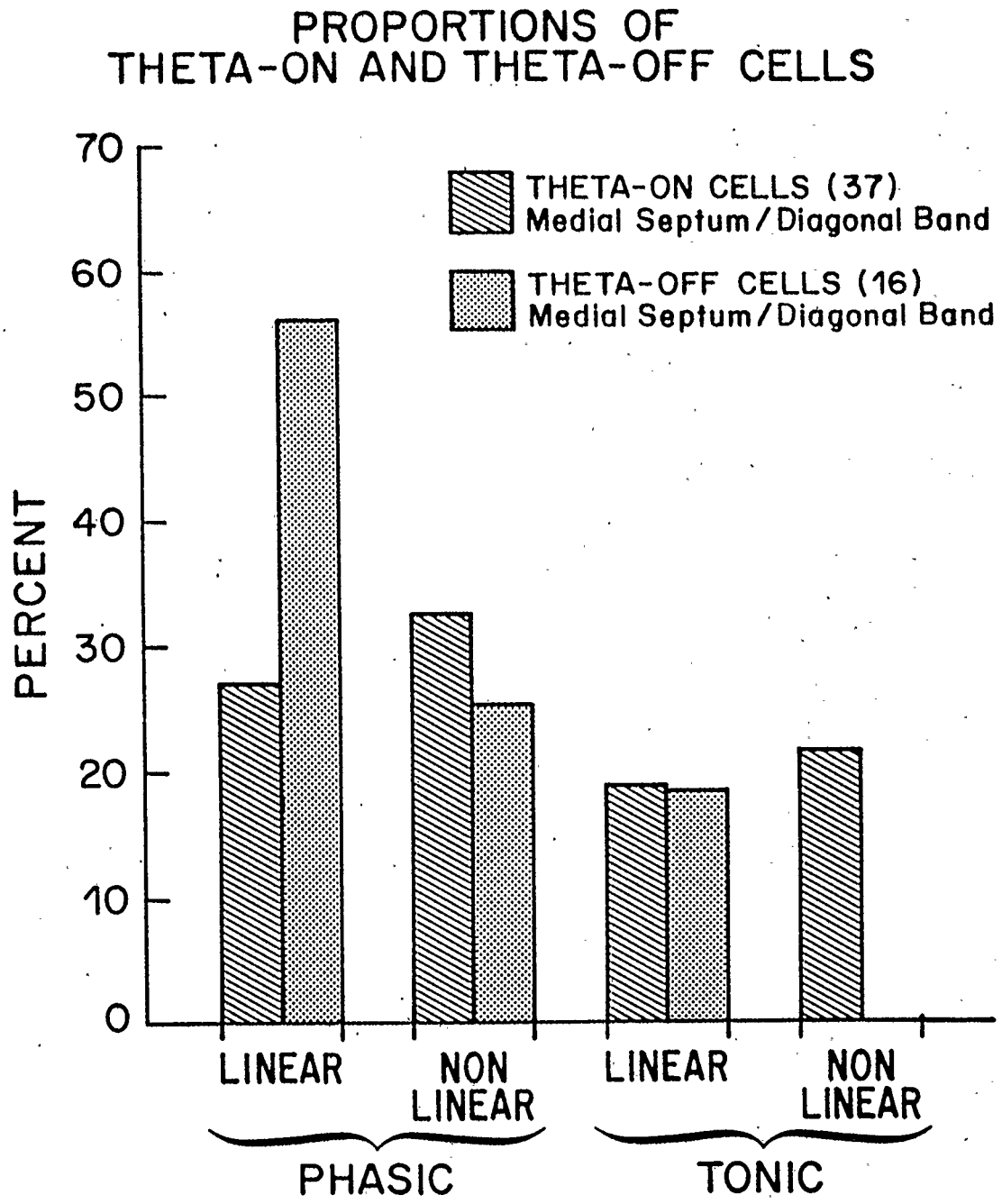
PROPORTIONS OF
THETA-ON AND THETA-OFF CELLS
70
60
50
40
30
20
10
0
PERCENT
THETA-ON CELLS (37)
Medial Septum/Diagonal Band
THETA-OFF CELLS (16)
Medial Septum/Diagonal Band
LINEAR
NON LINEAR
LINEAR
NON LINEAR
PHASIC
TONIC

differences between the subtypes of theta-on and theta-off cells. The largest difference was in the proportion of cells that were phasic linear (27.0 % - 56.2 %), although there was no real difference in the absolute number of cells. Ten cells were phasic linear theta-on (27.0 %) and nine cells were phasic linear theta-off (56.2 %). The other main difference between the theta-on and theta-off cells was that there were no tonic nonlinear theta-off cells while 21.6 percent of theta-on cells were tonic nonlinear. There seems to have been much more consistency as far as the proportion of theta-on cells that were within each possible subtype when compared to theta-off cells.

There were also differences in the location of the various cell types, as indicated by histology. Histology was not as accurate in determining the dorsal-ventral location as it was for the medial-lateral direction. Phasic cells were located on or very near to the midline in every case. On the other hand, tonic cells were recorded at virtually all medial-lateral areas of the MS/vDBB. Tonic cells that were linearly correlated to slow wave theta activity were located medially, very close to the midline. Tonic cells that were not related to slow wave theta in any way (n = 9) were the most laterally recorded cells. Seven of these cells were located at, or near the border between the medial and lateral septal nuclei. Two

were recorded on the midline and one of these was located in the ventral portion of the vDBB.

Stimulation Induced Activity

Twenty seven isolated neurons were recorded during stimulation of the DM-PH. Spontaneous activity was analyzed for 25 of these cells. Both of the remaining two cells could not be studied during spontaneous slow wave theta due to the level of anaesthesia. That is, theta could not be induced with a firm tail pinch and only continuous LIA was observed in the EEG record.

Stimulation of the DM-PH was confirmed by two criteria. A linear relationship between stimulation intensity and theta frequency was observed in 20 of the 27 neurons (see table 5). Histology demonstrated that the stimulating electrode was placed in the DM-PH for these 20 cells (13 animals). For each of these 20 cells, the frequency range of stimulation induced theta was larger than the frequency range observed during spontaneous theta. This was due to the fact that high intensity stimulation (400 - 500 μA) produced higher frequency theta than was observed spontaneously.

For the seven remaining cells, theta was either not observed following the stimulation period (n = 2), or was not linearly related to stimulation intensity (n = 5). Six

Table 5

Casewise summary of the relation between theta frequency and stimulation intensity

Spontaneous cell type		Cell Number	R^2	Slope (Hz/100μA)	p
Theta-on cells					
Phasic	Linear	4-2	0.673	0.455	<.001
		11-2	0.709	0.459	<.001
		17-3	0.920	0.671	<.001
	Nonlinear	1-2	0.329	0.323	<.01
		8-1	0.506	0.203	<.001
		15-5	0.345	0.228	<.01
		16-1	0.307	0.161	<.001
		25-1	0.359	0.381	<.01
		25-2	0.311	0.292	<.01
Tonic	Linear	2-2	0.707	0.358	<.001
	Nonlinear	2-4	0.318	0.205	<.001
		15-1	0.664	0.275	<.001
		19-3	0.524	0.419	<.001
		26-2	0.507	0.391	<.001
		26-3	0.495	0.299	<.01
Theta-off cells					
Phasic	Linear	4-1	0.474	0.286	<.001
	Nonlinear	21-1	0.461	0.379	<.01
No Relation					
Tonic		26-4	0.604	0.474	<.001
Unknown					
Phasic		2-3	0.185	0.201	<.01
Tonic		11-1	0.783	0.422	<.001

of these seven cells were recorded from three animals. Histology indicated that the stimulating electrode was not in the correct position in these three animals. Although the stimulating electrode was correctly positioned for the remaining cell, the cell discharged at a rate which could not be analyzed. One second did not contain a sufficient number of spikes to be interpreted, and the effects of stimulation could not be accurately assessed at longer post-stimulation intervals.

The spontaneous activity of 18 of the 20 cells indicated that 15 were theta-on cells, two were theta-off cells, and one was unrelated by discharge rate to the theta rhythm (tonic). Two of the 20 cells were not analyzed during spontaneous theta activity. Of the 15 theta-on cells: three were phasic linear, six were phasic nonlinear, one was tonic linear, and five were tonic nonlinear. Both theta-off cells which were recorded during stimulation were phasic; one of which was linear and the other nonlinear. Finally, one of the two cells without the analysis of spontaneous activity was determined; from the post-stimulation ACH, ISIH, TDH, and TCSH; to be phasic and the other tonic.

Stimulation of the DM-PH did not have an effect on the pattern of discharges observed for any neuron. Post-stimulation ACHs, ISIHs, TDHs,and TCSHs were used, as

they were for spontaneous activity, to determine the pattern of cell discharges and their relation to slow wave theta, following stimulation of the DM-PH. Of the 18 neurons recorded during spontaneous theta, none became phasic as a result of stimulation, at any intensity, that were previously tonic (n = 7), and none became tonic that were previously phasic (n = 11).

The majority of cells recorded during stimulation were theta-on cells (n = 15). In the case of phasic linear (n = 3) and tonic (n = 1) linear theta-on cells, stimulation of the DM-PH resulted in a positive linear relation between stimulation intensity and unit discharge rate ($p < .001$). Table 6 lists the R^2 values and slopes for each of these cells. The relationship between discharge rate and slow wave theta frequency was also linear positive ($p < .001$). The correlations between theta frequency and unit discharge rate were 0.800 for the tonic cell and ranged from 0.742 to 0.797 for the phasic cells ($\bar{r} = 0.772 \mp 0.028$). Thus, stimulation did not alter the nature of the relationship between the unit discharges and slow wave theta.

Figure 10A graphically demonstrates the relationships between unit discharge rate and stimulation intensity (left), and theta frequency and stimulation intensity (right) for phasic linear theta-on cell 11-2. The R^2 value

Table 6

Casewise summary of the relation between unit discharge rate and stimulation intensity

Spontaneous cell type		Cell Number	R^2	Slope (Hz/100μA)	p
Theta-on cells					
Phasic	Linear	4-2	0.818	7.28	<.001
		11-2	0.566	3.99	<.001
		17-3	0.621	7.40	<.001
	Nonlinear	1-2	0.288	4.17	<.01
		8-1	0.677	4.82	<.001
		15-5	0.532	9.35	<.001
		16-1	0.492	3.21	<.001
		25-1	0.241	2.89	<.01
		25-2	0.722	4.60	<.001
Tonic	Linear	2-2	0.816	6.07	<.001
	Nonlinear	2-4	0.185	-2.17	<.01
		15-1	0.310	-1.03	<.001
		19-3	0.001	----	n.s.
		26-2	0.296	0.85	<.01
		26-3	0.076	----	n.s.
Theta-off cells					
Phasic	Linear	4-1	0.279	2.74	<.001
	Nonlinear	21-1	0.029	----	n.s.
No Relation					
Tonic		26-4	0.622	4.06	<.01
Unknown					
Phasic		2-3	0.556	2.69	<.001
Tonic		11-1	0.805	6.06	<.001

Figure 10. Graphic representation of the relationship between unit discharge rate and stimulation intensity (left panels), and between theta frequency and stimulation intensity (right panels) for phasic linear theta-on cell 11-2 (part A) and tonic linear theta-on cell 2-2 (part B). Mean discharge rate and standard deviation (vertical bars) are plotted for each level of hypothalamic stimulation as are the mean and standard deviation of theta frequency for both the phasic (A) and the tonic (B) linear theta-on cell. A: The regression lines of unit discharge rate on hypothalamic stimulation ($y = 0.0399x + 1.25$, S.E. = 4.54) and theta frequency on hypothalamic stimulation ($y = 0.00459x + 2.54$, S.E. = 0.344) are provided for cell 11-2. B: The regression lines for unit discharge rate ($y = 0.0607x + 3.65$, S.E. = 2.97) and theta frequency ($y = 0.00358x + 3.69$, S.E. = 0.213) versus hypothalamic stimulation are also provided for cell 2-2.

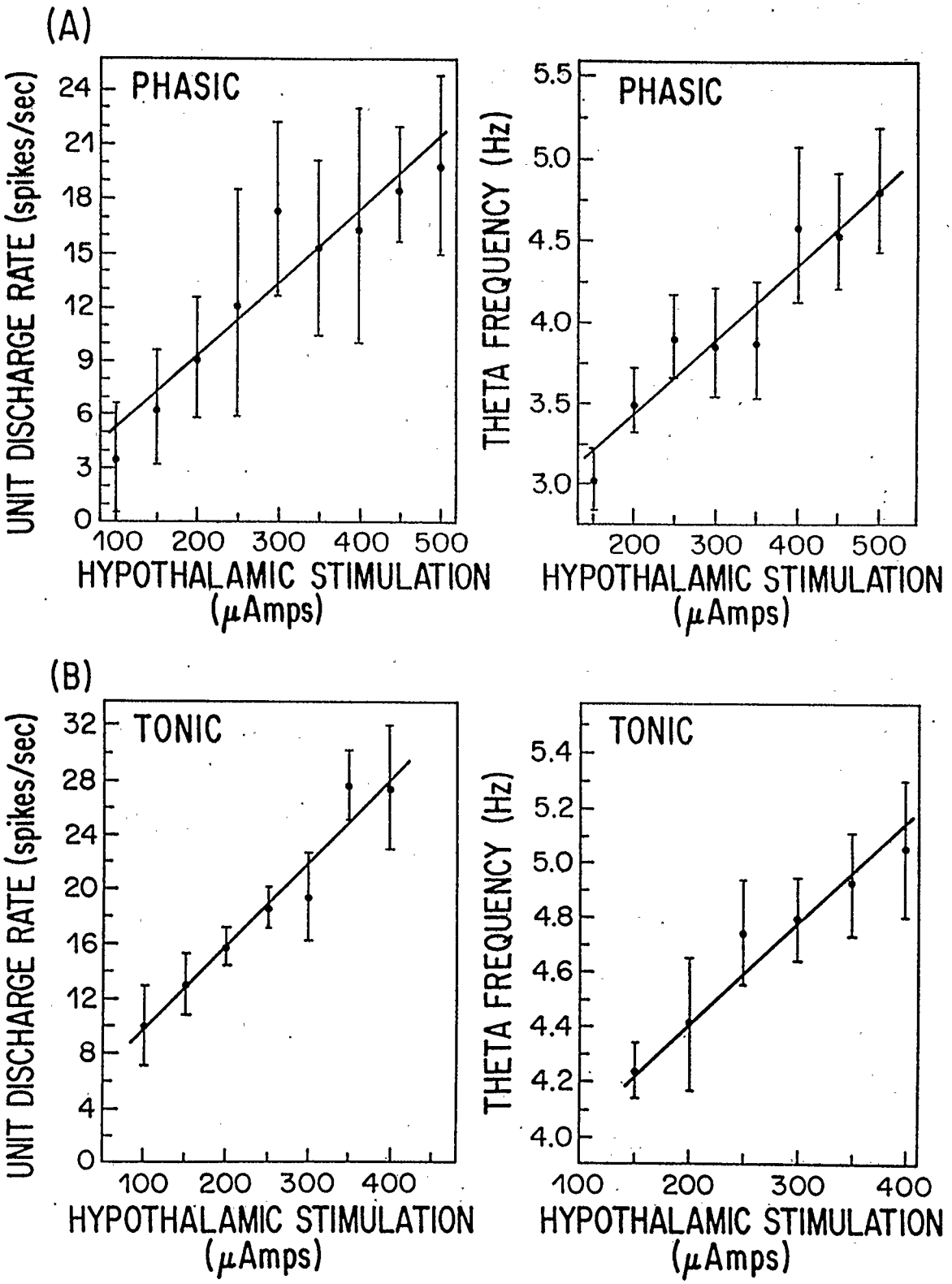
(A)
PHASIC
UNIT DISCHARGE RATE (spikes/sec)
0
3
6
9
12
15
18
21
24
100 200 300 400 500
HYPOTHALAMIC STIMULATION
(μAmps)
PHASIC
THETA FREQUENCY (Hz)
3.0
3.5
4.0
4.5
5.0
5.5
200 300 400 500
HYPOTHALAMIC STIMULATION
(μAmps)
(B)
TONIC
UNIT DISCHARGE RATE (spikes/sec)
0
4
8
12
16
20
24
28
32
100 200 300 400
HYPOTHALAMIC STIMULATION
(μAmps)
TONIC
THETA FREQUENCY (Hz)
4.0
4.2
4.4
4.6
4.8
5.0
5.2
5.4
100 200 300 400
HYPOTHALAMIC STIMULATION
(μAmps)

for the relationship of cell discharge rate to stimulation intensity was 0.566 with a slope of 3.99 spikes/s/100 μA. The R^2 value for the relation between theta frequency and stimulation intensity was 0.709 with a slope of 0.412 Hz/100 μA. Figure 10B shows the same graphs for tonic linear theta-on cell 2-2. The R^2 value for the relationship between unit discharge rate and stimulation of the hypothalamus was 0.816 with a slope of 6.07 spikes/s/100 μA and between theta frequency and stimulation intensity was 0.707 with a slope of 0.321 Hz/100 μA.

Eleven of the 15 theta-on cells recorded during stimulation induced theta were nonlinear theta-on cells. Six of these cells were phasic and five were tonic. An increase in stimulation intensity resulted in a linear increase in the discharge rate for all six phasic cells. R^2 values, which are listed in table 6, ranged from 0.241 to 0.722 while the slopes, which are also listed in table 6, ranged from 2.89 to 9.35 spikes/s/100 μA. During stimulation, the discharge rates for five of the six phasic cells became positively correlated to the frequency of the theta rhythm. The correlations for these five cells ranged from 0.540 to 0.705 ($\bar{r}$ = 0.612 ∓ 0.070). In the case of the sixth cell, the discharge rate remained unrelated to theta frequency (1-2; r = 0.195). The range of theta frequencies observed during stimulation was limited

(4.06 - 4.97 Hz), thus making a potential relationship difficult to detect. On the other hand, linearity was detected in situations where the frequency range of slow wave theta was less than 0.91 Hz.

An example of a phasic nonlinear theta-on cell which coded the level of activation of the DM-PH in a positive linear fashion, is provided in figure 11 Figure 11A shows that during spontaneous activity, cell 16-1 discharged at the same rate during lower and higher frequency theta and decreased its discharge rate during LIA. Figure 11B demonstrates that both theta frequency and discharge rate increased with an increase in the stimulation current. The cell decreased its discharge rate in the absence of DM-PH stimulation.

Table 6 shows that the effects of stimulation on discharge rate were much more variable for tonic nonlinear theta-on cells than for phasic nonlinear theta-on cells. Out of five tonic nonlinear theta-on cells, only one responded to increased stimulation intensity with a significant linear increase in discharge rate (26-2) and two cells responded with linear decreases in their discharge rates (2-4 and 15-1). One cell was inhibited by the stimulation (19-3). That is, its mean discharge rate during stimulation ($\bar{X}$ = 0.8 $\mp$ 0.8 spikes/s) was significantly less than ($p < .01$) its mean discharge rate

Figure 11. An example of the effects of stimulation on a phasic nonlinear theta-on cell (16-1). A: Spontaneously this cell discharged at approximately the same rate during lower frequency theta (left panel) as it did during higher frequency theta (middle panel) and decreased its discharge rate during LIA (right panel). B: Stimulation of the DM-PH at 200 μA (left panel) resulted in a discharge rate which was less than the discharge rate produced during 500 μA stimulation (middle panel). The cell discharged at a decreased rate in the absence of stimulation current (right panel).

PHASIC NONLINEAR THETA-ON CELL

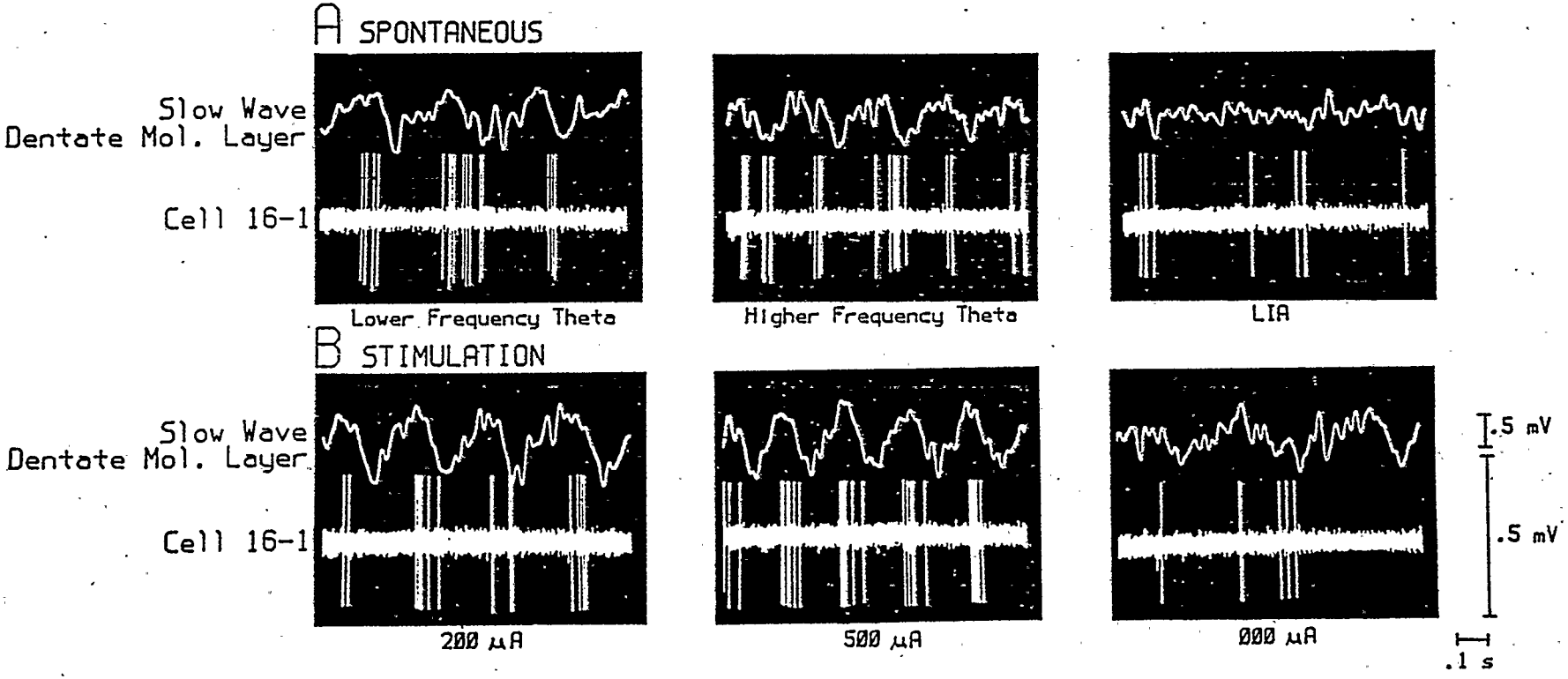

during slow wave theta ($\bar{X}$ = 4.4 ∓ 1.7 spikes/s) and during LIA ($\bar{X}$ = 3.0 ∓ 1.4 spikes/s). For the last cell (26-3), stimulation had no effect on the discharge rate. The mean discharge rate during stimulation induced theta was ($\bar{X}$ = 12.4 ∓ 3.2 spikes/s) not significantly different from the mean discharge rate during spontaneous theta ($\bar{X}$ = 12.4 ∓ 3.2 spikes/s).

During stimulation of the DM-PH, the relationship between discharge rate and theta frequency was also more variable for tonic nonlinear theta-on cells. Only one of two tonic nonlinear theta-on cells (15-1) whose discharge rates were negatively related to stimulation intensity, had a corresponding negative linear relationship between discharge rate and the frequency of theta ($r = -0.704$; $p < .01$). The other tonic nonlinear theta-on cell with a negative linear relationship between discharge rate and stimulation intensity (2-4), and the tonic nonlinear theta-on cell with a positive linear relationship (26-2) did not have significant relationships between their discharge rates and the frequency of theta. In addition, neither of the tonic nonlinear theta-on cells without linear relationships between their discharge rates and stimulation intensity had linear relationships between discharge rate and slow wave theta frequency during stimulation induced theta activity.

Although there were only two theta-off cells studied during stimulation of the DM-PH, it is interesting to note that both the linear and nonlinear phasic theta-off cells had increased discharge rates as a result of stimulation. During spontaneous activity, the discharge rate of phasic linear theta-off cell 4-1 was inversly related to the frequency of the slow wave theta (figure 12A). However, during stimulation its discharge rate was positively correlated to the frequency of the theta rhythm ($r = 0.518$; $p < .01$; figure 12B) and to the intensity of the stimulation (table 6; figure 12C). The relationship between theta frequency and the level of hypothalamic stimulation was also linear positive (table 5; figure 12D).

Although the discharge rate of phasic nonlinear theta-off cell 21-1 was not linearly related to the intensity of DM-PH stimulation, there was a nonlinear effect. Furthermore, during stimulation induced activity, as was the case with spontaneous activity, cell 21-1 discharged at a rate which was not linearly related to the frequency of theta ($r = 0.407$). However, unlike the spontaneous situation, the post-stimulation discharge rate of this cell ($\bar{X} = 11.8 \mp 2.7$ spikes/s), which was accompanied by hippocampal theta, was significantly greater than the mean discharge rate during spontaneously produced

Figure 12. Scatterplots of the data for cell 4-1 demonstrating the relationship between: cell discharge rate and theta frequency during spontaneous activity (A), cell discharge rate and theta frequency during stimulation of the DM-PH (B), cell discharge rate and stimulation intensity (C), and theta frequency and stimulation intensity (D). A: The discharge rate of phasic linear theta-off cell 4-1 was negatively related to theta frequency during spontaneous activity ($y = -15.48x + 99.84$, S.E. = 5.39). B: Stimulation of the DM-PH resulted in a positive linear relationship between discharge rate and theta frequency ($y = 6.33x + 7.84$, S.E. = 4.63). C: Increased stimulation current resulted in an increased discharge rate ($y = 0.0218x + 25.19$, S.E. = 4.34). D: The relationship between theta frequency and stimulation intensity was linear positive ($y = 0.00286x + 2.90$, S.E. = 0.2929), just as it was for all cells recorded during stimulation of the DM-PH.

PHASIC LINEAR THETA-OFF CELL

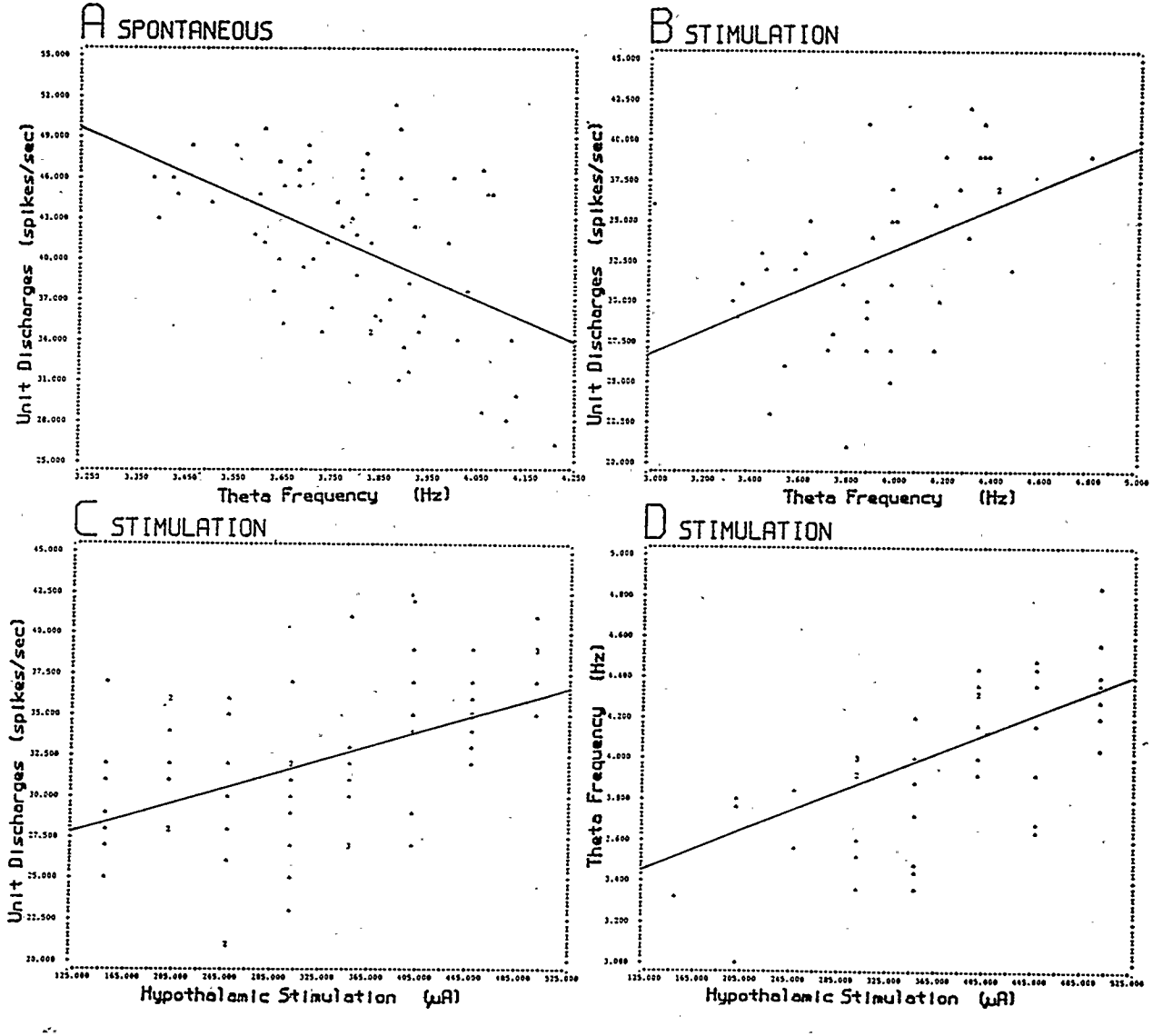

theta ($\bar{X}$ = 9.7 ∓ 2.0 spikes/s; $p < .001$) and equivalent to the discharge rate during LIA ($\bar{X}$ = 13.1 ∓ 3.9 spikes/s).

The last of the 18 cells which were recorded spontaneously and during the stimulation regimen (26-4), did not have a relationship, either linear or nonlinear, between discharge rate and spontaneous hippocampal theta. The discharge rate of this cell increased linearly with an increase in the intensity of the stimulation (see table 6), as did the frequency of the accompanying slow wave theta (see table 5). However, the frequency of the post-stimulation theta rhythm was not correlated to the unit discharge rate. This may have been due to the fact that the effects of stimulation on discharge rate were of short duration. Stimulation resulted in approximately 200 ms of high frequency discharges followed by a return to the mean spontaneous discharge rate ($\bar{X}$ = 2.5 spikes/s), for the remainder of the one second, post-stimulation period.

Finally, two cells were recorded during the stimulation regimen which were not analyzed during spontaneous activity. As was reported previously, the post-stimulation ACH, ISIH, and TCSH provided evidence that one cell was tonic (11-1) and that the other cell was phasic (2-3). The discharge rates of cells 11-1 and 2-3 were related to the intensity of DM-PH stimulation in a positive linear fashion.

Probably the most interesting result from the effects of stimulation was the fact that all phasic cells, regardless of their spontaneous relationship to theta frequency, were activated by stimulation of the DM-PH. Eleven of 12 phasic cells had a positive linear relation between discharge rate and the intensity of the stimulation. The same was not true for tonic cells. The effects of stimulation were much more variable, with only four of eight cells having been activated in a positive linear fashion. Two cells linearly decreased their rate of discharge to increased stimulation intensity, one cell responded to stimulation with a nonlinear decrease in discharge rate, and one tonic cell was not affected by stimulation of the DM-PH.

DISCUSSION

Spontaneous Activity

The majority of previous studies of cellular activity in the septal region concentrated on classifying neurons according to their degree of rhythmicity. Accordingly, the main emphasis was also on the EEG state of theta in the HF. The present results confirmed the basic findings of previous research and also extended them into two further dimensions that had received little or no attention. That is, while confirming the presence of rhythmic and arrhythmic neurons (pattern), the main conclusion was that MS/vDBB neurons were more precisely related to hippocampal EEG states according to details of their discharge rates (on-off, linear-nonlinear).

Cell Discharge Patterns

The results have confirmed previous findings regarding the rhythmicity of MS/vDBB neurons. In the present work, rhythmic neurons were classified as phasic if they exhibited regular alternating changes in their discharge pattern between firing and silence (often in bursts), with a phase relation to theta. Cells that were arrhythmic were classified as tonic if they exhibited irregular and

continuous firing patterns, and had no phase relation with hippocampal theta.

Like the original studies of Petsche, Stumpf, and colleagues (Petsche, et al., 1965; Stumpf, et al, 1962), and Apostol and Cruetzfeldt (1974), the present work defined two groups of neurons. However, several studies have classified MS/vDBB neurons into three groups (Petsche, et al., 1965; Wilson, et al., 1965; Gaztelu and Buno, 1982). Although there were differences between these three studies, the basic thrust was that there were neurons that were: rhythmic bursting, in phase with hippocampal theta; nonrhythmic bursting, with a greater probability of discharging on a preferred phase of hippocampal theta; and nonrhythmic, irregularly discharging neurons. The emphasis of the present work was not to define the specific nature of the phase relationship to theta, but simply to determine whether a phase relationship existed. It is likely that most of the nonrhythmic, bursting neurons recorded in this study were classified as tonic because these neurons would not have had a bimodal ISIH, nor a periodic ACH (Gaztelu and Buno, 1982), which was necessary for a cell to be classified as phasic. It is possible that some nonrhythmic, bursting neurons were classified as tonic, depending on the the nature of the phase relationship, and

whether these neurons could have exhibited periods of rhythmicity.

Cell discharges were phasically related to hippocampal theta in 58 % of the recorded MS/vDBB neurons. Phasic cells showed varying degrees of rhythmicity, however, this was not of central importance. The phase angle was constant between samples for a single cell, but varied from cell to cell. Tonic cells were also recorded in the MS/vDBB in proportions which were consistent with previous reports. The discharge patterns of these cells also varied.

Approximately 1/4 of the phasic MS/vDBB cells were rhythmic during LIA, which is consistent with previous results (Petsche, et al., 1962; Stumpf, et al., 1962; Macadar, et al., 1971; Wilson, et al., 1976). However, the LIA samples were not analyzed for the presence of a dominant frequency, which might have equalled the burst rate. The rhythmicity was not as consistent as in the theta state. No instances of rhythmicity were observed in tonic MS/vDBB cells during LIA.

Linear vs. Nonlinear Discharge Rates

Neurons were classified as linear if a regression analysis showed that their discharge rates changed in a significant positive, or negative manner in relation to

changes in theta frequency. Neurons were classified as nonlinear if the regression analysis failed to reveal a significant linear relationship between changes in discharge rate and changes in theta frequency. Approximately 45 % of the recorded cells demonstrated a linear relationship to the frequency of theta, 2/3 of which were positively related (theta-on), while 1/3 were negatively related (theta-off). Petsche, et al. (1962) noted a positive correlation between discharge rate and theta frequency, but did not report a negative relationship. The discharge rates of the remaining 55 % of the MS/vDBB neurons were not related to theta frequency in a linear fashion.

Theta-on vs. Theta-off

Neurons were classified as theta-on if they exhibited a positive linear relation to theta frequency and/or if their discharge rates were significantly greater during theta than during LIA. Neurons were classified as theta-off if they exhibited a negative linear relation to theta frequency and/or if their discharge rates were significantly greater during LIA than during theta.

Although 55 % of the neurons in the MS/vDBB did not have a linear relationship with theta frequency, 2/3 of these cells discharged at significantly different rates

during slow wave theta and LIA. Twenty of these 24 cells were theta-on cells and four were theta-off cells. The discharge rates of only 18 % of the recorded cells were not related to hippocampal theta, although 1/4 of these cells were phasic, and therefore were related to hippocampal theta by their discharge pattern.

The majority of the MS/vDBB cells with discharge rates related to hippocampal theta were theta-on cells. Theta-on cells out-numbered theta-off cells 2:1. Of the theta-on cell types, phasic theta-on cells were more frequently observed than were tonic theta-on cells. However, the proportions of phasic and tonic theta-on cells that were linear and nonlinear were approximately equal. In addition to the fact that theta-off cells were less frequently observed, theta-off cells were not as evenly distributed amongst the various subtypes. Phasic linear theta-off cells accounted for more than half of the theta-off cells and, suprisingly, were as common as phasic linear theta-on cells. Unlike phasic nonlinear theta-on cells, which were the most frequently observed theta-on cells, phasic nonlinear theta-off cells were rarely observed. The same holds true for tonic theta-off cells. Tonic linear theta-off cells were infrequently observed and no MS/vDBB cells could be classified as tonic nonlinear theta-off cells.

The differences between tonic and phasic, theta-on and theta-off cells were not analyzed statistically because it was the goal of this thesis to differentiate and describe theta-on and theta-off cells in the MS/vDBB based on the type of relation each cell had with hippocampal theta. Although the differences between tonic linear and phasic linear theta-on cells were not analyzed statistically, it is fairly clear that the mean percentage of variance shared by the two variables (theta frequency and unit discharge rate) did not differ a great deal. The slopes ($\bar{b}$) of the linear relations were generally greater for phasic linear theta-on cells than for tonic linear theta-on cells, however, there was considerable overlap between the observed ranges.

The discharge rates of phasic nonlinear theta-on cells appear to be greater than the discharge rates of tonic nonlinear theta-on cells during the theta state, and the LIA state. However, the difference in discharge rates during LIA is considerably less than during the theta state.

As was the case for linear theta-on cells, the percentage of variance shared by the relationship between theta frequency and cell discharge rates was approximately equal for tonic and phasic linear theta-off cell subtypes. Moreover, this value was consistent between all linear

cells, theta-on or theta-off, phasic or tonic. Slope ($\bar{b}$), unlike R^2, was much greater for the phasic linear theta-off cells than it was for the tonic linear theta-off cells. In fact, the magnitude was greater for phasic linear theta-off cells than for both tonic and phasic linear theta-on cells. Conversely, the magnitude of the slope for tonic linear theta-off cells was considerably less than any other linear group. This was probably due to the low mean discharge rates observed in these cells.

It is interesting that in five of nine phasic linear theta-off cells the mean discharge rate during theta was considerably greater than during LIA. However, since these cells were linear, it is possible that if higher frequency theta were more common in the EEG record, the mean discharge rate during theta might have been reduced considerably.

Topography of MS/vDDB Neuron Types

Topographically, there appeared to be a medial-lateral organization of cells related to the hippocampal EEG. The discharge rates of medially located cells tended to be linearly related to hippocampal theta, while the discharge rates of more laterally located cells tended to be either, nonlinearly related to the hippocampal slow wave activity, or not related to hippocampal slow wave activity.

Moreover, cells that were laterally located tended to have lower discharge rates, with cells at the MS-LS border having the lowest discharge rates. There also appeared to be a medial-lateral topographic organization with discharge patterns. That is, phasic cells tended to be located medially, while tonic cells were located at all medial-lateral levels.

Stimulation Induced Activity

The results of DM-PH stimulation on theta frequency confirm past research, which determined that theta frequency and stimulation intensity had a positive linear relation (Bland and Vanderwolf, 1972; Bland, 1986; Colom, et al., 1987). In addition, stimulation did not change the discharge patterns of phasic and tonic cell types. Those cells that were phasic during spontaneous activity remained phasic during stimulation and those that were tonic remained tonic. This was consistent with the results of Wilson, et al. (1976), who found that stimulation of the DM-PH only produced rhythmic behavior in those neurons that were previously identified to be rhythmic bursting neurons.

In addition to the effects of stimulation on pattern, stimulation intensity was also linearly related to the discharge rates in 17 of 20 recorded MS/vDBB cells. The remaining three cells were nonlinear. Even though Wilson,

et al. (1976) did use a variety of stimulation intensities, they did not systematically study the effects of the different levels on discharge rates.

Fifteen of the 17 linear cells were positively related to stimulation intensity. Of the three remaining MS/vDBB cells, the discharge rate of one cell was excited in a nonlinear fashion. That is, its discharge rate was significantly greater during stimulation of the DM-PH than during spontaneous theta and LIA. The proportion of cells with discharge rates which were positively related to stimulation intensity far exceeded the proportion which were linearly related to theta frequency in the spontaneous results. This was probably due to the fact that stimulation was carried out in only two theta-off cells.

Two of the linearly related cells were negatively related to stimulation intensity. One of the three nonlinear cells was inhibited by stimulation in that its discharge rate during stimulation (accompanied by theta) was significantly less than its discharge rate during spontaneously produced theta. Finally, the last cell was not affected by stimulation of the DM-PH at any intensity.

Stimulation of the DM-PH was primarily studied in theta-on cells because theta-off cells generally failed to discharge during stimulation. As was expected, the effects of stimulation were more consistent in phasic theta-on

cells as opposed to tonic theta-on cells. Stimulation of the DM-PH in the case of phasic linear theta-on cells did not alter the nature of the spontaneous relationship between slow wave theta frequency and discharge rate. The relationships between stimulation intensity, theta frequency, and cell discharge rates were all linear positive. The effects of stimulation on phasic nonlinear theta-on cells were not as predictable. The relationship between stimulation intensity and cell discharge rate was linear positive, as was the relationship between theta frequency and discharge rate. That is, activation of the input from the DM-PH altered the spontaneous relationship.

Comparing the results of DM-PH stimulation on MS/vDBB neuron discharges to results obtained from hippocampal theta cells (Colom, et al., 1987) revealed a more consistent positive linear relationship in phasic MS/vDBB neurons than hippocampal theta cells, which were also all phasic. Only in one case was a phasic MS/vDBB cell discharge rate not linearly related to stimulation intensity in a positive manner and that cell was a theta-off cell. In the HF, only 8 of 12 cells were linearly related to stimulation intensity, all of which were positive (Colom, et al., 1987). This would indicate a more direct pathway from the DM-PH to the MS/vDBB, which was suggested by Colom, et al. (1987). In addition to

phasic cells in the MS/vDBB, linear and nonlinear relations were observed between tonic theta-on cell discharge rates and stimulation intensity. Colom et al. (1987) reported that all cells studied were theta cells (ie. rhythmic bursting, related to theta phase).

Only one tonic linear theta-on cell was recorded during stimulation of the DM-PH. Stimulation resulted in a positive linear relationship between stimulation intensity and cell discharge rate, and did not alter the nature of the spontaneous relationship. As was predicted, the effects of stimulation on tonic theta-on cells were more variable. In only one instance did stimulation of the DM-PH produce a linear relation between theta frequency and cell discharge rate. Stimulation excited, inhibited, or had no effect on tonic nonlinear theta-on cells.

Even though theta-off cells were not generally studied during stimulation, two cells which increased their discharge rates in response to stimulation were recorded. All phasic cells recorded during stimulation of the DM-PH increased their discharge rates during stimulation. The phasic nonlinear theta-off cell was the only phasic MS/vDBB cell with a nonlinear relationship between discharge rate and stimulation intensity. On the other hand, tonic cells were not consistent in their response to stimulation.

Conclusions

Spontaneous Activity

Unlike many studies on MS/vDBB neurons, the results of this study were more likely to reflect the total population of the MS/vDBB since cells were isolated during both hippocampal theta and LIA. The results suggest that studies which have isolated cells during the theta state alone may have neglected a group of cells which were either silent during theta, or discharging at very low rates. In this study, as was the case with previous research, there is a sampling bias based on size and density of the population of neurons being studied. It has been demonstrated that there are small, medium, and large neurons in the MS/vDBB (Swanson and Cowan, 1976, 1979). Moreover, they are not distributed evenly throughout the MS/vDBB. The overall conclusions of this study must be tempered by this bias. Therefore, it is important to emphasize the actual spontaneous relationships observed in MS/vDBB cells, more than the reported proportions.

The results suggest that the the MS/vDBB is more than a rhythmic pacemaker for hippocampal theta. The relationships between discharge rates and hippocampal theta cells described by Colom and Bland (1987) were observed in MS/vDBB cells as was predicted. Moreover, the definitions

of theta-on and theta-off cells were extended to include MS/vDBB cell types which were not observed in the HF. This was due to the fact that there was a large group of tonically discharging cells with discharge rates linearly related to theta frequency, both positively and negatively in the MS/vDBB. Colom and Bland (1987) only reported tonic nonlinear cells in the HF. In the MS/vDBB there was also a group of phasically discharging cells with discharge rates which were not linearly related to theta frequency, but were nonlinearly related to the theta state. Once again, phasic nonlinear theta-on and theta-off cells were not reported by Colom and Bland (1987). The identification of tonic linear theta-on and theta-off cells in the MS/vDBB provides support for the hypothesis that the MS/vDBB input to the HF is both phasic and tonic. Not only does the MS/vDBB function as a rhythmic pacemaker, but it also provides an afferent drive related to hippocampal theta, which is both phasic and tonic.

The early observations of Petsche and colleagues (Petsche, et al., 1962) suggested that the MS provided a rhythmic afferent drive to the HF which was necessary for the production of hippocampal theta, in addition to setting the frequency of the theta rhtyhm. Further work lead to the conclusion that the rhythmic MS/vDBB activity was the cause of, rather than the result of, hippocampal theta

(Petsche, et al., 1962; Stumpf, et al., 1962; Petsche, et al., 1965; Gogolak, et al., 1968; Tombol and Petsche, 1969). Macadar, et al. (1970) suggested that a minimum number of cell discharges was required for theta to occur. In addition to a rhythmic input to the HF, the nonrhythmic MS/vDBB cells supposedly provide a tonic level of depolarization; that is, a tonic afferent drive which is necessary for the occurrence of theta (Macadar, et al., 1970).

This hypothesis was supported by the fact that nonrhythmic MS/vDBB cells were shown to change their discharge rates in relation to a change in the hippocampal EEG state (Apostol and Creutzfeldt, 1974). Also in support of this hypothesis, nonrhythmic infusions of carbachol and eserine into the HF were shown to produce slow wave theta (Rowntree and Bland, 1986). Conversely, infusions of atropine sulfate blocked the induced hippocampal theta (Rowntree and Bland, 1986). It has been proposed by Bland (1986) that the activity level of the tonic MS/vDBB input to the HF determines whether theta is present in the hippocampal EEG. Supposedly, the role of the rhythmic cells is to modulate the frequency of the theta rhythm according to the level of ascending activation from the brainstem and diencephalon (Bland, 1986).

This hypothesis has received support from the observations of a carbachol-induced theta rhythm in hippocampal slices (Konopacki, MacIver, Bland and Roth, 1987a; Konopacki, Bland, MacIver and Roth, 1987; Konopacki, MacIver, Bland and Roth, 1987b; Bland, Colom, Konopacki and Roth, in press). Theta in the hippocampal slice resembles type 2 theta in the intact animal in that it is induced by infusions of carbachol and blocked by infusions of atropine sulfate (Konopacki, MacIver, Bland and Roth, 1987; Konopacki, Bland, MacIver and Roth, 1987; Konopacki, MacIver, Bland and Roth, 1987; Bland, Colom, Konopacki and Roth, in press). Intracellular recordings of a theta rhythm, *in vitro*, in addition to a group of cells which discharged rhythmically, in phase with the intracellular and extracellular rhythm, suggest that theta in the hippocampal slice is not without a cellular basis, and is not an artifact (Bland, Colom, Konopacki and Roth, in press). The fact that theta has been produced in the HF without an intact septum suggests that the HF contains the necessary mechanisms for the production of slow wave theta, and that the MS/vDBB rhythmicity is not necessarily the cause of hippocampal theta.

The results of the present investigation support the importance of both rhythmic and nonrhythmic output to the HF from the MS/vDBB regarding modulation of theta frequency

and the occurrence of theta, respectively. However, it seems that both phasic and tonic neurons can change their discharge rates relative to theta frequency suggesting that both rhythmic and nonrhythmic MS/vDBB cells are involved in the modulation of theta frequency. That is, both the overall afferent input to the HF, regardless of whether it is phasic or tonic (as indicated by the linear relationship between MS/vDBB cell discharge rates and theta frequency), and the nature of the input (phasic vs. tonic) are important in the modulation of theta frequency. The results of this study also suggest that the MS/vDBB modulation of theta frequency (phasic and tonic) is inhibitory (linear theta-off) and excitatory (linear theta-on). Until now there has been no indication that this was possible.

As was indicated by Apostol and Cruetzfeldt (1974), MS/vDBB cells which are nonrhythmic appear to alter their discharge rates with changes in the hippocampal EEG activity from one state to another. In addition to nonrhythmic cells, MS/vDBB cells which are rhythmic also appear to alter their discharge rates in a similar fashion. Moreover, tonic and phasic nonlinear MS/vDBB cells were either theta-on or theta-off, suggesting that the afferent drive involved in the occurrence of theta is also excitatory and inhibitory. The results of this study

suggest that the nature of the afferent input to the HF from the MS/vDBB is more complicated than previously thought, and that both theta frequency and the occurrence of theta are dependent on the discharge rates of MS/vDBB neurons in addition to their phasic output.

It is important to note that, according to anatomic research, approximately 50 % of the recorded neurons could have been septal-hippocampal projection neurons, while the other 50 % could have been interneurons or neurons which projected to other structures (Lamour, et al., 1984). Lamour, et al. (1984) reported that cholinergic and noncholinergic neurons projecting to the HF were both rhythmic and nonrhythmic. The various cell groups recorded in this study might correspond to the various types of septal-hippocampal and unidentified neurons reported by these authors. Therefore, the conclusions regarding the nature of the afferent input of the MS/vDBB to the HF are limited by the fact that only 50 % of the recorded neurons were likely to be septal-hippocampal neurons, just as was the case with the previous work on the septal pacemaker hypothesis.

Septal-hippocampal and unidentified MS/vDBB neurons respond to iontophoretic administration of different neurotransmitters, agonists, and antagonists in different ways (Lamour, et al., 1984). It would be informative to

study the relationships between MS/vDBB cells and slow wave theta reported herein with antidromic activation and/or with iontophoresis as was done by Lamour, et al. (1984).

The observation of opposite relationships between MS/vDBB cell discharge rates and theta frequency, and discharge rates with hippocampal EEG states, supports the anatomic, physiologic, and pharmacologic evidence of excitatory and inhibitory mechanisms in the septal-hippocampal system. However, the results of this study cannot differentiate between the various possibilities such as: the influence of excitatory and inhibitory hippocampal-septal projections, inhibitory recurrent collaterals, inhibitory interneurons from the LS to the MS/vDBB, or the cholinergic and noncholinergic septal-hippocampal projections.

The use of an acute paradigm limits the conclusions regarding the natural physiologic state. Increasing the concentration of urethane was previously shown to reduce theta frequency and the discharge rates of MS/vDBB cells (Stumpf, et al., 1962). This study clearly demonstrated that theta frequency and cell discharge rates could be inversely related in urethane anaesthetized preparations. This was the case for both tonic and phasic cells.

Urethane also limited the range of theta frequency observed in the hippocampal EEG. For this reason the use

of the terms linear and nonlinear are appropriate. At this time these terms adequately describe the relationships observed within the frequency window. Further study of these relationships in the freely moving animal may yield the same types of relationships over the entire frequency range of theta. Currently there is a paucity of information about the correlates of MS/vDBB cells, both to the hippocampal EEG and behavior.

A study by Ranck (1976) reported theta cells and tight group cells in the MS/vDBB of freely moving rats. Ranck (1976) reported what would be termed phasic nonlinear theta-on cells in the present work. These cells increased their discharge rates during type 1 theta behaviors, which resulted in the production of type 1 theta. In addition, he reported theta cells (phasic) which increased their discharge rates when the animal produced an orienting response. Unfortunately, he did not analyze the relationship of cell discharge rate to theta frequency. Tight group cells (tonic) were reported to have behavioral correlates to automatic behaviors such as face washing, and other undetermined behaviors. Finally, Ranck (1976) reported a group of constant firing fast cells (tonic) with discharge rates which were not related to the EEG state. The present work in concert with Ranck (1976) suggests that there may also be cells in the MS/vDBB which have further

correlations to the hippocampal EEG and necessarily to certain groups of behavior.

It is also likely that a maximum discharge rate will be reached somewhere within the frequency range of theta. Since the frequency range of theta is much larger than that observed in urethane anaesthetized animals, it is possible that the slope of the relationship will change with larger changes in theta frequency than could be observed in this study.

Nonlinear cells observed in the present study could have exponential, or logarithmic (nonlinear) relationships with theta frequency, if higher frequencies of theta were observed. That is, the slope of the relationship within the frequency window could have been zero, and had higher frequency theta been observed, the slope might have increased . Linear cells in this study may also have exponential relations to theta frequency. Therefore, it must be remembered that until further work is completed in freely moving animals, the terms linear and nonlinear merely describe the relationships observed in a urethane anaesthetized preparation.

An investigation of this nature in freely moving animals, rabbits in particular because they clearly produce large amplitude type 1 and type 2 theta, might also serve to clarify whether there are one or two types of theta.

Analysis of relationships in the type 1 behavioral conditions compared to the type 2 theta conditions could yield a single continuous function, a function with an abrupt change in slope, or it could yield a discontinuous function. A continuous function would support the hypothesis that type 1 (high frequency) theta is produced by an increasing input from the brainstem (proposed by Brazhnik and Vinogradova, 1986). A discontinuous function, or a sudden change in slope might indicate that an additional input has been activated, causing the cell discharge rate to suddenly increase or decrease.

Finally, the spontaneous relations observed in this study were obtained over one second samples of theta. There is considerable inconsistency in the literature over whether intraburst discharge rates and burst durations vary with theta frequency (Vinogradova, et al., 1980; Petsche, et al., 1962; Petsche, et al., 1965; Gaztelu and Buno, 1982; Wilson, et al., 1976). It would be useful to compare the results of the present second by second analysis with the relations observed in a cycle by cycle analysis. It is possible, depending on the slope observed in the present linear analysis, that a cycle by cycle analysis could result in a linear positive, a linear negative, or a constant relationship between discharge rate and cycle duration (period). With the low number of spikes/burst

that can be observed in MS/vDBB cells, there may not be enough variation in discharge rates. It is also possible that discharge rates might not reflect such precise changes in the theta rhythm.

Stimulation Induced Activity

Stimulation of the DM-PH had some interesting effects on the spike trains of MS/vDBB cells. Stimulation of the DM-PH at different intensities, when recording phasically discharging neurons, suggested that the input from the DM-PH to these cells is direct and excitatory. Cell discharge rates were linearly related to the stimulus intensity regardless of their spontaneous relationship to hippocampal EEG activity. Phasic linear and nonlinear theta-on cells, and phasic linear and nonlinear theta-off cells increased spontaneous discharge rates to stimulation of the DM-PH.

As was predicted, tonic cells did not respond to stimulation of the DM-PH in a consistent fashion. These cells could increase or decrease discharge rates linearly or nonlinearly with increased stimulation intensity. However, these results must be interpreted cautiously, and in concert with previous research due to the small number of cells studied. These results suggest that tonic cells receive several inputs, directly or indirectly, from the

DM-PH. This is supported by the anatomic interconnections of the hypothalamic nuclei with the septal nuclei (see Anatomy). The results of DM-PH stimulation have confirmed and extended the findings of previous research, which demonstrated more predictable effects of brainstem and diencephalic stimulation on rhythmic bursting neurons of the MS/vDBB (Vinogradova, et al., 1980; Petsche, et al., 1962; Petsche, et al., 1965; Gaztelu and Buno, 1982; Wilson, et al., 1976).

The effects of stimulation on the spontaneously observed relationship between hippocampal theta and MS/vDBB cell discharge rates and patterns provided some interesting results. The results of this study were consistent with previous research in that MS/vDBB cells which discharged tonically remained tonic during stimulation and phasic cells remained phasic (Petsche, et al., 1962; Wilson, et al., 1976; Gaztelu and Buno, 1982). As was already reported, the effects of stimulation on the spontaneous relationship between discharge rates and the hippocampal EEG, for phasically discharging cells was to overide the spontaneous relationship, except for phasic linear theta-on cells, which were already positively correlated to theta frequency. Tonically discharging cells did not appear to have a consistent relationship between stimulation induced activity and the spontaneous activity.

In summary, this study demonstrated that a variety of MS/vDBB neurons were related to hippocampal EEG activity along a number of axes, in addition to rhythmicity. Future models of the septal-hippocampal system must take into account the multiple ways in which MS/vDBB cells can be related to the hippocampal EEG. Furthermore, it is possible that the relationships described in this work may still be over-simplified. However, the reported results provide a platform for further study and elaboration on the models of septal-hippocampal function.

REFERENCES

Alonso, A., Gaztelu, J. M. Buno, W. Jr. and Garcia-Austt, E. (1987) Cross-correlation analysis of septohippocampal neurons during θ-rhythm. Brain Research, 413, 135-146.

Alonso, A. and Kohler, C. (1982) Evidence for separate projections of hippocampal pyramidal and non-pyramidal neurons to different parts of the septum in the rat brain. Neuroscience Letters, 31, 209-214.

Amaral, D. G. (1978) A golgi study of cell types in the hilar region of the hippocampus in the rat. The Journal of Comparative Neurology, 182, 851-914.

Amaral, D. G. and Kurz, J. (1985) An analysis of the origins of the cholinergic and noncholinergic septal projections to the hippocampal formation of the rat. The Journal of Comparative Neurology, 240, 37-59.

Anchel, H. and Lindsley, D. B. (1972) Differentiation of two reticulo-hypothalamic systems regulating hippocampal activity. Electroencephalography and Clinical Neurophysiology, 32, 209-226.

Andersen, P., Bland, B. H. and Dudar, D. (1973) Organization of the hippocampal output. Experimental Brain Research, 17, 152-168.

Andersen, P., Bland, B. H., Myhrer T. and Schwartzkroin, P. A. (1979) Septohippocampal pathway necessary for dentate theta production. Brain Research, 165, 13-22.

Apostol, G. and Creutzfeldt, O. D. (1974) Cross-correlation between the activity of septal units and hippocampal EEG during arousal. Brain Research Bull, 8, 211-222.

Baisden. R. H., Woodruff. M. L. and Hoover. D. B. (1984) Cholinergic and non-cholinergic septo-hippocampal projections: A double-label horseradish peroxidase-acetylcholinesterase study in the rabbit. Brain Research, 290, 146-151.

Berger, T. W., Semple-Rowland, S, and Basset, J. L. (1980) Hippocampal polymorph neurons are the cells of origin for ipsilateral assocation and commissural afferents to the dentate gyrus. Brain Research, 215, 329-336.

Blackstad, T. W. (1956) Commissural connections of the hippocampal region in the rat, with special reference to their mode of termination. The Journal of Comparative Neurology, 105, 417-537.

Bland, B. H. (1986) The physiology and pharmacology of hippocampal formation theta rhythms. Progress in Neurobiology, 26, 1-54.

Bland, S. K. and Bland, B. H. (1986) Medial septal modulation of hippocampal theta cell discharges. Brain Research, 375, 102-116.

Bland, B. H. and Vanderwolf, C. H. (1972) Diencephalic and hippocampal mechanisms of motor activity in the rat: Effects of posterior hypothalamic stimulation on behavior and hippocampal slow wave activity. Brain Research, 43, 67-88.

Bland, B. H., Andersen, P. and Ganes, T. (1975) Two generators of hippocampal theta activity in rabbits. Brain Research, 94, 199-218.

Bland, B. H., Colom, L. V., Konopacki, J. and Roth, S. H. (in press) Intracellular records of carbachol-induced theta rhythm in hippocampal slices. Brain Research.

Bland, B. H., Seto, M. G. and Rowntree, C. J. (1983) The relation of multiple hippocampal theta cell discharge rates to slow wave theta frequency. Physiology and Behavior, 31, 111-117.

Brazhnik, E. S., and Vinogradova, O. S. (1986) Control of the neuronal rhythmic bursts in the septal pacemaker of theta-rhythm: Effects of anaesthetic and anticholinergic drugs. Brain Research, 380, 94-106.

Brodal, A. (1947) The hippocampus and the sense of smell. Brain, 70, 179-222.

Chandler, C. P. and Crutcher, K. A. (1983) The septo-hippocampal projections in the rat: An electron microscopic horseradish peroxidase study. Neuroscience, 10, 685-696.

Chronister, R. B. and DeFrance, J. F. (1979) Organization of projection neurons of the hippocampus. Experimental Neurology, 66, 509-523.

Colom, L. V. and Bland, B. H. (1987) State-dependent spike train dynamics of hippocampal formation neurons:

Evidence for theta-on and theta-off cells. Brain Research, 422, 277-286.

Colom, L. V., Ford, R. D. and Bland, B. H. (1987) Hippocampal formation neurons code of level of activation of the cholinergic septohippocampal pathway. Brain Research, 410, 12-20.

Cooper, J. R., Bloom, F. E. and Roth, R. H. (1986) The Biochemical Basis of Neuropharmacology. New York; Oxford University Press.

Costa, E., Panula, P., Thompson, H. K. and Cheney, D. L. (1983) The transynaptic regulation of the septal-hippocampal cholinergic neurons. Life Science, 32, 165-179.

Crutcher, V. A., Madison, R. and Davis, J. N. (1981) A study of the rat septohippocampal pathway using anterograde transport of horseradish peroxidase. Neuroscience, 6, 1961-1973.

Destrades, C. (1982) Two types of diencephalically driven RSA (theta) as a means of studying memory formation in mice. Brain Research, 234, 486-493.

Dutar, P., Lamour, Y. and Jobert, A. (1983) Acetylocholine excites identified setpo-hippocampal neurons in the rat. Neuroscience Letters. 43, 43-47.

Dutar, P., Lamour, Y. and Jobert, A. (1985) Septohippocampal neurons in the rat: an in vivo intracellular study. Brain Research, 340, 135-142.

Dutar, P., Lamour, Y., Rascol,. O. and Jobert, A. (1986) Septo-hippocampal neurons in the rat: further study of their physiological and pharmacological properties. Brain Research, 365, 325-334.

Edgington, E. S. (1980) Randomization Tests. New York: Marcel Dekker, Inc.

Fonnum, F. and Walaas, I. (1978) The effect of intrahippocampal kainic acid injections and surgical lesions on neurotransmitters in the hippocampus and septum. Journal of Neurochemistry, 31, 1178-1181.

Gaarskjaer, F. B. (1986) The organization and development of the hippocampal mossy fiber system. Brain Research Reviews, 11, 335-357.

Garcia Austt, E. (1984) Hippocampal level of neural integration. In: Cortical Integration: Basic Archicortical and Cortical Association Level of Neural Integration. International Brain Research Organization, Monograph Series. Vol. 11. Reinoso-Suarez, F. and Agmone-Marsan, C. (Eds.) New York: Raven Press.

Gaztelu, J. M. and Buno, W, Jr. (1982) Septo-hippocampal relationships during EEG theta rhythm. Electroencephalography and Clinical Neurophysiology, 54, 375-387.

Gerfen, C. R. and Sawchenko, P. E. (1984) An anterograde neuroanatomical tracing method that shows the detailed morphology of neurons, their axons and terminals: immunohistochemical localization of an axonally transported plant lectin, *Phaseolus vulgaris* leucoagglutinin (PHA-L). Brain Research, 290, 219-238.

Gogolak, G., Stumpf, C., Petsche, H. and Sterc, J. (1968) The firing pattern of septal neurons and the form of the hippocampal theta wave. Brain Research, 7, 201-207.

Green, J. D. and Arduini, A. (1954) Hippocampal electrical activity in arousal. Journal of Neurophysiology, 17, 533-557.

Hjorth-Simonsen, A. (1972) Projection of the lateral part of the entorhinal area to the hippocampus and fascia dentata, The Journal of Comparative Neurology, 146, 219-232.

Hjorth-Simonsen, A. (1973) Some intrinsic connections of the hippocampus in the rat: An experimental analysis. The Jounal of Comparative Neurology, 147, 145-162.

Hjorth-Sinomsen, A. and Jeune, B. (1972) Origin and termination of the hippocampal perforant path in the rat studied by silver impregnation. The The Journal of Comparative Neurology, 114, 215-232.

Houser, C. R., Crawford, G. D., Barber, R. P., Salvaterra, P. M. and Vaughn, J. A. (1983) Organization of morphological characteristics of cholinergic neurons: an immunocytochemical study with a monoclonal antibody to choline acetyltransferase. Brain Research, 286, 97-119.

Joels, M. and Urban, I. J. A. (1985) Topographic organization of fimbria-fornix fibers projecting to the lateral septum of rats: A single and field response analysis. Experimental Neurology, 87, 474-486.

Kimura, H., McGeer, P. L., Peng, J. H. and McGeer, E. G. (1981) The central cholinergic system studied by CAT immunohistochemistry in the cat. The Journal of Comparative Neurology, 200, 151-201.

Kita, H. and Oomura, Y. (1982a) An HRP study of the afferent connections to rat medial hypothalamic region. Brain Research Bulletin, 8, 53-62.

Kita, H. and Oomura, Y. (1982b) An HRP study of the afferent connections to rat lateral hypothalamic region. Brain Research Bulletin, 8, 63-71.

Kohler, C. and Chan-Palay, V. (1983) Distribution of γ-aminobutyric acid containing neurons and terminals in the septal area. Anatomical Embryology, 167, 53-65.

Kohler, C., Chan-Palay, V. and Wu, J. Y. (1984) Septal neurons containing glutamic acid decarboxylase immunoreactivity project to the hippocampal region in the rat brain. Anatomical Embryology, 169, 41-44.

Konopacki, J., Bland, B. H., MacIver, M. B. and Roth, S. H. (1987) Cholinergic theta rhythm in transected hippocampal slices: independent CA1 and dentate generators. Brain Research, 436, 217-222.

Konopacki, J., MacIver, M. B., Bland, B. H. and Roth, S. H. (1987a) Carbachol-induced EEG 'theta' activity in hippocampal brain slices. Brain Research, 405, 196-198.

Konopacki, J., MacIver, M. B., Bland, B. H. and Roth, S. H. (1987b) Theta in hippocampal slices: relation to synaptic responses of dentate neurons. Brain Research Bulletin, 18, 25-27.

Kramis, R. C. and Routtenberg, A. (1977) Dissociation of hippocampal EEG from its behavioral correlates by septal and hippocampal electrical stimulation. Brain Research, 125, 37-49.

Kramis, R. and Vanderwolf, C. H. (1980) Frequency-specific RSA-like hippocampal patterns

elicited by septal hypothalamic, and brainstem electrical stimulation. Brain Research, 192, 383-399.

Kramis, R. C., Vanderwolf, C. H. and Bland, B. H. (1975) Two types of hippocampal rhythmical slow activity in both the rabbit and the rat: Relations to behavior and effects of atropine , diethyl ether, urethane and, pentobarbital. Experimental Neurology, 49, 58-85.

Lamour, Y., Dutar, P. and Jobert, A. (1984) Septo-hippocampal and other medial septum-diagonal band neurons: electrophysiological and pharmacological properties. Brain Research, 309, 227-239.

Leung, L. S., Lopes Da Silva, S. J. and Wadman, W. J. (1982) Spectral characteristics of hippocampal EEG in the freely moving rat. Electroencephalography and Clinical Neurophysiology, 54, 203-219.

Lewis, P. R. and Shute, C. C. C. (1967) The cholinergic limbic system. Projections to hippocampal formation, medial cortex, neclei of the ascending cholinergic reticular system, and the subfornical organ and supra-optic crest. Brain, 90, 521-540.

Liberson, W. R. and Cadilhac, J. G. (1954) Hippocampal responses to sensory stimulation in the guinea pig. Electroencephalography and Clinical Neurophysiology, 6, 710-711.

Lorente de No, R. (1934) Studies on the structure of the cerebral cortex. II. Continuation of the study of the Ammonic system. Journal fur Psychologie und Neurologie, 46, 113-177.

Luiten, P. G. M. and Room, P. (1980) Interrelations between lateral, dorsomedial and ventromedial hypothalamic nuclei in the rat. An HRP study. Brain Research, 190, 321-332.

Lynch, G. S., Rose, G. and Gall, C. M. (1978) Anatomical and functional aspects of the septo-hippocampal projections. In: Functions of the Septo-Hippocampal System, pp 5-20. Eds. K. Elliot and J. Whelan. Ciba Foundation Symposium, 58, Elsevier, Amsterdam.

Macadar, O., Roig, J. A., Monti, J. M. and Budelli, R. (1970) The functional relationship between septal and hippocampal unit activity and hippocampal theta rhythm. Physiology and Behavior, 5, 1443-1449.

Macadar, A. W., Chalupa, L. M. and Lindsley, D. B. (1974) Differentiation of brain stem loci which affect hippocampal and neocortical electrical activity. Experimental Neurology, 43, 499-514.

McKinney, M., Coyle, J. T. and Hedreen, J. C. (1983) Topographic analysis of the innervation of the rat neocortex and hippocampus by the basal forebrain cholinergic system. The Journal of Comparative Neurology, 217, 103-121.

McLennan, H, and Miller, J. J. (1974a) The hippocampal control of neuronal discharges in the septum of the rat. Journal of Physiology (London), 237, 607-624.

McLennan, H, and Miller, J. J. (1974b) γ-Aminobutyric acid and inhibition in the septal nuclei of the rat. Journal of Physiology (London), 237, 625-633.

McNaughton, N. and Miller, J. J. (1984) Medial septal projections to the dentate gyrus of the rat: electrophysiological analysis of distribution and plasticity. Experimental Brain Research, 56, 243-256.

Meibach, R. C. and Siegel, A. (1977a) Efferent connections of the hippocampal formation in the rat. Brain Research, 124, 197-224.

Meibach, R. C. and Siegel, A. (1977b) Efferent connections of the septal area of the rat: An analysis utilizing retrograde and anterograde transport methods. Brain Research, 119, 1-20.

Mellgren, S. I. and Srebro, B. (1973) Changes in acetylcholinesterase and distribution of degenerating fibres in the hippocampal region after septal lesions in the rat. Brain Research, 52, 19-36.

Mesulam, M. M., Mufson, E. J., Wainer, B. H. and Levey, A. I. (1983) Central cholinergic pathways in the rat: an overview basd on an alternative nomenclature (Ch1-Ch6). Neuroscience, 10, 1185-1201.

Milner, T. A., Loy, R. and Amaral, D. G. (1983) An anatomical study of the development of the septo-hippocampal projection in the rat. Developmental Brain Research, 8, 366-378.

Monmaur, P. and Thomson, M. A. (1983) Topographic organization of septal cells innervating the dorsal hippocampal formation of the rat: special reference

to both the CA1 and dentate θ-generators. Experimental Neurology, 82, 366-378.

Morales, F. R., Roig, J. A., Monti, J. M. Macadar, O. and Budelli, R. (1971) Septal unit activity and hippocampal EEG during the sleep-wakefulness cycle of the rat. Physiology and Behavior, 6, 563-567.

Mosko, S., Lynch, G. and Cotman, C. W. (1973) The distribution of septal projections to the hippocampus of the rat. The Journal of Comparative Neurology, 152, 163-174.

Nyakas, C., Luiten, P. G. M., Spencer, D. G. and Traber, J (1987) Detailed projection patterns of septal and diagonal band efferents to the hippocampus in the rat with emphasis on innervation of CA1 and dentate gyrus. Brain Research Bulletin, 18, 533-545.

Panula, P. Revuelta, A. V., Cheney, D. L., and Wu, J. Y. and Costa, E. (1984) An immunohistochemical study on the location of GABAergic neurons in rat septum. The Journal of Comparative Neurology, 222, 69-80.

Paxinos, G. and Watson, C. (1986) The Rat Brain: in Stereotaxic Coordinates. New York: Academic Press

Petsche, H., Gogolak, G. and Van Zwieten, P. A. (1965) Rhythmicity of septal cell discharges at various levels of reticular excitation. Electroencephalography and Clinical Neurophysiology, 19, 25-33.

Petsche, H. and Stumpf, C. (1960) Topographic and toposcopic study of origin and spread of the regular synchronized arousal pattern in the rabbit. Electroencephalography and Clinical Neurophysiology, 12, 589-600.

Petsche, H., Stumpf, G. and Gogolak, G. (1962) The significance of the rabbit's septum as a relay station between the midbrain and the hippocampus. I. The control of hippocampus arousal activity by the septum cells. Electroencephalography and Clinical Neurophysiology, 19, 25-33.

Raisman, G. (1966) The connexions of the septum. Brain, 89, 317-348.

Raisman, G., Cowan, W. M. and Powell, T. P. S. (1965) The extrinsic afferent, commissural and association fibres of the hippocampus. Brain, 88, 963-996.

Raisman, G., Cowan, W. M. and Powell, T. P. S. (1966) An experimental analysis of the efferent projections of the hippocampus. Brain, 89, 83-108.

Ramon y Cajal, S. (1911) Histologie du Systeme Nerveux de l'Homme et des Vertebres Tome 2. Paris: A. Maloine.

Ranck, J. B. (1973) Studies of the single neurons in dorsal hippocampal formation and septum in unrestrained rats. Part 1. Behavioral correlates and firing repertoires. Experimental Neurology, 41, 461-531.

Ranck, J. B. (1976) Behavioral correlates and firing repertoires of neurons in septal nuclei of unrestrained rats. In: The Septal Nuclei. J. F. DeFrance (Ed.). New York: Plenum Publishing Corporation.

Rawlins, J. N. P., Feldon, J. and Gray, J. A. (1979) Septo-hippocampal connections and the hippocampal theta rhythm. Experimental Brain Research, 37, 49-63.

Riley, J. N. and Moore, R. Y. (1981) Diencephalic and brainstem afferents to the hippocampal formation of the rat. Brain Research Bulletin, 6, 437-444.

Robinson, T. E. (1980) Hippocampal rhythmic slow activity (RSA; theta): a critical analysis of selected studies and discussion of possible species-differences. Brain Research Reviews, 2, 69-101.

Robinson, T. E. and Vanderwolf, C. H. (1978) Electrical stimulation of the brain stem in freely moving rats: II. Effects on hippocampal and neocortical electrical avtivity, and relations to behavior. Experimental Neurology, 61, 485-515.

Rowntree, C. I. and Bland, B. H. (1986) An analysis of cholinoceptive neurons in the hippocampal formation by direct microinfusion. Brain Research, 362, 98-113.

Sainsbury, R. S. and Bland, B. H. (1981) The effects of selective septal lesions on theta production in CA1 and the dentate gyrus of the hippocampus, Physiology and Behavior, 26, 1097-1101.

Saper, C. B., Swanson, L. W. and Cowan, W. M. (1979) An autoradiographic study of the efferent connections of the lateral hypothalamic area in the rat. The Journal of Comparative Neurology, 184, 689-706.

Schwerdtfeger, W. K. and Buhl, E. (1986) Various types of non-pyramidal hippocampal neurons project to the septum and contralateral hippocampus. Brain Research, 386, 146-154.

Segal, M. (1974) Responses of septal neuclei to microiontophoretically administered putative neurotransmitters. Life Sciences, 14, 1345-1351.

Segal, M. (1986) Properties of rat medial septal neurones recorded in vitro. Journal of Physiology (London), 379, 309-330.

Segal, M. and Landis, S. (1974) Afferents to the hippocampus of the rat studied with the method of retrograde transport of horseradish peroxidase. Brain Research, 78, 1-15.

Shinoda, K., Tohyama, M. and Shiotani, Y. (1987) Hippocampofugal γ-aminobutyric acid (GABA)-containing neuron system in the rat: a study using a double-labeling method that combines retrograde tracing and immunocytochemistry. Brain Research, 409, 181-186.

Sinclair, B. R., Seto, M. G. and Bland, B. H. (1982) Theta cells in CA1 and dentate layers of the hippocampal formation: Relations to slow wave activity and motor behavior in the freely moving rabbit. Journal of Neurophysiology, 5, 1214-1225.

Steward, A. and Scoville, S. A. (1976) Cells of origin of entorhinal cortical afferents to the hippocampus and fascia dentata of the rat. The Journal of Comparative Neurology, 169, 347-370.

Stewart, D. J. and Vanderwolf, C. H. (1987) Hippocampal rhythmical slow activity following ibotenic acid lesions of the septal region. I. Relations to behavior and effects of atropine and urethane. Brain Research, 423, 88-100.

Storm-Mathisen, J. and Opsahl, M. W. (1978) Aspartate and/or glutamate may be transmitters in hippocampal efferents to septum and hypothalamus. Neuroscience Letters, 9, 65-70.

Stumpf, C., Petsche, H. and Gogolak, G. (1962) The significance of the rabbit's septum as a relay station between the midbrain and the hippocampus. II. The differential influence of drugs upon the septal cell firing pattern and the hippocampus theta activity. Electroencephalography and Clinical Neurophysiology, 14, 212-219.

Swanson, L. W. and Cowan, W. M. (1976) Autoradiographic studies of the development and connections of the septal area in the rat. In J. F. DeFrance (Ed.), The Septal Nuclei. New York: Plenum Press.

Swanson, L. W. and Cowan, W. M. (1977) An autoradiographic study of the organization of the efferent connections of the hippocampal formation in the rat. The Journal of Comparative Neurology, 172, 49-84.

Swanson, L. W. and Cowan, W. M. (1979) Connections of the septal region in the rat. The Journal of Comparative Neurology, 186, 621-656.

Swanson, L. W., Sawchenko, P. E. and Cowan, W. M. (1980) Evidence that the commissural, associational and septal projections of the regio inferior of the hippocampus arise from the same neurons. Brain Research, 197, 207-212.

Ter Horst, G. J. and Luiten, P. G. M. (1986) The projections of the dorsomedial hypothalamic nucleus in the rat. Brain Research Bulletin, 16, 231-248.

Tombol, T. and Petsche, H. (1969) The histological organization of the pacemaker for the hippocampal theta rhythm in the rabbit. Brain Research, 12, 414-426.

Vanderwolf, C. H., Bland, B. H. and Whishaw, I. Q. (1973) Diencephalic hippocampal and neocortical mechanisms in voluntary movement. In: Efferent Organization and the Intergration of Behavior. pp. 229-262. Maser., J. D. (Ed.) New York: Academic.

Vertes, R. P. (1980) Brain stem activation of the hippocampus: A role for the magnocellular reticular formation and the MLF. Electroencephalography and Clinical Neurophysiology, 50, 48-58.

Vertes, R. P. (1981) An analysis of ascending brain stem systems involved in hippocampal synchronization and

desynchronization. Journal of Neurophysiology, 46, 1140-1159.

Vertes R. P. (1982) Brain stem generation of the hippocampal EEG. Progress in Neurobiology, 19, 159-186.

Vinogradova, O. S., Brahzhnik, E. S, Karanov, A. M. and Zhadina, S. D. (1980) Neuronal activity of the septum following various types of deafferentation, Brain Research, 187, 353-368.

Wainer, B. H., Levey, A. I., Rye, D. B., Mesulam, M-M. and Mufson, E. J. (1985) Cholinergic and non-cholinergic septohippocampal pathways. Neuroscience Letters, 54, 45-52.

Wilson, C. L., Motter, B. C. and Lindsley, D. B. (1976) Influences of hypothalamic stimulation upon septal and hippocampal electrical activity in the cat. Brain Research, 107, 55-68.

Winson, J. (1974) Patterns of hippocampal theta rhythm in the freely moving rat. Electroencephalography and Clinical Neurophysiology, 36, 291-301.

Wyss, J. M., Swanson, L. W. and Cowan, W. M. (1979) A study of subcortical afferents to the hippocampal formation in the rat. Neuroscience, 4, 463-476.

Zaczek, R., Hedreen, J. C. and Coyle, J. T. (1979) Evidence for a hippocampal-septal glutamatergic pathway in the rat. Experimental Neurology, 65, 145-156.